AD-A185 667 CODING FOR SPREAD-SPECTRUM COMMUNICATIONS NETWORKS(U) 1/2
MICHIGAN UNIV ANN ARBOR COMMUNICATIONS AND SIGNAL
PROCESSING LAB B G KIM MAR 87 022793-2-T
UNCLASSIFIED N00014-85-K-0545 F/G 25/2 NL

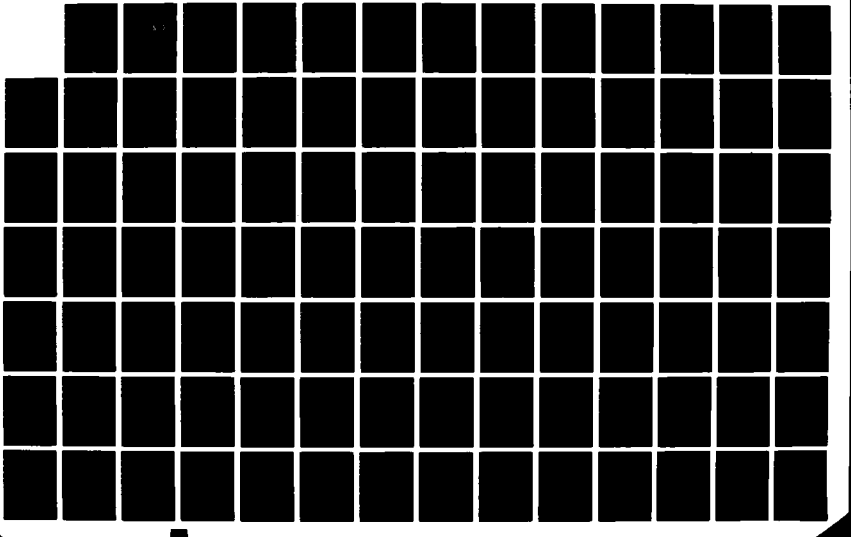

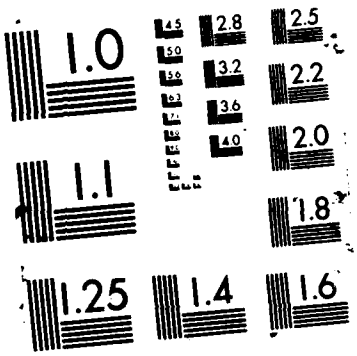
1.0
1.1
1.25
1.4
1.6
1.8
2.0
2.2
2.5
2.8
3.2
3.6
4.0
4.5

(2)

Report 022793-2-T

CODING FOR SPREAD-SPECTRUM COMMUNICATIONS NETWORKS

Bal Gi Kim

COMMUNICATIONS & SIGNAL PROCESSING LABORATORY
Department of Electrical Engineering and Computer Science
The University of Michigan
Ann Arbor, Michigan 48109

March 1987

Technical Report No. 244
Approved for public release; distribution unlimited.

Prepared for

OFFICE OF NAVAL RESEARCH
Department of the Navy
Arlington, Virginia 22217

UNCLASSIFIED
SECURITY CLASSIFICATION OF THIS PAGE

AD-A185667

REPORT DOCUMENTATION PAGE

1a. REPORT SECURITY CLASSIFICATION UNCLASSIFIED	1b. RESTRICTIVE MARKINGS NONE
2a. SECURITY CLASSIFICATION AUTHORITY	3. DISTRIBUTION/AVAILABILITY OF REPORT Approved for Public Release; Distribution Unlimited
2b. DECLASSIFICATION/DOWNGRADING SCHEDULE	
4. PERFORMING ORGANIZATION REPORT NUMBER(S) Report 022793-2-T TR 244	5. MONITORING ORGANIZATION REPORT NUMBER(S)
6a. NAME OF PERFORMING ORGANIZATION Communications & Signal Processing Laboratory 6b. OFFICE SYMBOL (If applicable)	7a. NAME OF MONITORING ORGANIZATION Office of Naval Research
6c. ADDRESS (City, State, and ZIP Code) The University of Michigan Ann Arbor, Michigan 48109-2122	7b. ADDRESS (City, State, and ZIP Code) 800 North Quincy Street Arlington, Virginia 22217
8a. NAME OF FUNDING/SPONSORING ORGANIZATION 8b. OFFICE SYMBOL (If applicable)	9. PROCUREMENT INSTRUMENT IDENTIFICATION NUMBER Contract No. N00014-85-K-0545
8c. ADDRESS (City, State, and ZIP Code)	10. SOURCE OF FUNDING NUMBERS PROGRAM ELEMENT NO. / PROJECT NO. / TASK NO. / WORK UNIT ACCESSION NO.

11. TITLE (Include Security Classification)
Coding for Spread-Spectrum Communication Networks

12. PERSONAL AUTHOR(S)
Bal Gi Kim

13a. TYPE OF REPORT	13b. TIME COVERED	14. DATE OF REPORT (Year, Month, Day)	15. PAGE COUNT
Tech. Report	FROM _____ TO _____	March 1987	158

16. SUPPLEMENTARY NOTATION

17. COSATI CODES			18. SUBJECT TERMS (Continue on reverse if necessary and identify by block number)
FIELD	GROUP	SUB-GROUP	Digital Communications; Parallel decoding; Error correcting codes; Reed-Solomon codes

19. ABSTRACT (Continue on reverse if necessary and identify by block number)

The multiple-access capability of a frequency-hop packet radio network is investigated from a coding point of view. The achievable region of code rate and channel traffic and the normalized throughput are considered as performance measures.

We model the communication system from the modulator input to the demodulator output as an I-user interference channel, and evaluate the asymptotic performance of various coding schemes for channels with perfect side information, no side information, and imperfect side information. The coding schemes being considered are Reed-Solomon codes, concatenated codes, and parallel decoding schemes. We derive the optimal code rate and the optimal channel traffic at which the normalized throughput is maximized, and from these optimum values the asymptotic maximum normalized throughput is derived. The results are then compared with channel capacities.

20. DISTRIBUTION/AVAILABILITY OF ABSTRACT ☒ UNCLASSIFIED/UNLIMITED ☐ SAME AS RPT. ☐ DTIC USERS	21. ABSTRACT SECURITY CLASSIFICATION UNCLASSIFIED
22a. NAME OF RESPONSIBLE INDIVIDUAL Wayne E. Stark	22b. TELEPHONE (Include Area Code) (313) 763-0390 22c. OFFICE SYMBOL

DD FORM 1473, 84 MAR 83 APR edition may be used until exhausted. All other editions are obsolete.

SECURITY CLASSIFICATION OF THIS PAGE
UNCLASSIFIED

19. Abstract (cont.)

It is shown that the capacity of interference channels with perfect side information and no side information can be achieved by Reed-Solomon codes and concatenated code respectively. For channels with imperfect side information, it is found that the parallel decoder performs better than the errors-and-erasures decoder. The performance improvement becomes more significant as the side information becomes less reliable.

To my parents

ACKNOWLEDGEMENTS

I wish to express my sincere gratitude to Professor Wayne E. Stark, my thesis advisor, for his invaluable advice and support during the research carried out for this study. His keen insight and observations have been essential for the realization of this work.

I also wish to express my appreciation to Professors David Neuhoff, William Root, and Demosthenis Teneketzis, for their time reading and providing the helpful comments on this thesis. My education and research work are impossible without financial support over the years. For this, I would like to acknowledge the funding by Fulbright Scholarship and the Office of Naval Research under Contract N00014-85-K-0545.

Finally, I would like to thank my parents and brothers for their enduring encouragement and advice. To them I dedicate this dissertation.

TABLE OF CONTENTS

LIST OF FIGURES

Figure

LIST OF TABLES

Table

LIST OF APPENDICES

Appendix

LIST OF SYMBOLS

Anything

A_j	Weight distribution of a code
$C_j(I)$	Capacity of the j^{th} component channel given I users
$C_{sum}(I)$	Sum capacity of the interference channel given I users
d_{min}	Minimum distance of a code
D	Dimensionality of the signal set per frequency slot
η	Constant defined in (3.9)
G	Mean value of Poisson distribution
I	Number of users
I_{opt}	Optimum number of users at which normalized throughput is maximized
k	Number of information symbols in a codeword
K	Number of information symbols in an inner code
L	Diversity level
λ	Channel traffic intensity per frequency slot, I/q
M_i	Inner code alphabet size
M_o	Outer code alphabet size
n	Code length
N	Inner code length
N_b	Number of code symbols per hop
$p_{e,I}$	Probability of symbol error given I users

$p_{er,I}$	Probability of symbol erasure given I users
$p_{\rho,I}$	Probability of symbol erasure given I users with assumption 2
p_h	Probability of hit
$p_{h,I}$	Probability of hit given I users
$\hat{P}_m$	Probability of symbol erasure given m hits
$P_c(I)$	Probability of correctly decoding a codeword (packet)
P_d	Probability of detected error
P_F	Probability of erasure given no hit
$P_{I,L}$	Probability of symbol erasure given L diversity, I users
$P_{L,e}$	Probability of symbol error given L diversity, I users
P_m	Probability of symbol error given m hits
P_M	Probability of no erasure given hit
$P_E(I)$	Probability of codeword (packet) error given I users
P_{ud}	Probability of undetected error
q	Number of frequency slots
r_{opt}	Optimum code rate at which the normalized throughput is maximized
ρ	Fraction of the hop duration time that can be tolerated
$S(I)$	Unnormalized throughput given I users
T_h	Hop duration time
$W(I)$	Normalized throughput given I users
W_{max}	Maximum normalized throughput

CHAPTER I

INTRODUCTION

1.1. Spread-Spectrum Multiple-Access Communication

In recent years there has been increased interest in a class of multiple-access techniques known as spread-spectrum multiple-access (SSMA). The SSMA techniques are those multiple-access methods in which the multiple-access capability is due primarily to coding and in which - unlike traditional time- and frequency-division multiple-access - there is no requirement for precise time or frequency coordination between the transmitters in the system. One attractive feature of SSMA is the difficulty of detection by an unauthorized receiver. Another advantage of SSMA is that it is relatively easy to add additional users to the system. However, probably the dominant reason for considering SSMA is the need for some type of external interference rejection capability such as multipath rejection or resistance to intentional jamming.

SSMA techniques have been considered for a variety of satellite systems [San 81], systems to provide communication to aircraft and other mobile users [Leb 71], [Coo 78], [Goo 80], air traffic control systems [Sti 73].

The two most common forms of SSMA are frequency-hopped (FH) SSMA and direct-sequence (DS) SSMA. In DS-SSMA [Leh 84], [Pur 81b], each user

is given its own code, which is approximately orthogonal (i.e., has low cross correlation) with the codes of the other users. The carrier is phase modulated by the digital data sequence and the code sequence. In FH-SSMA [Pur 84], each user is assigned a unique frequency hopping pattern, so that the RF signal from a given transmitter is hopped from slot to slot by changing the carrier frequency according to its own hopping pattern.

This thesis is concerned with the application of FH-SSMA techniques to communication networks. We are interested in the multiple-access capability of a frequency-hop packet radio network as characterized by the user-channel model described in section 1.2. The goals of this thesis are to find the theoretical limit in performance and to show how to achieve the limit through the use of channel coding techniques.

1.2. The User-Channel Model

We consider a frequency-hop spread-spectrum (FH/SS) packet radio network in which I transmitter-receiver pairs (also called user pairs) of terminals wish to communicate over a common channel (see Figure 1.1). Each source generates messages (information), independent of messages generated by other users. There are I separate encoders, one for each source. The j^{th} encoder has as input only the messages from the j^{th} source and produces a codeword $(x_{j1}, x_{j2}, \cdots, x_{jn})$, $x_{ji} \in X$, where X is a common input alphabet. At the j^{th} receiver the j^{th} frequency dehopper, which has knowledge of the j^{th} hopping pattern, dehops the received signal and the dehopped signal is demodulated to produce the output vector $(y_{j1}, y_{j2}, \cdots, y_{jn})$, $y_{ji} \in Y$, where Y is a common output alphabet. Decoding is done independently at each of the I receivers and thus there is no cooperation between users on either the transmitting or the receiving side. We thus model

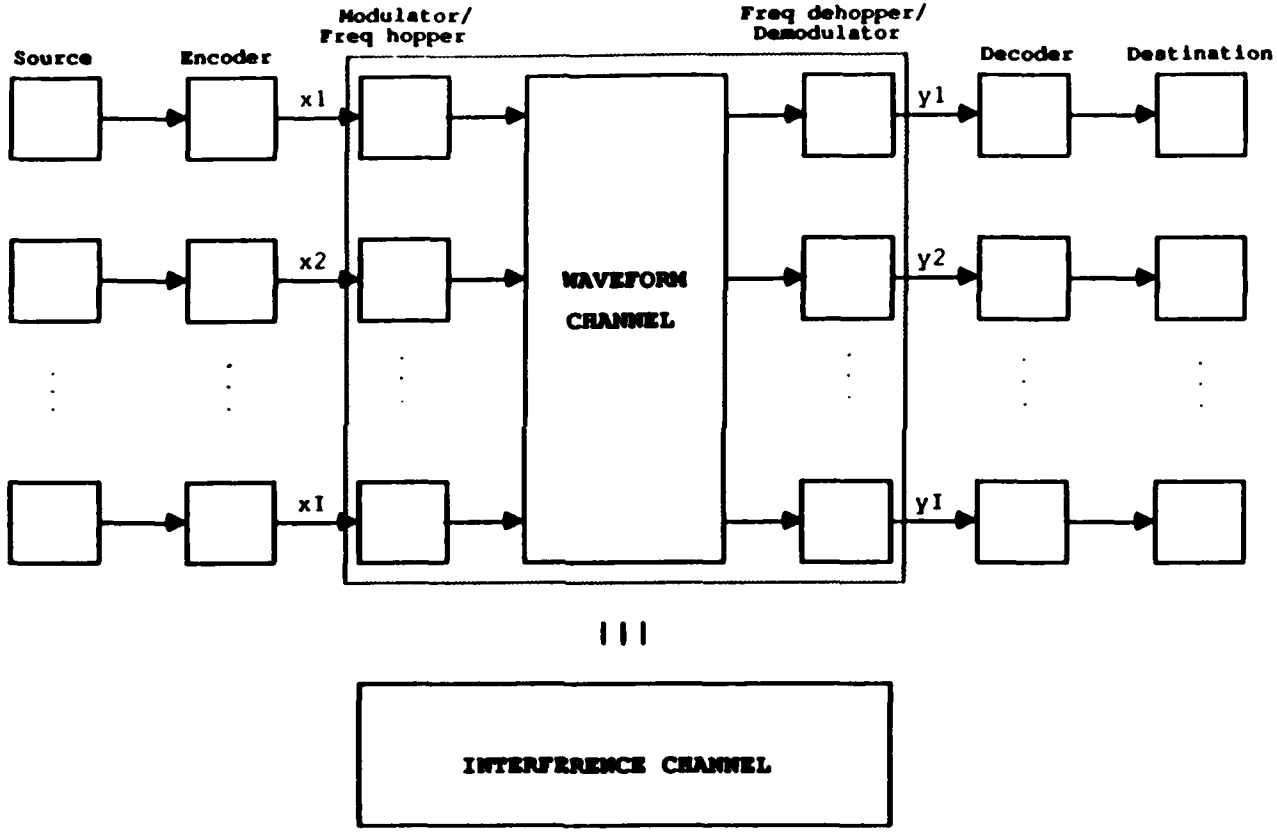

Figure 1.1: *I*-user channel model.

the communication system from the modulator input to the demodulator output as an I-user interference channel [Gam 80].

We assume that each receiver is able to hear the transmissions of each of the I transmitters. Each receiver does not attempt to dehop and demodulate signals other than its own. The signal of each user is, however, present in the front end of each receiver and is a potential source of interference. An example of this is a satellite multiple access broadcast system or a fully connected network. Thus the interference traffic level will be the same at each receiver in the network, which makes the component channels for all user pairs be identical. We thus assume that exactly the same code is used for all user pairs in the network.

The users are assumed to transmit data in fixed-length packets, and the packet may consist of several codewords. In this thesis we will assume that a "packet" consists of exactly one codeword from the code. This provides us with a natural definition of a "successfully transmitted packet": A packet is declared successfully transmitted if the number of errors and/or erasures occuring due to multi-user interference is within the errors-and-erasures correcting capability of the code.

In our model of a frequency-hop radio network, there is a band of q frequency slots available and each user pair has a frequency hopping pattern that randomly hops among all q frequency slots with probability $1/q$ for each slot independent of previous hop frequencies (i.i.d. hopping). In each hopping time-slot, N_b code symbols are transmitted using a common type of modulation whose spectrum falls within the specified frequency slot. In general, frequency hopping for the terminals in the network can be either synchronous or asynchronous. The requirement for *synchronous* frequency hopping is that the hop intervals from all of the transmitters in the network must be aligned at each receiver in the network. The term *asynchronous* frequency hopping is reserved for the situation where

this requirement is not met. We also assume that packet time slotting is employed, that is, time is divided into intervals called packet (time) slots, and each packet transmission must take place wholly within a packet slot. The conditions required for slotted transmission are much less strict than the requirements for synchronous frequency hopping: Because the packet slot size is typically one to three orders of magnitude greater than the hop size (hop duration time), it is considerably easier to implement a slotted packet transmission system than to synchronize the frequency hopping among all of the terminals in the network. In particular, a guard time of a few percent of the packet length is sufficient to permit slotted operation in the packet radio network, and therefore represents a small degree of added overhead.

Whenever two or more code symbols from different radios are transmitted simultaneously in the same frequency slot, we say a "hit" occurs. Suppose two packets are transmitted in the same packet slot on two different hopping patterns, and consider a single symbol from one of them. The probability that the other packet has symbol transmitted in the same frequency slot at any time during the transmission interval for that symbol is called the probability of a hit and is denoted by p_h. It is known that p_h can be calculated as [Ger 82]

$$p_h = \begin{cases} \frac{1}{q}\left[1 + \frac{1}{N_b}(1 - \frac{1}{q})\right], & \text{asynchronous frequency hopping} \\ \frac{1}{q}, & \text{synchronous frequency hopping,} \end{cases} \tag{1.1}$$

where N_b is the number of code symbols per hop. If there are I simultaneous transmissions, the probability of a particular symbol being hit is

$$p_{h,I} = 1 - (1 - p_h)^{I-1}. \tag{1.2}$$

Since each receiver can hear the transmissions of all I transmitters, the probability of a particular symbol being hit will be the same at all receivers, namely $p_{h,I}$. We will assume that the background noise power is small compared with

the signal power, so that when there is no interference at a particular hop, the data is correctly received.

1.3. Previous Work

Studies of the multiple-access capability of frequency-hop spread-spectrum communication systems have begun quite recently. Geraniotis and Pursley [Ger 82] have obtained the (uncoded) bit error probability in an asynchronous frequency-hop SSMA communication system. Soon after, the use of frequency-hopping, M-ary modulation, and Reed-Solomon coding in a multiple-terminal communication system was considered in [Haj 82], [McE 82], [Pur 81a]. In particular, Hajek [Haj 82], [Pur 81a] have evaluated the throughput of frequency-hopped communications with error-correction coding for a Poisson traffic model. Musser and Daigle [Mus 82] derived the throughput of an unslotted code division multiple access (CDMA) network with fixed length packets. Pursley [Pur 83a] examined the improved multiple-access capability available through the use of frequency-hopping with side information and erasure-correction. In [Pur 84] he also evaluated error probabilities and local throughput of the frequency-hop radio networks which incorporate the standard slotted and unslotted ALOHA channel-access protocols, and Reed-Solomon error-control coding. Hegde and Stark [Heg 85] considered the multiple-access capability of frequency-hop spread-spectrum communication from an information theoretic (capacity) point of view. It was shown that there is an optimal number of users that maximizes the total information being reliably transmitted.

Spread-spectrum network protocols have been discussed in the literature [Pur 83b], [Sil 84], [Sou 84], [Wie 82], but the design and analysis of these protocols are still an active area of basic research, and several problems remain un-

solved. Raychaudhuri [Ray 81] presented analytical techniques for performance evaluation (such as steady-state throughput, delay) of slotted ALOHA CDMA systems. In [Wie 83], [Wie 86] a distributed reservation scheme for SSMA channels has been introduced and analyzed.

1.4. Thesis Outline

In this section we briefly outline the remaining chapters of this thesis. In chapter II, several performance measures of the multiple-access capability which are to be discussed throughout this thesis are stated. Those are the channel capacity, the achievable region, and the throughput. In brief, the channel capacity is the maximum average amount of information that can be transmitted over the channel with the best possible code. The achievable region is the set of all code rate, channel traffic pairs such that it is possible to have the packet (codeword) error probability to be less than a desired error probability. The throughput is the average number of successful transmissions that can take place within the range of a given receiver.

Chapter III is concerned with the multiple-access capability of a frequency-hop packet radio network which utilizes Reed-Solomon coding. Reed-Solomon (RS) codes are employed to correct the errors and/or erasures occurring due to multi-user interference. If the receiver can detect the presence of interference in the same frequency slot in which the signal of interest is present (side information) and erase the corrupted channel symbols, the unique erasure-correcting capability of the RS codes can be exploited. In general, an (n, k) RS code can correct up to $e \triangleq n - k$ erasures out of n symbols or up to $t \triangleq \lfloor (n-k)/2 \rfloor$ errors out of n symbols: this is the best value of e and t that can be achieved by any code of the same block length and rate. This is often a strong justification for

using RS codes. For both the perfect side information and no side information cases, we derive the achievable regions of code rate and channel traffic, and the optimal code rate and optimal channel traffic at which the normalized throughput is maximized. From these optimum points we derive the maximum possible throughputs, and compare them with the corresponding channel capacities. It is found that for the perfect side information case, the maximum sum capacity (defined in section 2.2) is achieved by the optimal rate RS code with bounded distance decoding. However it is shown that the maximum (normalized) throughput achievable without side information is only 39.3% (worst case) of that achievable with perfect side information. The loss in using Reed-Solomon codes in a no side information environment is partially due to the use of a non maximum likelihood decoder (i.e., bounded distance decoder).

In chapter IV, we investigate a technique for obtaining the side information. This is done by partitioning the data stream into blocks, encoding each block using an error-detecting code, and transmitting the encoded block (codeword) during a single hop. On the basis of the received version of the codeword the decoder makes a statistical decision about which of the channel states (*hit* or *no hit*) each codeword was transmitted over. Clearly, as the rate of the error-detecting code decreases, the error detection capability increases, therefore the reliability of side information obtained will increase. However, decreasing the code rate implies a decrease in the efficient use of the channel. An interesting question that arises from this discussion is "How does the reliability of the side information change as the code rate changes?", or "What is the maximum allowable code rate to obtain a certain reliability of the side information?". In this chapter we give the answer to the above question for both the synchronous and asynchronous frequency-hopping systems.

The combination of encoder, channel, and decoder generates in general an

errors-and-erasures channel. The above encoder and decoder will be called later as *inner encoder* and *inner decoder* respectively. We employ an *outer code* to correct the errors (caused by undetected errors) and the erasures (caused by detected errors). In this way the inner decoder informs the outer decoder which symbols (inner codewords) in the received packet have been hit by symbols from other packets in the same time slot. We find that the normalized throughput achievable with perfect side information can indeed be achieved through the use of this *concatenated* coding scheme, even though the channel provides no side information. This chapter ends by evaluating the performance of diversity / RS code as an example of the concatenated coding schemes.

In chapter V, we consider the performance of frequency-hopping multiple-access systems which have *imperfect* side information at the demodulator. In fact, perfect side information and no side information are special cases of the imperfect side information. When imperfect side information is available at the demodulator, its output is, in general, a sequence of errors, erasures, and correct symbols. In order to correct the errors and erasures we employ a Reed-Solomon code, and consider two different decoders for it: one is the errors-and-erasures decoder and the other is a parallel decoder. We first evaluate the performance of errors-and-erasures decoder and discuss an idea for improving the performance. Based on this idea we suggest a parallel decoding scheme and evaluate the performance of it over the imperfect side information channel.

Finally in chapter VI, conclusions are made.

CHAPTER II

PERFORMANCE MEASURES

2.1 Introduction

Up to now our characterization of the performance of frequency-hop multiple access systems has been qualitative. In this chapter, this characterization is made more precise by examining specific quantitative performance measures: these are the capacity region, the achievable (rate, traffic) region, and the throughput. Such measures not only are needed for analytical and numerical comparisons of the effectiveness of different multiple access systems, but are also used in optimizing the performance of a given multiple access system. In the latter case, the performance measure acts as the objective function in the problem of selecting the best system parameter values and/or operational modes.

2.2 The Interference Channel

The I-user interference channel has I transmitters and I receivers. Transmitter j wishes to send information to receiver j. He does not care what other receivers receive or understand. It is not quite a broadcast channel because

there is only one intended receiver for each transmitter, nor is it a multiple access channel because each receiver is only interested in what is being sent by the corresponding transmitter.

The I-user interference channel is characterized, in general, by $(X_1 \times X_2 \times \cdots \times X_I,\ P(y_1, y_2, \cdots, y_I \mid x_1, x_2, \cdots, x_I),\ Y_1 \times Y_2 \times \cdots \times Y_I)$ consisting of $2I$ finite sets $X_1, X_2, \cdots, X_I, Y_1, Y_2, \cdots, Y_I$ and a collection of conditional probability distributions $P(\cdot, \cdot, \cdots, \cdot \mid x_1, x_2, \cdots, x_I)$ on $Y_1 \times Y_2 \times \cdots \times Y_I$, one for each vector $(x_1, x_2, \cdots, x_I)$ where $x_1 \in X_1, x_2 \in X_2, \cdots, x_I \in X_I$. Here $x_1, x_2, \cdots, x_I$ are inputs to the channel and $y_1, y_2, \cdots, y_I$ are outputs from the channel (see Figure 1.1). In our interference channel model, $X_1 = X_2 = \cdots = X_I$ and $Y_1 = Y_2 = \cdots = Y_I$.

Using Sato's terminology [Sat 77], if the marginal transition probabilities $P(y_j \mid x_1, x_2, \cdots, x_I)$, do not depend on x_i, $i \neq j$, i.e.,

$$P(y_j \mid x_1, x_2, \cdots, x_I) = P(y_j \mid x_j), \quad j = 1, 2, \cdots, I, \tag{2.1}$$

then the interference channel is called "separated". The interference channels created by a specific frequency-hopping modulation will be characterized by the marginal transition probabilities $P(y_j \mid x_1, x_2, \cdots, x_I)$, $j = 1, 2, \cdots, I$. We will show later how the marginal transition probabilities depend on the frequency-hopping modulation (e.g. number of frequency slots, hopping pattern) and availability of side information. If the interference channel is separated, the individual channels characterized by $P(y_j \mid x_j)$ are called "component" channels. In our model the component channels for all user pairs are identical.

2.3 Capacity Region

In general, by the "capacity region" of any interference channel, one means the set of all joint user rates such that it is possible to communicate with arbitrarily

small error probability at any joint rate inside this set, but it is impossible to do so at any joint rate outside this set. To define the capacity region for such channels precisely, it is convenient to make use of the concept of the "achievable rate". An $((M_1, M_2, \cdots, M_I), n)$ code for an I-user interference channel consists of I sets of integers called the message set

$$\mathbf{M}_j = \{1, 2, \cdots, M_j\}, \quad j = 1, 2, \cdots, I, \tag{2.2}$$

I encoding functions

$$f_j : \mathbf{M}_j \rightarrow X_j^n, \quad j = 1, 2, \cdots, I, \tag{2.3}$$

and I decoding functions

$$g_j : Y_j^n \rightarrow \mathbf{M}_j, \quad j = 1, 2, \cdots, I. \tag{2.4}$$

Assuming an uniform distribution over the product message sets $\mathbf{M}_1 \times \mathbf{M}_2 \times \cdots \times \mathbf{M}_I$, i.e., that the messages are independent and equally likely, we define the "average probability of error" for the j^{th} channel to be

$$P_j^{(n)}(e) = \frac{1}{M_1 \cdots M_I} \sum_{(m_1, \cdots, m_I) \in \mathbf{M}_1 \times \cdots \times \mathbf{M}_I} P(\, g_j(\mathbf{y}_j) \neq m_j \mid (m_1, \cdots, m_I) \text{ sent}), \tag{2.5}$$

where $\mathbf{y}_j \in Y_j^n$.

We define the rate vector $(r_1, r_2, \cdots, r_I)$ of an $((M_1, M_2, \cdots, M_I), n)$ code by

$$r_j = \frac{\log_2 M_j}{n}, \quad j = 1, 2, \cdots, I. \tag{2.6}$$

The rate vector $(r_1, r_2, \cdots, r_I)$ is said to be *achievable* by an I-user interference channel if, for any $\epsilon > 0$ and for all n sufficiently large, there exists an $((M_1, M_2, \cdots, M_I), n)$ code with

$$M_1 \geq 2^{nr_1}, \;\; M_2 \geq 2^{nr_2}, \;\; \cdots \;\; , M_I \geq 2^{nr_I},$$

such that

$$P_1^{(n)}(e) < \epsilon, \;\; P_2^{(n)}(e) < \epsilon, \;\; \cdots, \;\; P_I^{(n)}(e) < \epsilon.$$

The *capacity region* of the I-user interference channel is defined as the set of all achievable rate vectors in the $(r_1, r_2, \cdots, r_I)$-space.

Notice that the notions of achievable rates and capacity region depend only on the marginal transition probabilities of the channel, $P(y_j \mid x_1, x_2, \cdots, x_I)$, and not directly on the joint conditional probability $P(y_1, y_2, \cdots, y_I \mid x_1, x_2, \cdots, x_I)$. This is because the average probability of error $P_j^{(n)}(e)$ $(j = 1, 2, \cdots, I)$ depends only on the corresponding marginal probability

$$P_j(y_j \mid x_1, x_2, \cdots, x_I) = \sum_{y_k, k \neq j} P(y_1, y_2, \cdots, y_I \mid x_1, x_2, \cdots, x_I). \tag{2.7}$$

From this, we can conclude that the capacity region is the same for all I-user channels that have the same marginal probabilities.

The capacity region for the interference channel is not, in general, known, but various inner and outer bounds have been developed for it [Ahl 71], [Sat 77]. However, if the channel is *separated*, i.e.,

$$P_j(y_j \mid x_1, x_2, \cdots, x_I) = P_j(y_j \mid x_j), \quad j = 1, 2, \cdots, I, \tag{2.8}$$

then using the properties given in [Sat 77] it can be shown that the inner bounds and the outer bounds coincide, thus giving us the capacity region:

$$\{(r_1, r_2, \cdots, r_I) \; : \; 0 \leq r_j < C_j(I)\}, \tag{2.9}$$

where

$$C_j(I) = \max_{Q_j} I(X_j; Y_j) \tag{2.10}$$

is the capacity of the j^{th} component channel which is described by $(X_j, P(y_j|x_j), Y_j)$. This implies that the capacity regions of the separate interference channel are determined by the individual channel parameters only. Reducing the rate of one user is of no benefit to other users.

The sum capacity, $C_{sum}(I)$, is defined as the largest possible total rate that

can be achieved by all users, and if the channel is separated

$$\begin{aligned} C_{sum}(I) &= \max_{Q_1 \cdots Q_I} \sum_{j=1}^{I} I(X_j ; Y_j) \\ &= \sum_{j=1}^{I} \max_{Q_j} I(X_j ; Y_j) \\ &= \sum_{j=1}^{I} C_j(I). \end{aligned} \tag{2.11}$$

2.4 Achievable Region

In the previous section we have considered the performance achievable with the best possible codes, i.e., the capacity region. The coding theorem guarantees the existence of codes, but does not provide any criteria for construction or selection of such codes. The capacity region is a property of a channel. This section and the next section are focused on a coding viewpoint. We assume that all encoders have same rate and are identical. We first consider an achievable region of a family of interference channels with a family of codes. The achievable region is defined as the set of all code rate (r), channel traffic (I) pairs such that there exists a code with rate r and codeword error probability less than some desired value, $\hat{P}_E$, for I users (packet transmissions). The codeword error probability is the probability of the number of errors and erasures occuring in the received sequence being greater than the correcting capability of the code. The set of all (r, I) such that the codeword (packet) error probability is less than $\hat{P}_E$ is the "$\hat{P}_E$ achievable region". The requirement for $\hat{P}_E$ on the individual links is closely coupled to the system delay: a larger packet error probability implies that a larger number of retransmissions will be required, and this implies increased delay.

The effectiveness of a class of coding schemes on a given channel (i.e., given I) can be measured by letting the code length become sufficiently large and comparing the resulting maximum possible (maximized over all codes in a specific class)

code rate for the codeword error probability to be less than an arbitrarily small constant with the absolute maximum rate, i.e., the capacity. Many people have been searching for practical realization of Shannon's promises, but the search has been difficult and only partially completed. In fact, the problem of finding an explicitly constructable, practical sequence of codes for which the probability of error approaches zero for all rates less than the capacity region remains open in general.

2.5 Throughput

Throughput is a widely-accepted performance measure for a satellite packet broadcasting system [Kle 76]. Basically, it is intended to be a measure of the information flow in the neighborhood of an arbitrary terminal in the network. It is defined as the average number of successful packet transmissions that can take place simultaneously within the range of a given receiver. If the network is homogeneous in the sense that the interference traffic is the same at each receiver, the codeword (packet) error probability given I simultaneous transmissions, $P_E(I)$, is the same for each packet, and the unnormalized throughput given I simultaneous transmissions, $S(I)$, is the number of transmissions times the probability of success; that is,

$$S(I) = I \cdot (1 - P_E(I)). \tag{2.12}$$

Notice that this throughput measure does not distinguish between packets according to their destination. It is a measure of the multiple-access capability of the modulation and coding technique which is divorced from the particular protocols being used in the network. A packet is correctly received if the number of errors and erasures it encounters is within the correction capability of the code.

In order to make valid comparisons between frequency-hop and narrowband

radio networks, it is necessary to normalize $S(I)$ to give throughput per unit bandwidth. If the code has rate r and the number of frequency slots is q, the normalized throughput at traffic level I is

$$\begin{aligned} W(I) &= rS(I)/q \\ &= rI(1 - P_E(I))/q; \end{aligned} \tag{2.13}$$

this is the total amount of information being reliably sent over the network per unit time per unit bandwidth. As the code rate decreases, the amount of bandwidth required (for fixed q and information bit rate) increases so that the normalization factor, r/q, decreases. However, the smaller the code rate the greater the error and erasure correcting capability of the code. The larger error and erasure correcting capability of the code tends to increase the unnormalized throughput. These two competing factors cause there to be an optimum code rate that maximizes the normalized throughput. Alternatively we can imagine that for fixed q as the number of transmitter-receiver pairs increase there will be a decrease in the reliability of the information being transmitted. This is because the chances of more than one user hopping to the same frequency slot, i.e. the probability of a hit, are larger for larger I. On the other hand as the number of user pairs increases, the total amount of information being transmitted is increasing. From this discussion one is led to believe that for a fixed q there will be an optimum number of users simultaneously transmitting that maximizes the normalized throughput. The values of I and r for which $W(I)$ is maximized is denoted by I_{opt} and r_{opt} respectively. For frequency-hop radio networks with error-control coding, the value of I_{opt} depends on the code and the bandwidth used by the spread spectrum, but it is typically much larger than one. The value of r_{opt} depends on the number of users simultaneously transmitting and the bandwidth used by the spread spectrum. From these two optimum values we can derive the maximum possible normalized throughput W_{max}.

CHAPTER III

REED-SOLOMON CODES

3.1 Introduction

An important and popular subclass of nonbinary BCH codes is the class of Reed-Solomon codes often abbreviated as RS codes [Cla 82], [Bla 83]. They are BCH codes over GF(M) with the special property that the block length n is $M-1$, M, or $M+1$, where M is a power of a prime. Besides serving as illuminating examples of BCH codes, they are of considerable practical and theoretical importance. They are convenient for building other codes, either alone or in combination with other codes, as in concatenated codes which will be discussed in chapter IV. In this chapter we investigate the achievable region and the throughput for the family of interference channels generated by our spread-spectrum frequency-hopping model of Chapter I, when only RS codes are used.

An important property of any (n, k) RS code is that the minimum distance is given by

$$d_{min} = n - k + 1, \tag{3.1}$$

where n is the block length and k is the number of information symbols in each block. A code for which the minimum distance equals $n-k+1$ is called a

maximum-distance-separable (MDS) code. Therefore, every RS code is an MDS code and is optimum in the sense of the Singleton bound [Bla 83]. This means that for fixed n and k, no code can have a larger minimum distance than a RS code. This is often a strong justification for using RS codes. Furthermore, it can be readily verified that shortening the block length of a RS code by omitting information symbols can not reduce its minimum distance, and therefore any shortened RS code is also an MDS code.

Another important property of a RS code is the fact that any k positions in the codeword may be used as an information set. That is, given an (n, k) RS code over GF(M), for any k symbol positions there will be one and only one codeword corresponding to each of the M^k assignments in those k positions. An important and very useful consequence of this property is that it enables one to write down the exact weight distribution for any RS code. The weight distribution $\{A_j\}$ for a RS code or any MDS code defined over GF(M) having block length n and minimum distance d_{min} is given by

$$A_j = \binom{n}{j} (M-1) \sum_{l=0}^{j-d_{min}} (-1)^l \binom{j-1}{l} M^{j-d_{min}-l}, \qquad (3.2)$$

for $d_{min} \leq j \leq n$. Derivation of this weight distribution formula can be found in Forney [For 66], Berlekamp [Ber 68], Peterson and Weldon [Pet 72].

From the above minimum distance property, an (n, k) RS code with bounded distance decoding will correct up to $e \triangleq n - k$ erasures out of n symbols or up to $t \triangleq \lfloor (n-k)/2 \rfloor$ errors out of n symbols. More generally, it will correct any combination of ϵ erasures and τ errors provided that $2\tau + \epsilon$ does not exceed $n - k$.

3.2 Perfect Side Information

Since the RS code can correct twice as many erasures as errors, it can be

expected that the multiple-access capability of frequency-hop packet radio networks is considerably enhanced if the receiver can determine which symbols in the packet have been hit. This information, typically called side information, is used in the demodulator and decoder to improve error control. The received symbols that have been hit by other transmissions are erased in order to take advantage of the powerful erasure correction capability of RS codes. An (n, k) RS code can correct any pattern of $n - k$ or fewer erasures.

We consider the spread-spectrum frequency-hopping model described in Chapter I. If there are I users transmitting, we model it as an I user interference channel. We assume that the background noise is negligible compared to the signal power and perfect side information is available to the demodulator and decoder. However, these assumptions will be relaxed in chapter V. The main purpose of the present section is to examine the improved multiple-access capability available through the use of frequency-hopping with perfect side information and erasure correction.

3.2.1 Assumption 1: No Discrimination Against Partially Overlapping Interference

We assume first that all symbols that have been hit, even if only partially overlapping in time (due to the asynchronous nature of frequency hopping process), are detected and erased. When there are I simultaneous users the probability that a particular symbol is hit is given by $p_{h,I}$ (see (1.2)), The marginal transition probability in this case is given by

$$P(y_j|x_1, x_2, \cdots, x_I) = \begin{cases} 1 - p_{h,I}, & y_j = x_j \\ p_{h,I}, & y_j = ?. \end{cases}$$

Since the j^{th} channel output does not depend on the symbols transmitted from other users, the interference channnel is separated. The component channel

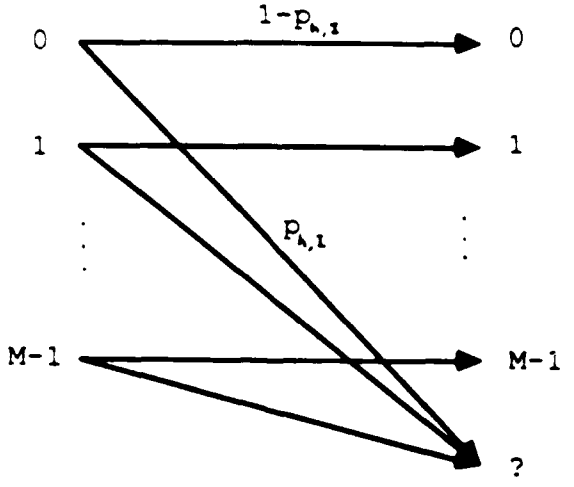

Figure 3.1: M-ary erasure channel.

model (seen by each user pair) will be an M-ary erasure channel with erasure probability equal to $p_{h,I}$ as shown in Figure 3.1.

Achievable Region

A given codeword (packet) is correctly received if the number of erasures does not exceed the erasure-correction capability of the RS code. By the memorylessness of the random hopping pattern, the hits at different hop durations are conditionally independent given I. Thus the probability of correct codeword for a bounded distance decoder given I simultaneous transmissions, $P_c(I)$, is given by

$$P_c(I) = \sum_{j=0}^{n-k} \binom{n}{j} p_{h,I}^j (1 - p_{h,I})^{n-j}. \tag{3.3}$$

Asymptotically, as n and k approach infinity while the code rate, $r \triangleq k/n$, is

held constant, it can be shown (see Appendix A) that

$$\lim_{n,k\to\infty} P_e(I) = \begin{cases} 1, & 1-r > p_{h,I} \\ 0.5, & 1-r = p_{h,I} \\ 0, & 1-r < p_{h,I}. \end{cases} \tag{3.4}$$

This implies that "error-free" communication is possible asymptotically provided that the code rate is less than $1 - p_{h,I}$, i.e.,

$$r < (1-p_h)^{I-1}, \tag{3.5}$$

or equivalently

$$I < 1 + \frac{\ln(r)}{\ln(1-p_h)}. \tag{3.6}$$

This represents an asymptotic $(n, k \to \infty)$ achievable region of I and r for arbitrarily small error probability with perfect side information. The limiting value for the asymptotic achievable region as both the number of users and the number of frequency slots get large (i.e., $I, q \to \infty$ with $\lambda \triangleq I/q$ held constant) is given by

$$r < e^{-\eta\lambda}, \tag{3.7}$$

or

$$\lambda < \frac{1}{\eta}\ln(\frac{1}{r}), \tag{3.8}$$

where

$$\eta = \begin{cases} 1, & \text{synchronous frequency hopping} \\ 1 + \frac{1}{N_h}, & \text{asynchronous frequency hopping.} \end{cases} \tag{3.9}$$

It can be easily shown that the capacity of the component channel shown in Figure 3.1 is given by

$$\begin{aligned} C(I) &= 1 - p_{h,I} \\ &= (1-p_h)^{I-1}, \end{aligned}$$

which is the same as the right hand side of (3.5). This implies that the capacity of the channel with perfect side information can be achieved by the Reed-Solomon code.

Now we consider the achievable region for finite block length Reed-Solomon codes. We want to find the maximum number of simultaneous transmissions (or channel traffic) and the maximum code rate for the packet error probability to be less than $\hat{P}_E$ when Reed-Solomon codes of finite block length are used to correct the erasures due to the multi-user interferences. Unfortunately it is very difficult to derive the exact maximums analytically, because (3.3) is a complicated function of I and k. However, we can derive a simple approximation to the maximum channel traffic and code rate as follows. If we apply the Demoivre-Laplace theorem [Pap 65] to (3.3), we can get an approximation

$$P_c(I) \approx F\left(\frac{n-k-np_{h,I}}{\sqrt{np_{h,I}(1-p_{h,I})}}\right), \tag{3.10}$$

where

$$F(x) \triangleq \int_{-\infty}^{x} (2\pi)^{-\frac{1}{2}} e^{-u^2/2} du.$$

By combining (3.10) with the constraint, $P_E(I) \triangleq 1 - P_c(I) \leq \hat{P}_E$, we obtain

$$r \leq 1 - p_{h,I} - \alpha\sqrt{p_{h,I}(1-p_{h,I})/n} \tag{3.11}$$

or equivalently

$$I \leq 1 + \frac{\ln(A)}{\ln(1-p_h)} \tag{3.12}$$

where

$$\alpha \triangleq F^{-1}(1-\hat{P}_E)$$
$$A \triangleq \frac{2nr+\alpha^2+\alpha\sqrt{4nr(1-r)+\alpha^2}}{2(n+\alpha^2)}.$$

Figure 3.2 shows the achievable regions of I and r for $P_E(I) \leq 10^{-2}$ with Reed-Solomon codes of length 32 and 256 and also the asymptotic achievable regions for arbitrarily small error probability with perfect side information. We see that the exact values and the approximations are very close, where the exact values have been obtained by computer search.

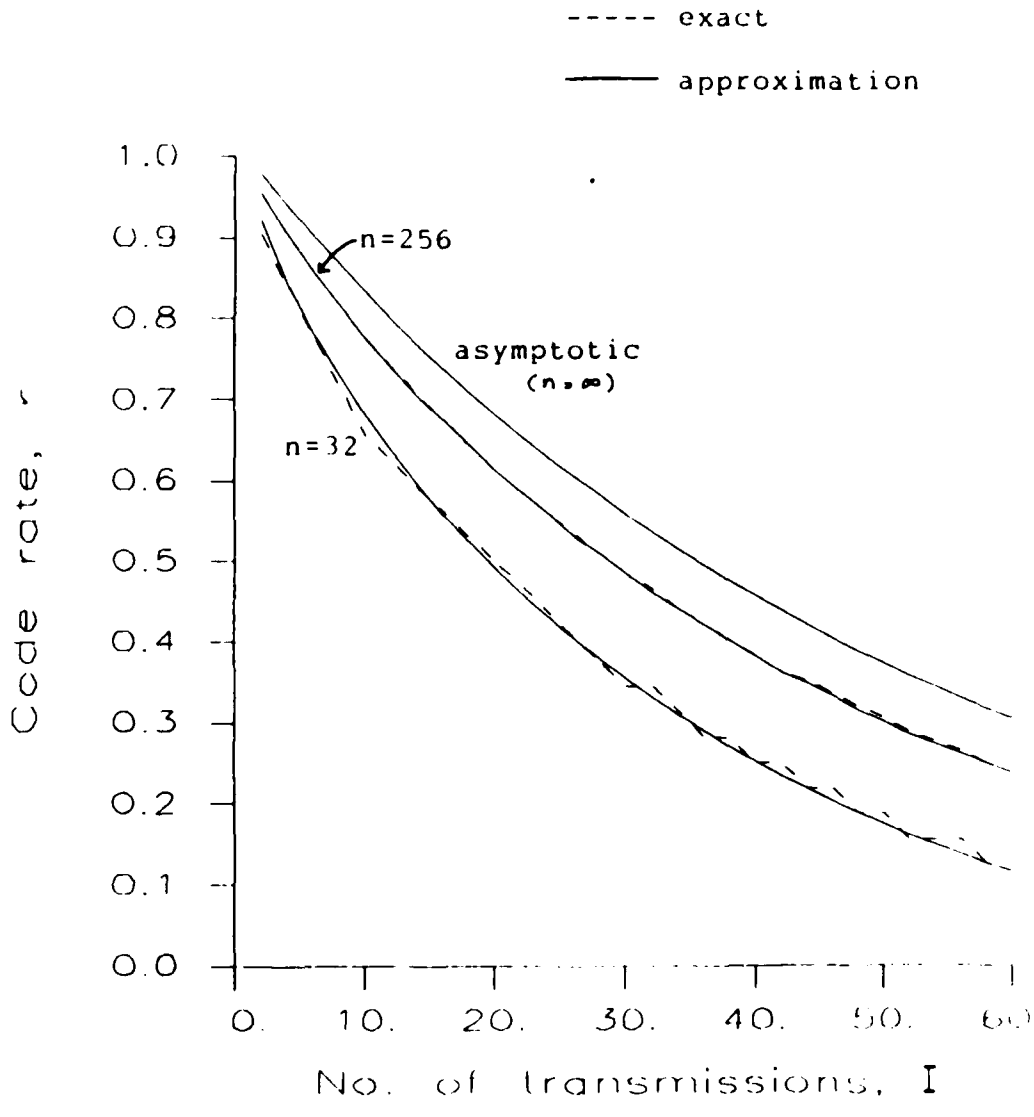

Figure 3.2: Achievable regions of (r, I) for $P_E(I) \leq 10^{-2}$ and the asymptotic achievable region, perfect side information, $q = 100$, η=2.

When there is a distribution on the number of packet transmissions (Poisson with mean G), we have the average probability of correct decoding, P_C, given by

$$P_C = \sum_{I=0}^{\infty} P_c(I+1) f(I), \tag{3.13}$$

where

$$f(I) = G^I e^{-G}/I!.$$

It is shown in [Pur 84] that as G and q approach infinity while $\mu \triangleq G/q$ is held constant,

$$P_C = \sum_{j=0}^{n-k} \binom{n}{j} (1-e^{-\eta\mu})^j (e^{-\eta\mu})^{n-j}, \tag{3.14}$$

where η is given by (3.9). By applying the Gaussian approximation of (3.14) to the constraint, $P_E \triangleq 1 - P_C \leq \hat{P}_E$, we obtain

$$r \leq e^{-\eta\mu} - \alpha\sqrt{e^{-\eta\mu}(1-e^{-\eta\mu})/n}, \tag{3.15}$$

or equivalently

$$\mu \leq \frac{1}{\eta} \ln(1/A). \tag{3.16}$$

Equations (3.11) and (3.12) will be especially useful for the use of *adaptive* transmissions and coding techniques. The idea is to observe the channel and respond to an unfavorable channel (e.g. heavy traffic) by controlling the channel traffic level (restricting the number of packet transmissions according to (3.12)) or by improving the error-correction capability of the system (reducing the code rate according to (3.11)) such that the packet error probability on the individual communication links is less than some desired value, $\hat{P}_E$. Estimation of channel traffic is fairly easy to implement in a frequency-hop radio network [Pur 83a]. Perhaps the simplest estimate of channel traffic is the number of frequency slots that have signal strengths above a certain threshold. Another alternative is to monitor a few of the frequency slots and count the number of times signals are present on these slots during a few hop periods.

Throughput

For a system employing an (n, k) code and q frequency slots, the normalized throughput given I simultaneous transmissions is given by

$$W = \frac{k}{nq} I P_c(I). \tag{3.17}$$

The asymptotic normalized throughput as n and k approach infinity while $r \triangleq k/n$ is held constant can be obtained by using (3.6) and (3.17) as

$$\lim_{n,k\to\infty} W = \frac{r}{q}\left(1 + \frac{\ln(r)}{\ln(1-p_h)}\right). \tag{3.18}$$

This means that the asymptotic normalized throughput approaches *arbitrarily close* to the RHS of (3.18). The unit of the above normalized throughput is information symbols per channel use per frequency slot. To change it to information bits per channel use per dimension, it must be multiplied by $\log_2 M/D$, where D is the dimensionality of the signal set per frequency slot. In all that follows we will consider the former unit: information symbols per channel use per frequency slot.

By optimizing over r, we get the optimum code rate, r_{opt}, given by

$$r_{opt} = e^{-1}(1-p_h)^{-1}, \tag{3.19}$$

which for reasonable values of q is very close to e^{-1}. This asymptotic optimal code rate also seems to give a very good approximation to the optimal code rate for finite length codes, even the length 32 codes. We can see from Figures 3.3 and 3.4 that the maximum normalized throughput is obtained by the (32,12) code and (256,94) code: but the optimum values of k obtained from the asymptotic optimum code rate, e^{-1}, are $32 \times e^{-1} = 11.77$ and $256 \times e^{-1} = 94.18$, which are very close to the exact optimum values of k, namely 12 and 94 respectively. At

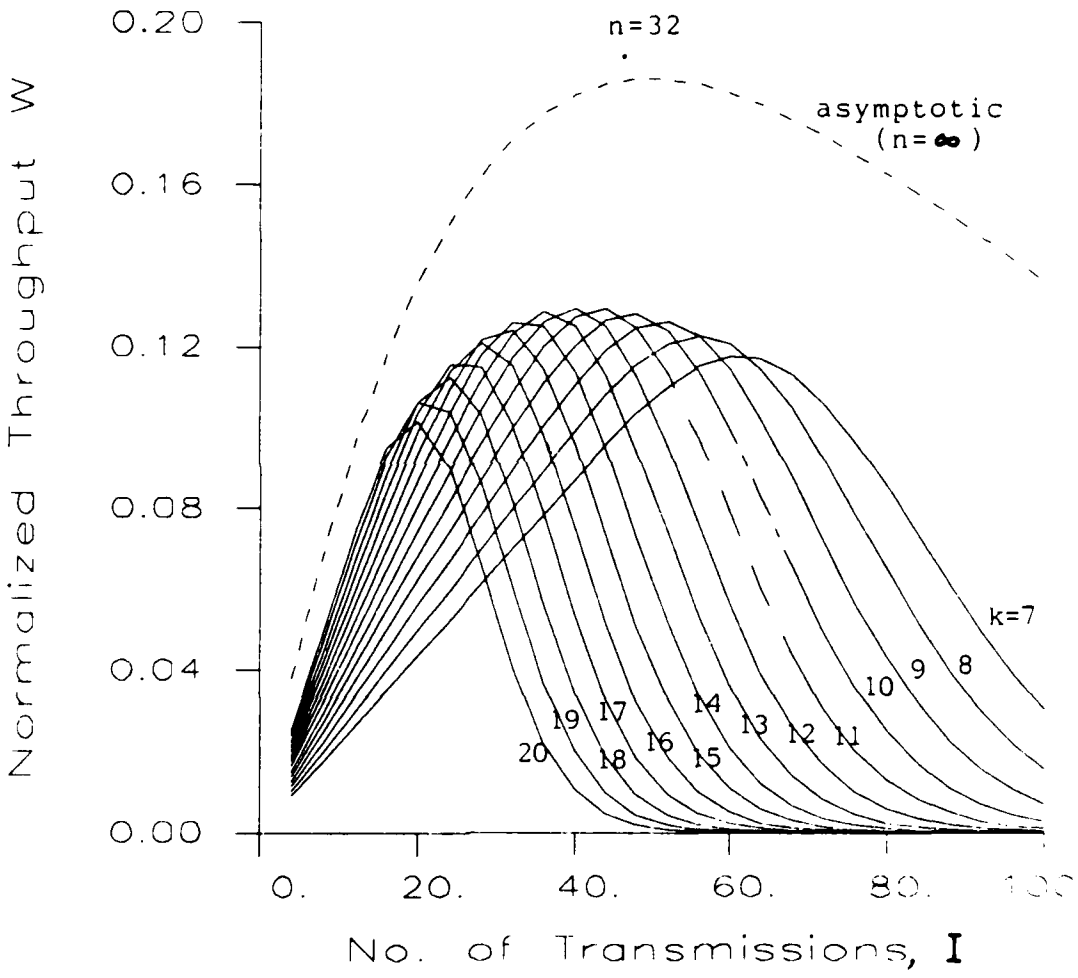

Figure 3.3: Normalized throughputs, perfect side information, $q = 100$, $n = 32$, η=2.

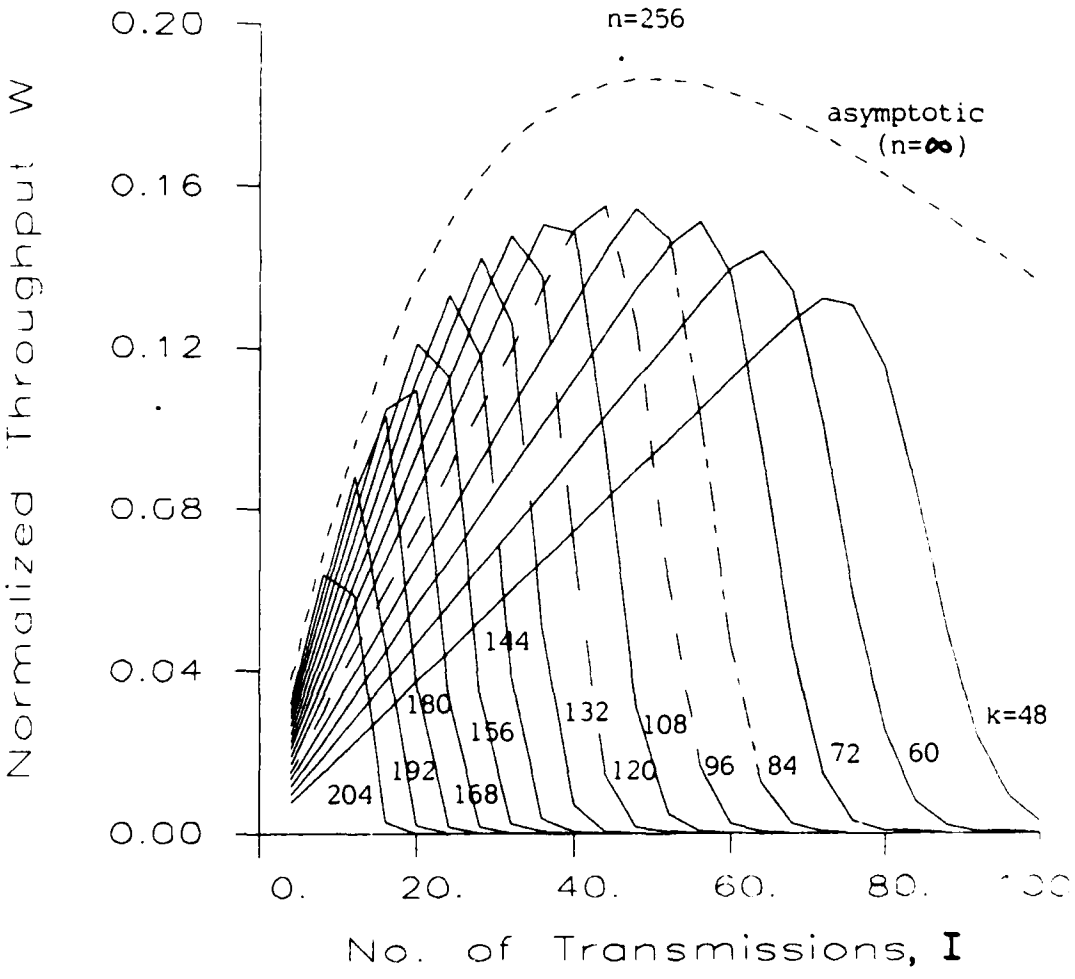

Figure 3.4: Normalized throughputs, perfect side information, q = 100, n = 256, η=2.

this optimum code rate the optimum number of transmissions is given by

$$I_{opt} = [\ln(1 - p_h)^{-1}]^{-1}, \tag{3.20}$$

thus the limiting optimum value of the channel traffic per frequency slot, $\lambda \triangleq I/q$, is

$$\lambda_{opt} = \eta^{-1}, \tag{3.21}$$

as $q \rightarrow \infty$. At r_{opt} and I_{opt} the maximum possible throughput, W_{max} becomes

$$W_{max} = 1/[qe(1 - p_h)\ln(1 - p_h)^{-1}], \tag{3.22}$$

which approaches e^{-1}/η for large enough q. This is also the asymptotic sum capacity of the interference channel with perfect side information in information symbols per channel use [Haj 83], [Heg 85]. Therefore it can be concluded that if perfect side information is available, the asymptotic sum capacity is achieved by the optimal rate Reed-Solomon code with bounded distance decoding. However, this is not true if side information is not available as we will see in section 3.3.

Comparisions With Narrowband Slotted ALOHA System

For Poisson traffic model (the number of packet transmissions in a time slot is given by a Poisson random variable) and slotted ALOHA [Tan 81] without frequency hopping, the optimum average number of transmissions attempted per time (packet) slot is 1. The throughput at this traffic level is e^{-1}, and the resulting packet error probability is $1-e^{-1}$ which is approximately 0.632 [Abr 70], [Tan 81].

For frequency-hop radio networks with error-control coding (RS code with perfect side information) and Poission traffic, the normalized throughput can be

derived as

$$\begin{aligned} W &= \tfrac{k}{nq}\textstyle\sum_{I=0}^{\infty} I P_c(I) f(I) \\ &= \tfrac{k}{nq}\textstyle\sum_{I=0}^{\infty} I \sum_{j=0}^{n-k} \binom{n}{j} (1-(1-p_h)^{I-1})^j ((1-p_h)^{I-1})^{n-j} \tfrac{G^I e^{-G}}{I!} \\ &= \tfrac{k}{n} \cdot \tfrac{G}{q} \textstyle\sum_{I=0}^{\infty} \sum_{j=0}^{n-k} \binom{n}{j} (1-(1-p_h)^{I})^j ((1-p_h)^{I})^{n-j} \tfrac{G^I e^{-G}}{I!} \\ &\to \tfrac{k\mu}{n} \textstyle\sum_{j=0}^{n-k} \binom{n}{j} (1-e^{-\eta\mu})^j (e^{-\eta\mu})^{n-j}, \end{aligned} \tag{3.23}$$

as $G, q \to \infty$, while $\mu \triangleq G/q$ is held constant. From (3.4), as $n, k \to \infty$ while $r \triangleq k/n$ is held constant, we can show that the summation term approaches 1 if $r < e^{-\eta\mu}$. Therefore the normalized throughput becomes

$$W \to \mu e^{-\eta\mu}, \tag{3.24}$$

as $n, k, G, q \to \infty$. The optimum traffic level can be shown to be η^{-1} and the throughput at this optimum traffic level is e^{-1}/η: for synchronous frequency hopping $\eta = 1$, and even for asynchronous frequency hopping η can be 1 asymptotically by forming each M-ary symbol from binary signals (e.g. BFSK) of length $\log_2 M$ bits, and thus making $N_b = \log_2 M$ in (3.9). Therefore, it can be concluded that frequency-hop spread-spectrum modulation can be just as bandwidth-efficient as narrowband modulation in the sense that for a given bandwidth it can achieve the same throughput. However, for the narrowband ALOHA system without frequency hopping the throughput of e^{-1} is achieved when the packet error probability is 0.632 (which may be too large in practical system) and with binary feedback, while for the spread-spectrum modulation it is achieved with arbitrarily small packet error probability and without feedback. Error-control coding can not improve the situation very much (if at all) in the narrowband ALOHA system, because the symbol error probability is approximately

1/2 for M-ary signal set of interest whenever the symbol is hit by another transmission of equal power. Thus the average number of errors within the received version of a codeword (packet) of length n will be approximately $n/2$, while for any (n,k) code the maximum number of correctable errors is $\lfloor (n-k)/2 \rfloor$. This implies that coding can hardly improve the performance of narrowband ALOHA system. Numerical datas given in [Haj 82] support the above arguments.

3.2.2 Assumption 2: Discrimination Against Partially Overlapping Interference

In this section we assume the use of noncoherent M-ary FSK signaling (each frequency slot thus consists of M orthogonal tone positions), and assume that the packet radio network operates asynchronously at the hop level (asynchronous frequency hopping). Then the occurence of hits generally results in *partial*, rather than total, overlap among tones of different users; it is assumed that the degree of overlap in time experienced by any pair of hops that suffer a hit is uniformly distributed over the interval from 0 to the total hop duration time, T_h. Without loss of generality we assume T_h=1. It was assumed in subsection 3.2.1 that any degree of hop overlap results in the loss of the information (erasure) carried in that hop. In this subsection we make a departure from this assumption.

We assume that a symbol erasure will be necessitated if and only if in any one (or more) of the M tone positions of the frequency slot the amount of time overlap between the symbol (tone) of interest and those of other users exceed a fraction ρ of the hop duration time. Otherwise, the symbol is received correctly. This modified model in which partial overlaps can be tolerated was introduced in [Wie 84].

Therefore we must examine each of the M tone positions of the frequency slot to determine whether any of them experience interference for more than a fraction ρ of the hop duration. Note that this interference may arise from one or

more other users' signals in the same tone position whose combined overlap at the same or at opposite ends of the hop lasts for a fraction of a hop greater than ρ. However, it is shown in Appendix B that as M becomes large, the probability of the event that all users sharing the same frequency slot transmit distinct tones approaches 1. Therefore if τ denotes the amount of time overlap between the tone of interest and that of an interferer, the probability of symbol erasure given m hits, $\hat{P}_m$, is given by

$$\begin{aligned} \hat{P}_m &= 1 - [P(\tau < \rho)]^m \\ &= 1 - \rho^m. \end{aligned} \tag{3.25}$$

Thus, by averaging over the number of hits we obtain the symbol erasure probability, $p_{\rho,I}$, given as

$$\begin{aligned} p_{\rho,I} &= \sum_{m=1}^{I-1}(1-\rho^m)\begin{pmatrix} I-1 \\ m \end{pmatrix} p_h^m(1-p_h)^{I-1-m} \\ &= 1-(1-(1-\rho)p_h)^{I-1}. \end{aligned} \tag{3.26}$$

The marginal transition probability in this case is given by

$$P(y_j|x_1,x_2,\cdots,x_I) = \begin{cases} 1-p_{\rho,I}, & y_j = x_j \\ p_{\rho,I}, & y_j = ?. \end{cases}$$

Since the j^{th} channel output does not depend on the symbols transmitted from other users, the interference channnel is separated. The component channel model is again M-ary erasure channel, but with erasure probability equal to $p_{\rho,I}$.

Achievable Region

By following the same procedure as in subsection 3.2.1, we can show that "error-free" communication is possible asymptotically provided that the code rate is less than $1 - p_{\rho,I}$, i.e.,

$$r < (1-(1-\rho)p_h)^{I-1}, \tag{3.27}$$

or equivalently,

$$I < 1 + \frac{\ln(r)}{\ln(1-(1-\rho)p_h)}. \tag{3.28}$$

Throughput

By following the same procedure as in subsection 3.2.1, the asymptotic normalized throughput as n and k approach infinity while $r \triangleq k/n$ is held constant can be shown to be

$$\lim_{n,k\to\infty} W = \frac{r}{q}\left(1 + \frac{\ln(r)}{\ln(1-(1-\rho)p_h)}\right). \tag{3.29}$$

By optimizing over r, we get the optimum code rate, r_{opt}, given by

$$r_{opt} = e^{-1}(1-(1-\rho)p_h)^{-1}, \tag{3.30}$$

which for reasonable values of q is very close to e^{-1}. At this optimum code rate the optimum number of transmissions is given by

$$I_{opt} = [\ln(1-(1-\rho)p_h)^{-1}]^{-1}, \tag{3.31}$$

thus the limiting ($I, q \to \infty$ with $\lambda \triangleq I/q$ held constant) optimum traffic intensity per frequency slot, λ_{opt}, is given by

$$\lambda_{opt} = 1/[\eta(1-\rho)]. \tag{3.32}$$

At r_{opt} and I_{opt} the asymptotic maximum possible throughput, W_{max}, becomes

$$W_{max} = 1/[qe(1-(1-\rho)p_h)\ln(1-(1-\rho)p_h)^{-1}], \tag{3.33}$$

which approaches $e^{-1}/[\eta(1-\rho)]$ for large enough q. This is also the asymptotic sum capacity of the interference channel as modeled by M-ary erasure component channels with erasure probability, $p_{\rho,I}$, given in (3.26). We see that the ability to discriminate against interfering signals results in dramatic increase in throughput by the factor of $1/(1\text{-}\rho)$.

3.3 No Side Information

We now assume that side information is not available at the demodulator, thus it does not produce any erasure symbol, but instead makes an estimate (hard decision) on the received signal. The demodulated symbols are fed into an error-correction decoder. As long as there are no more than $\lfloor \frac{n-k}{2} \rfloor$ errors, the (n, k) RS code can correct them, where $\lfloor x \rfloor$ denotes the integer part of x.

3.3.1 Demodulator Model 1: Worst Case

We assume that if a received symbol is hit by one or more symbols, then the demodulator output is equally likely one of the M possible symbols, and if there is no hit it is correctly received. That is, the conditional probability of symbol error given hit is given by $1 - 1/M$, and it is 0 given no hit. Thus the probability that a received symbol is in error given I simultaneous transmissions, $p_{e,I}$, is given by

$$p_{e,I} = (1 - 1/M)(1 - (1 - p_h)^{I-1}). \tag{3.34}$$

This is the worst case assumption in the sense of minimizing the capacity: The minimum of the capacity of an M-ary channel is obtained when all the transition probabilities are equal to $1/M$, and the resulting minimum capacity can be shown to be zero. Therefore, the resulting achievable regions and throughputs are pessimistic results.

The marginal transition probability in this case is given by

$$P(y_j|x_1, x_2, \cdots, x_I) = \begin{cases} 1 - p_{e,I}, & y_j = x_j \\ p_{e,I}, & y_j \neq x_j. \end{cases}$$

Since the j^{th} channel output does not depend on the symbols transmitted from other users, the interference channnel is separated. The component channel

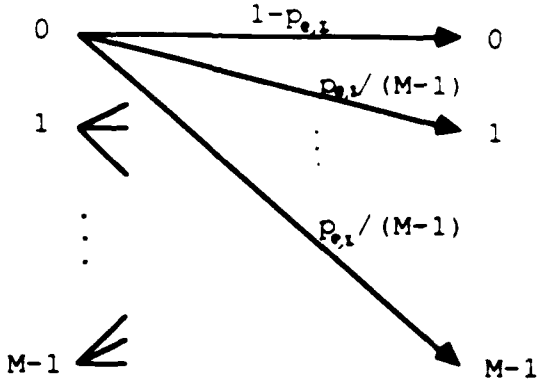

Figure 3.5: M-ary symmetric channel.

model will be an M-ary symmetric channel with crossing probability $p_{e,I}$ as shown in Figure 3.5.

Achievable Region

When an (n, k) Reed-Solomon code is employed to correct the errors, the probability of correctly decoding a codeword (packet) given I simultaneous transmissions, $P_c(I)$, with bounded distance decoding is given by

$$P_c(I) = \sum_{j=0}^{\lfloor (n-k)/2 \rfloor} \binom{n}{j} p_{e,I}^j (1 - p_{e,I})^{n-j}. \tag{3.35}$$

Asymptotically, as n and k approach infinity while the code rate, $r \triangleq k/n$, is held constant, it can be shown that

$$\lim_{n,k \to \infty} P_c(I) = \begin{cases} 1, & 1 - r > 2p_{e,I} \\ 0.5, & 1 - r = 2p_{e,I} \\ 0, & 1 - r < 2p_{e,I}. \end{cases} \tag{3.36}$$

This implies that "error-free" communication is possible asymptotically provided that the code rate is less than $1 - 2p_{e,I}$, i.e.,

$$r < 2(1 - p_h)^{I-1} - 1, \tag{3.37}$$

or equivalently

$$I < 1 + \frac{\ln((1+r)/2)}{\ln(1-p_h)}. \tag{3.38}$$

This represents an asymptotic achievable region of I and r for arbitrarily small error probability without side information. The limiting value for the asymptotic achievable region as both the number of users and the number of frequency slots get large (i.e., $I, q \to \infty$ with $\lambda \triangleq I/q$ held constant) is given by

$$r < 2e^{-\eta\lambda} - 1,$$

or equivalently

$$\lambda < \frac{1}{\eta} \ln(\frac{2}{1+r}).$$

It can be shown that as $M \to \infty$, the capacity of the channel shown in Figure 3.5 is given by

$$C(I) = (1 - p_h)^{I-1},$$

which is the same as that obtainable with perfect side information.

For the case of finite block length codes, we can derive a similar approximation to the maximum channel traffic and code rate for the packet error probability to be less than $\hat{P}_E$. By applying the Demoivre-Laplace theorem to (3.35), we can get an approximation

$$P_c(I) \approx F\left(\frac{\lfloor (n-k)/2 \rfloor - np_{e,I}}{\sqrt{np_{e,I}(1-p_{e,I})}}\right). \tag{3.39}$$

By combining (3.39) with the constraint, $P_E(I) \triangleq 1 - P_c(I) \leq \hat{P}_E$, we obtain

$$r \leq 1 - \frac{2}{n}\lceil np_{e,I} + \alpha\sqrt{np_{e,I}(1-p_{e,I})}\rceil \tag{3.40}$$

or equivalently

$$I \leq 1 + \ln(B)/\ln(1 - p_h) \tag{3.41}$$

where

$$B \triangleq 1 - \frac{2t + \alpha^2 - \alpha\sqrt{4t + \alpha^2 - 4t^2/n}}{2(1 - 1/M)(n + \alpha^2)}.$$

Figure 3.6 shows the achievable regions of I and r for $P_E(I) \leq 10^{-2}$ with Reed-Solomon codes of length 32 and 256 and also the asymptotic achievable regions for arbitrarily small error probability without side information. We see that the exact values and the approximations are very close.

When there is a distribution on the number of packet transmissions (Poisson with mean G), it can be shown that

$$P_C = \sum_{j=0}^{\lfloor \frac{n-k}{2} \rfloor} \binom{n}{j} [(1 - 1/M)(1 - e^{-\eta\mu})]^j [1 - (1 - 1/M)(1 - e^{-\eta\mu})]^{n-j}, \tag{3.42}$$

as G and q approach infinity while $\mu \triangleq G/q$ is held constant. By applying the Gaussian approximation of (3.42) to the constraint, $P_E \leq \hat{P}_E$, we can obtain

$$r \leq 1 - \frac{2}{n}\lceil np_{e,\mu} + \alpha\sqrt{np_{e,\mu}(1 - p_{e,\mu})}\rceil, \tag{3.43}$$

or equivalently

$$\mu \leq \frac{1}{\eta}\ln(1/B), \tag{3.44}$$

where

$$p_{e,\mu} \triangleq (1 - 1/M)(1 - e^{-\eta\mu}).$$

As in perfect side information case, the equations (3.40)and (3.41) will be useful for the use of *adaptive* transmissions and coding techniques.

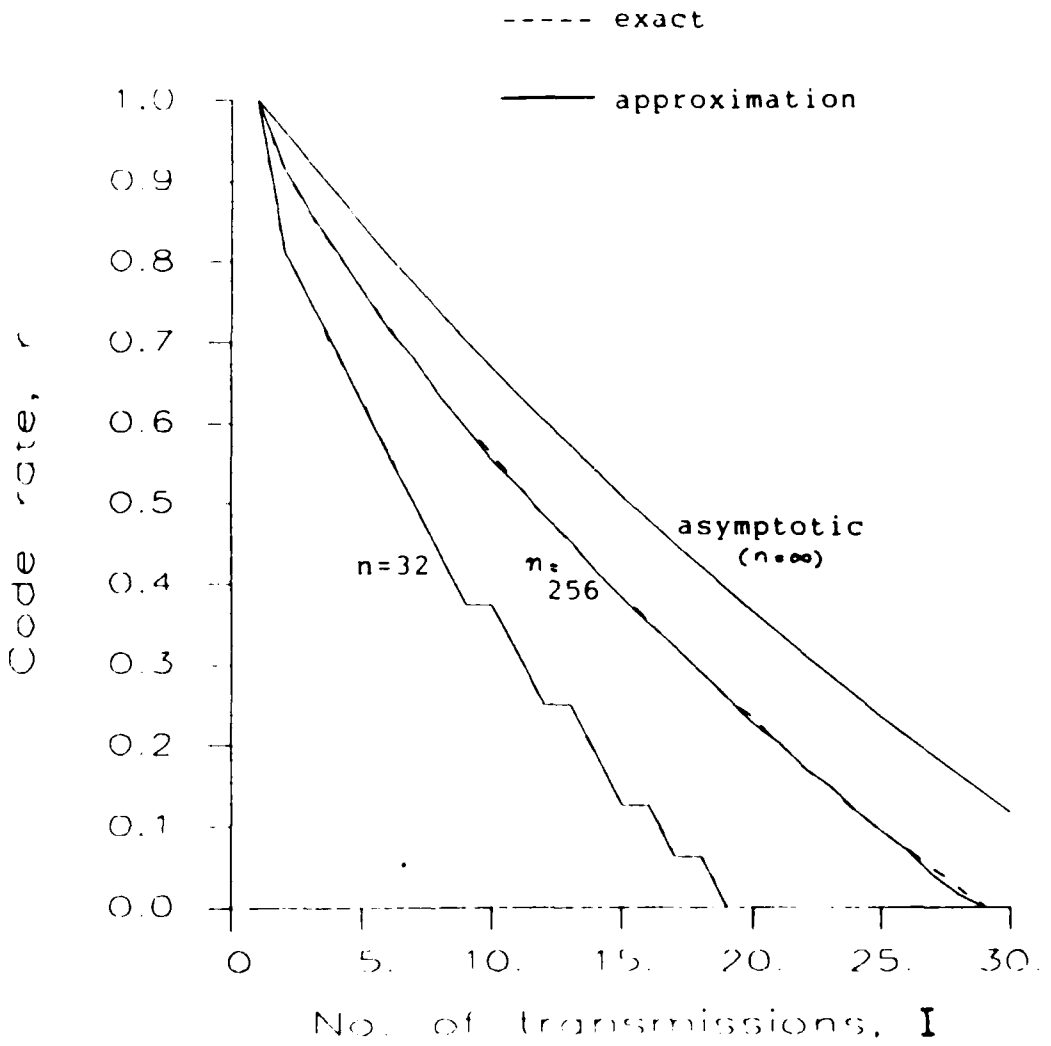

Figure 3.6: Achievable regions of (r, I) for $P_E(I) \leq 10^{-2}$ and the asymptotic achievable region, no side information, $q = 100$, η=2.

Throughput

The asymptotic normalized throughput can be obtained from (3.17) and (3.38) as

$$\begin{aligned} \lim_{n,k\to\infty} W &= \frac{r}{q}\left(1+\frac{\ln((1+r)/2)}{\ln(1-p_h)}\right) \\ &\to \frac{r}{\eta}\ln\left(\frac{2}{1+r}\right), \end{aligned} \tag{3.45}$$

for large enough q. By optimizing over r we get the optimal code rate, r_{opt}

$$r_{opt} = 0.4597. \tag{3.46}$$

This asymptotic optimal code rate also seems to give a very good approximation for finite length codes, even the length 32 codes. We can see from Figures 3.7 and 3.8 that the maximum normalized throughput is obtained by the (32,14) code and (256,118) code: the optimum values of k obtained from the asymptotic optimum code rate, 0.4597, are $32 \times 0.4597 = 14.71$ and $256 \times 0.4597 = 117.68$, which are very close to the exact optimum values of k, namely 14 and 118 respectively. At this optimum code rate the optimum channel traffic per frequency slot, λ_{opt}, is

$$\lambda_{opt} = 0.3148/\eta, \tag{3.47}$$

which is also a good approximation for finite n and q. At r_{opt} and λ_{opt} the asymptotic maximum possible throughput, W_{max}, becomes

$$W_{max} = 0.1448/\eta, \tag{3.48}$$

which is only 39.3% of that achievable with perfect side information.

We can also show that the asymptotic $(I, q \to \infty)$ maximum sum capacity without side information approaches e^{-1}/η as $M \to \infty$. The loss in using Reed-Solomon codes is partially due to the use of a non maximum likelihood decoder (i.e., bounded distance decoder). However, we will show in chapter IV that the normalized throughput achievable with perfect side information can be achieved

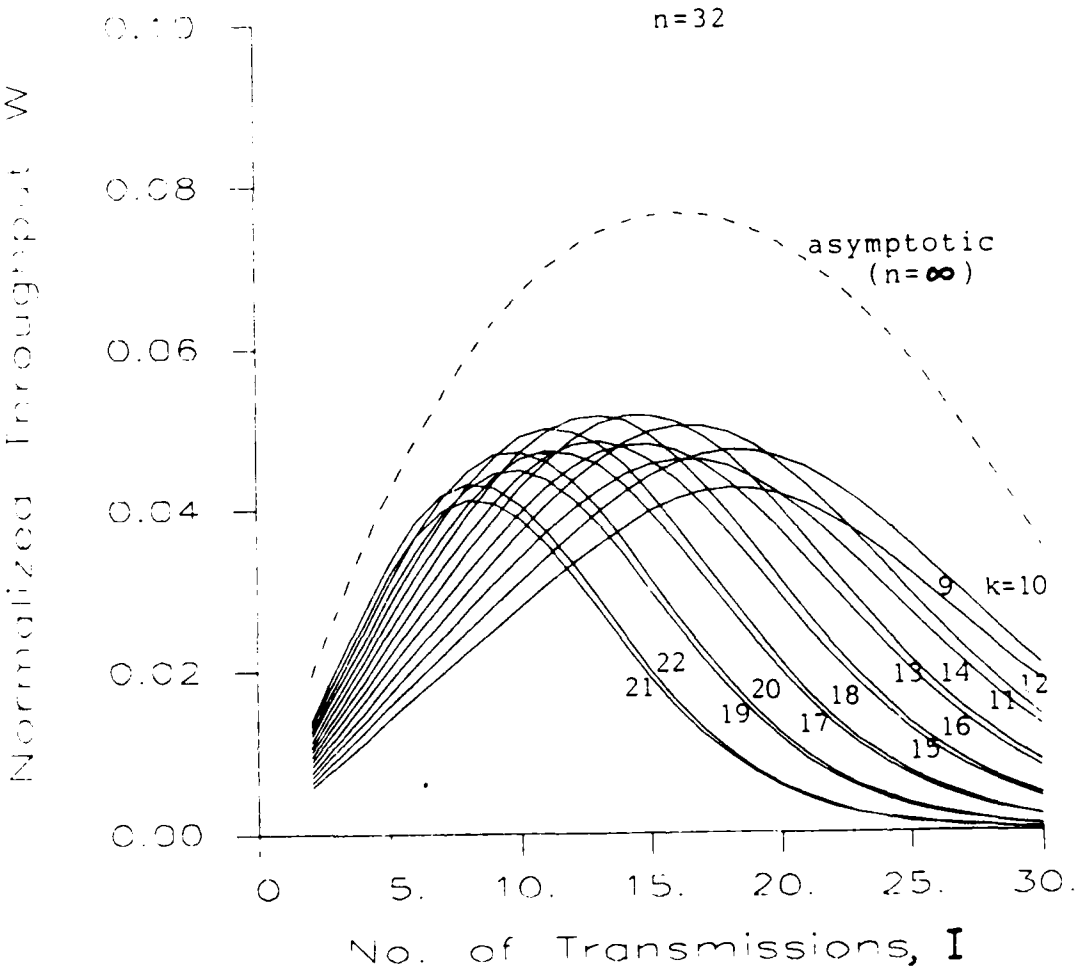

Figure 3.7: Normalized throughputs, no side information, $q = 100$, $n = 32$, η=2.

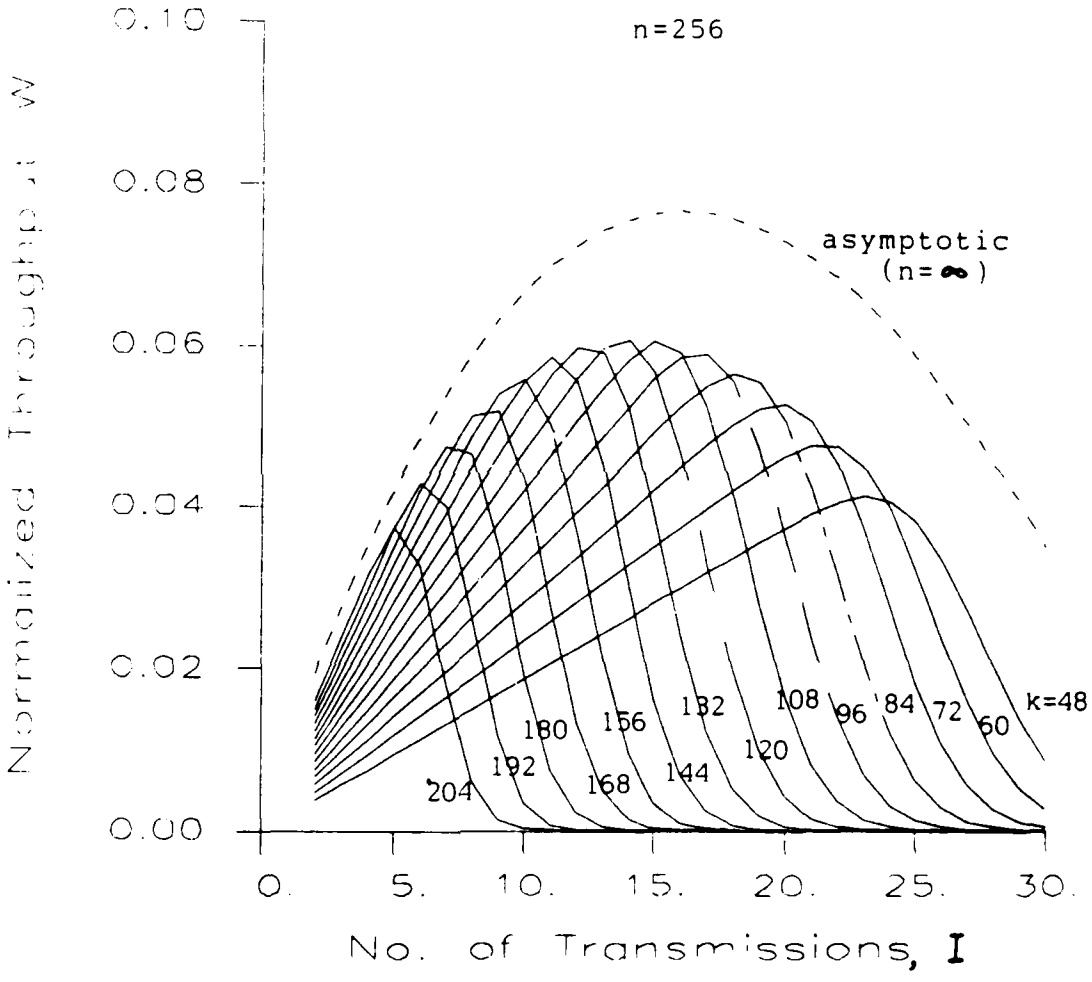

Figure 3.8: Normalized throughputs, no side information, $q = 100$, $n = 256$, η=2.

through the use of concatenated coding scheme, even though the channel provides no side information.

3.3.2 Demodulator Model 2: Realistic Case

Notice that in the previous model we have not distinguished one hit from more than one hit in the calculation of $p_{e,I}$. This can be taken into account as follows. If two users hop to the same frequency slot at the same time, i.e. one hit, the probability of symbol error is $1/2$ if the two users have different symbol and 0 if they have the same symbol. If three users collide, i.e. two hits, the symbol error probability is $2/3$ if all three users transmit different symbols, and $1/2$ if two of the users transmit the same symbol but the third transmits a different symbol, and 0 if they have the same symbol. This modeling is valid for the M-orthogonal signaling, such as MFSK. Notice that the j^{th} channel output depends on the symbols transmitted from other users. Therefore, the interference channel in this case is not separated.

If each symbol is transmitted with equal probability, i.e., $1/M$, then the probability of symbol error for this situation with m hits, P_m, can be derived as (see Appendix B)

$$\begin{aligned}
P_1 &= 0\tfrac{1}{M} + \tfrac{1}{2}(1-\tfrac{1}{M}) = \tfrac{1}{2}(\tfrac{M-1}{M}) \\
P_2 &= 0\tfrac{1}{M^2} + \tfrac{1}{2}\tfrac{3(M-1)}{M^2} + \tfrac{2}{3}\tfrac{(M-1)(M-2)}{M^2} = \tfrac{4M^2-3M-1}{6M^2} \\
P_3 &= \tfrac{3M^3-2M^2-M}{4M^3} \\
P_4 &= \tfrac{24M^4-15M^3-10M^2+1}{30M^4} \\
P_5 &= \tfrac{10M^5-6M^4-5M^3+M}{12M^5}.
\end{aligned} \tag{3.49}$$

$$\vdots$$

As M becomes larger, P_m becomes

$$P_m = m/(m+1). \tag{3.50}$$

That is, the probability of symbol error tends to depend more on the *number* of interfering signals than on which symbols are being transmitted from interferers as M becomes large. The above probability is also an upper bound for finite M, and can also be used as a good approximation: for example, P_4=0.784 for M=32 and 0.798 for M=256, while the upper bound is 0.8. By averaging over the number of hits we can determine the average symbol error probability given I simultaneous transmissions, $p_{e,I}$, as

$$\begin{aligned} p_{e,I} &= \sum_{m=1}^{I-1} \frac{m}{m+1} \binom{I-1}{m} p_h^m (1-p_h)^{I-1-m} \\ &= 1 - \frac{1-(1-p_h)^I}{I p_h}. \end{aligned} \tag{3.51}$$

Achievable Region

From (3.36) and (3.51) we can show that asymptotically as $n, k \to \infty$ while $r \triangleq k/n$ is held constant, "error-free" communication is possible, i.e, $P_c(I)$=1, provided

$$\begin{aligned} r &< \frac{2-2(1-p_h)^I}{I p_h} - 1 \\ &\to \frac{2}{\eta\lambda}\left(1 - e^{-\eta\lambda}\right) - 1, \end{aligned} \tag{3.52}$$

as $I, q \to \infty$ while $\lambda \triangleq I/q$ is held constant. Figure 3.9 shows the asymptotic achievable regions of code rate and number of packet transmissions for arbitrarily small packet error probability for the cases of perfect side information and no side information.

Throughput

From (3.17) and (3.52) the asymptotic normalized throughput can be shown

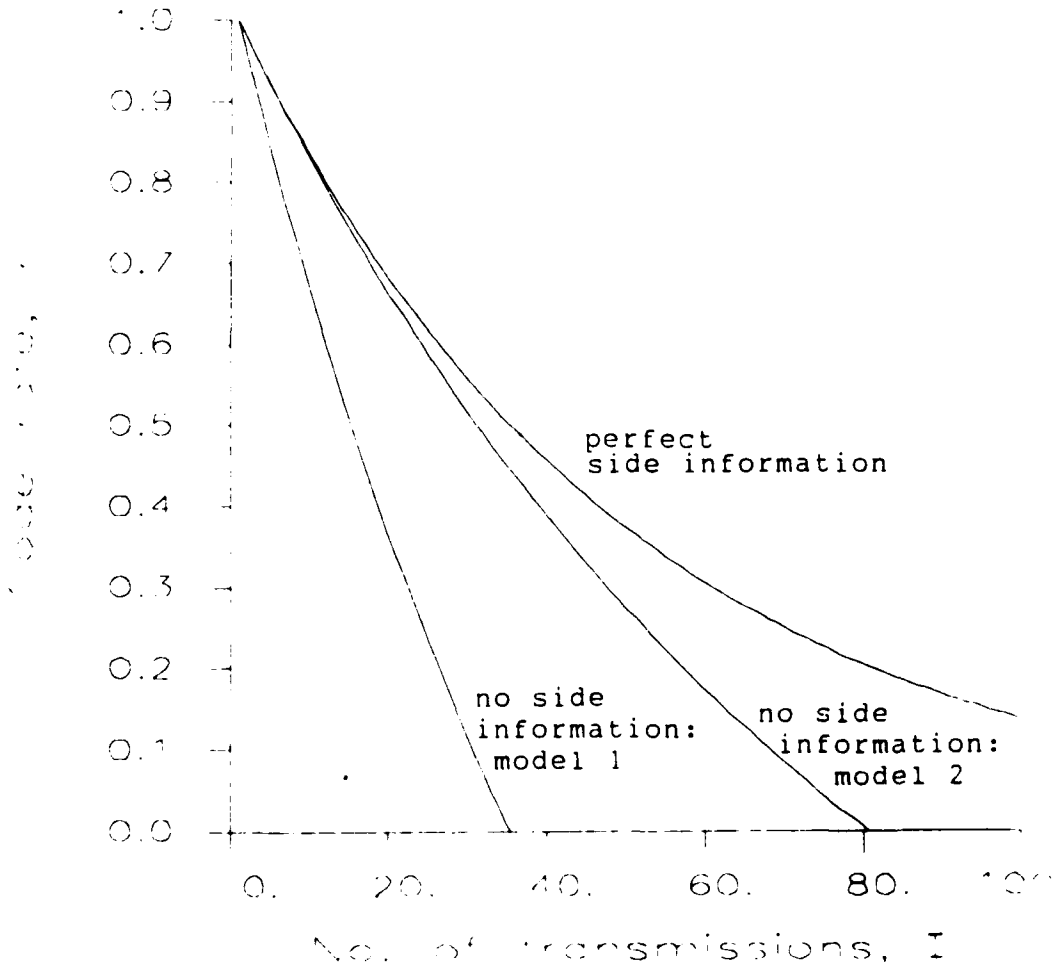

Figure 3.9: Asymptotic achievable regions of (r, I) for arbitrarily small error probability, $q = 100$, $\eta = 2$.

to be

$$\begin{aligned} \lim_{n,k\to\infty} W &= \frac{I}{q}\left(\frac{2-2(1-p_h)^I}{Ip_h} - 1\right) \\ &\to \frac{2}{\eta}\left(1 - e^{-\eta\lambda}\right) - \lambda, \end{aligned} \tag{3.53}$$

as $I, q \to \infty$ while $\lambda \triangleq I/q$ is held constant. By optimizing over λ we get the optimum channel traffic, λ_{opt}

$$\lambda_{opt} = \ln(2)/\eta = 0.6931/\eta, \tag{3.54}$$

and the optimum code rate, r_{opt}

$$\begin{aligned} r_{opt} &= \frac{2(1-e^{-\eta\lambda_{opt}})}{\eta\lambda_{opt}} - 1 \\ &= \ln(e/2)/\ln(2) = 0.4427, \end{aligned} \tag{3.55}$$

and the asymptotic maximum possible throughput, W_{max}

$$W_{max} = \ln(e/2)/\eta = 0.3069/\eta. \tag{3.56}$$

However, the capacity region with this model is not known, because the channel is not separated. Figure 3.10 shows the asymptotic normalized throughputs for the perfect side information and no side information cases.

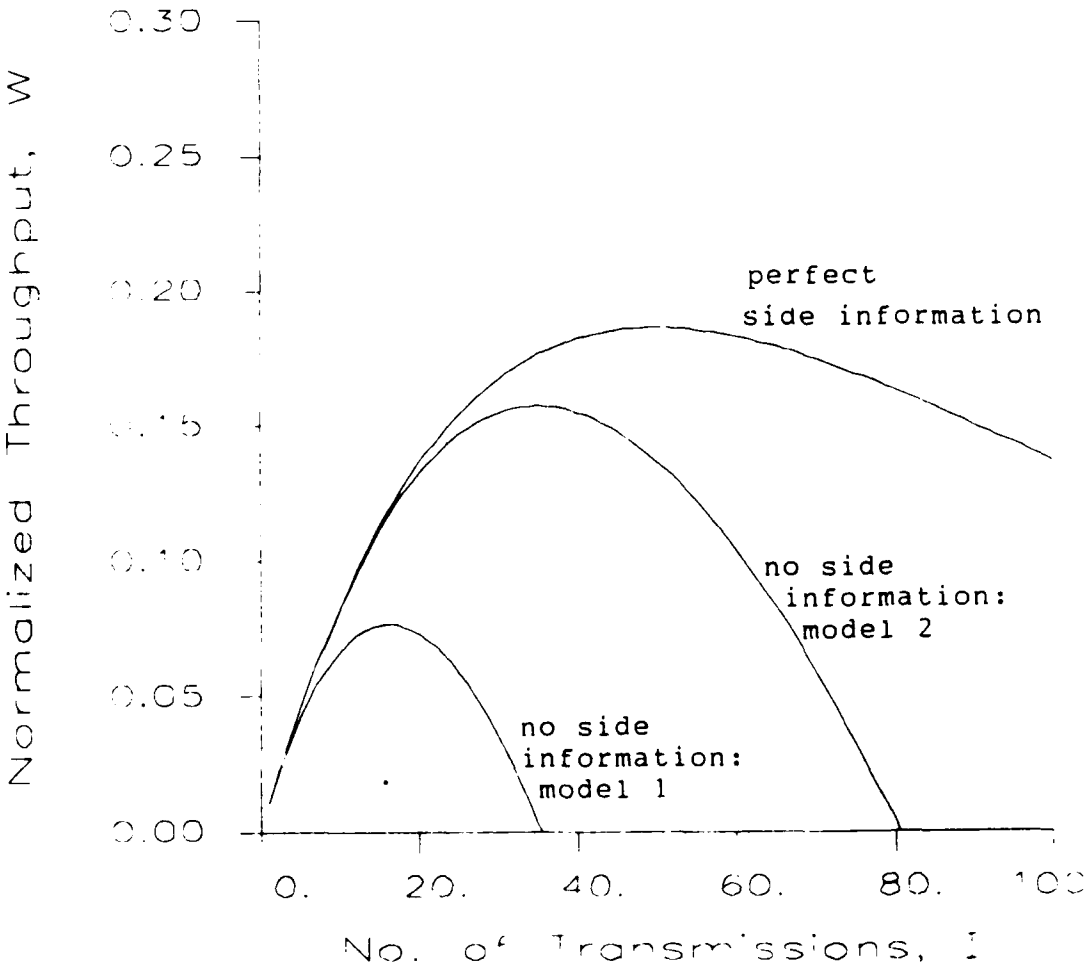

Figure 3.10: Asymptotic normalized throughputs vs. I, $q = 100$, $\eta = 2$.

CHAPTER IV

CONCATENATED CODES

4.1. Introduction

It has been shown in Section 3.3 that the maximum throughput achievable without side information is only 39.3% (worst case) of that achievable with perfect side information. This gives us a quantitative measure of the importance of side information in improving the multiple-access capability of frequency-hop packet radio networks.

One technique for obtaining the side information is to partition the data stream into blocks of K digits and to encode each block into a codeword of length $N(\geq K)$ and to transmit the codeword during a single hop. On the basis of the received version of the codeword the decoder attempts to detect errors in the received sequence: if there are errors then at least one code symbol must have been hit. However, not all error patterns are detectable, so there is a nonzero probability of undetected error. If an error is detected then symbols transmitted on that hop are erased, and if the error is undetected it results in an error.

A similar technique has been suggested by McEliece and Stark [McE 84] using a test pattern. It is however a special example of the class of error detecting codes considered in this chapter, and the underlying assumption in [McE 84] is

that interference occurs in a whole block if it occurs: that is, the interference during a hop remains the same throughout the hop. This assumption is very restrictive, and certainly many real channels such as asynchronous frequency-hopping multi-user systems do not have constant interference in the block. In general, interference occurs partially during a hop.

One can expect that as the code rate decreases, the probability of undetected error decreases and the probability of detected error increases because of the increased minimum distance among the codewords. That is, the reliability of the side information obtained from the code increases. However, decreasing the code rate implies a decrease in the efficient use of the channel. An interesting question that arises from this discussion is "How does the reliability of the side information change as the code rate changes?", or "What is the maximum allowable code rate to obtain a certain reliability of the side information?". In this chapter we give the answer to the above question for both the constant and partial interference cases.

The combination of encoder, channel, and decoder generates in general an errors-and-erasures channel. The above encoder and decoder will be called later an *inner encoder* and *inner decoder* respectively. We employ an *outer code* to correct the errors (caused by undetected errors) and the erasures (caused by detected errors). In this way the inner decoder informs the outer decoder which symbols (inner codewords) in the received packet have been hit by symbols from other packets in the same time slot. We find that the normalized throughput achievable with perfect side information can be achieved through the use of this *concatenated coding scheme*, even though the channel provides no side information. This chapter ends by evaluating the performance of diversity / RS code as an example of the concatenated coding schemes.

4.2. Concatenated Coding

The basic concept of concatenated codes for two levels of coding is illustrated in Figure 4.1. This figure provides the general outline of a powerful class of codes which were introduced by Forney in 1966 [For 66]. Information to be transmitted is first encoded with an (n, k) outer code. The symbols from the outer encoder are further encoded with an (N, K) inner code. Clearly, if the symbol alphabets of the inner and outer codes are not the same, it is necessary to reformat the data between the encoders for the inner and outer codes. At the receive side, the demodulated data is first decoded with the inner decoder, and the symbols from the inner decoder are then decoded with the outer decoder. The combination of inner encoder, channel, and inner decoder is referred to as the *super channel.* The alphabet sizes of the inner code and outer code are denoted as M_i and M_o respectively.

Several characteristics of concatenated codes are evident from Figure 4.1. First, the resulting concatenated code has overall length of nN channel symbols (M_i-ary) with kK information symbols per overall codeword and with code rate $rR = kK/nN$, where $R = K/N$ and $r = k/n$. Although the overall length of the code is nN, the structure imposed by the concatenation concept allows decoding operation to be performed by two decoders for codes of length N and n, respectively. This allows a significant reduction in complexity over that which would be required to provide the same overall error rate with a single level of coding. The most natural choice for outer codes are the RS codes. This is because the RS codes, being maximum-distance-separable codes, make highly efficient use of redundancy, and block lengths and symbol sizes can be readily adjusted to accomodate a wide range of message sizes.

The concatenated scheme we consider uses an inner code to correct or detect

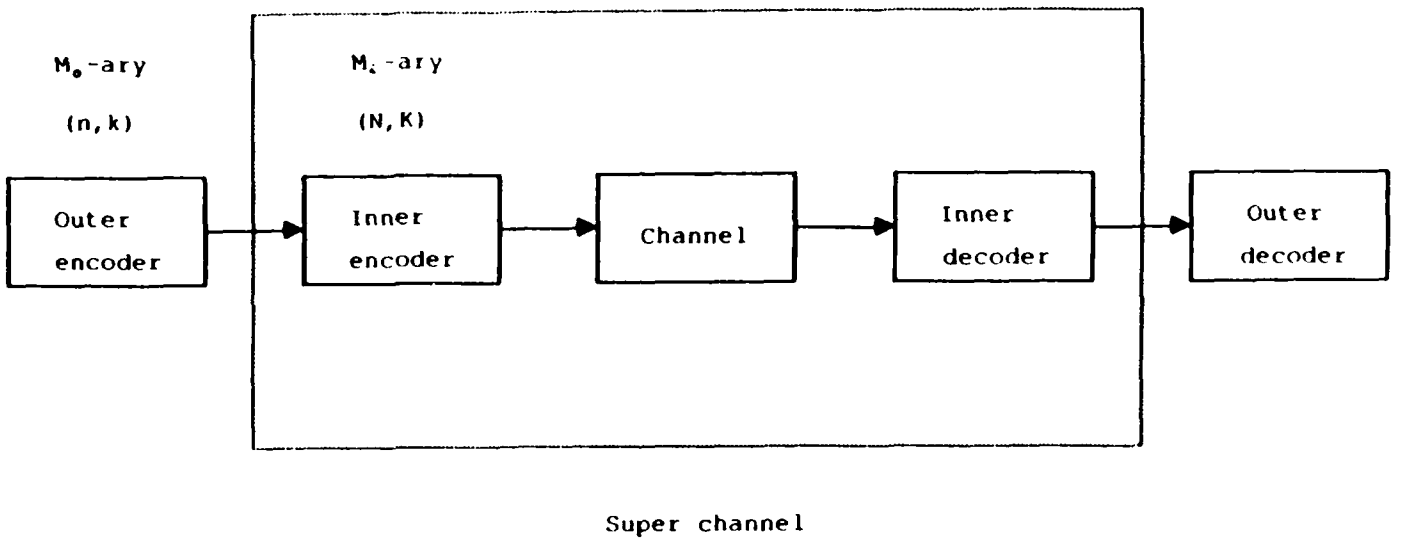

Figure 4.1: Concatenated coding system.

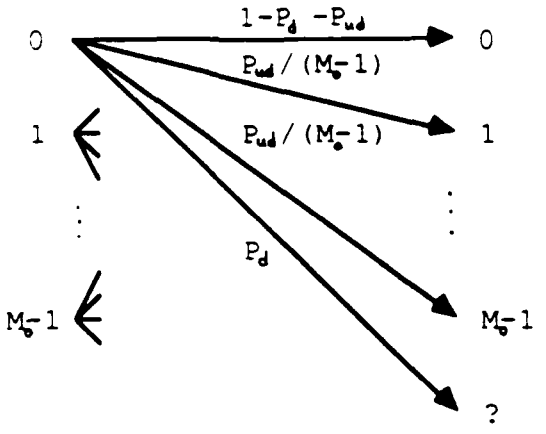

Figure 4.2: Super channel model created by inner code.

errors within a hop. The codewords of the inner code are transmitted during a single hop and one outer code symbol consists of one inner codeword ($\rightarrow M_i^K = M_o$). The inner code can correct e errors and detect f errors ($e \leq f$) provided $e + f < d_{min}$, where d_{min} is the minimum distance of the inner code [Mac 77]. When an error is detected every symbol of the inner code is erased. There are, however, errors that are not detected nor corrected by the inner code which result in errors at the output of the inner decoder. Therefore, the inner code creates an errors-and-erasures channel, as shown in Figure 4.2, where P_d and P_{ud} denotes the probability of detected error and the probability of undetected error respectively. The purpose of the outer code is to correct the errors and erasures of the inner code.

Achievable Region

Since an (n, k) RS outer code can correct t errors and e erasures provided $e + 2t \leq n - k$, for a memoryless channel of Figure 4.2 the probability of correctly decoding a codeword (packet) is given by [Ber 80]

$$P_c(I) = \sum_{l+2m \leq n-k} \binom{n}{l, m} P_d^l \, P_{ud}^m (1 - P_d - P_{ud})^{n-l-m}, \tag{4.1}$$

where

$$\binom{n}{l, m} \triangleq \frac{n!}{l!m!(n-l-m)!}.$$

Asymptotically as both n and k approach infinity while the outer code rate $r \triangleq k/n$ is held constant, it can be shown (see Appendix C) that

$$\lim_{n,k \to \infty} P_c(I) = \begin{cases} 1, & r < 1 - P_d - 2P_{ud} \\ 0.5, & r = 1 - P_d - 2P_{ud} \\ 0, & r > 1 - P_d - 2P_{ud}. \end{cases} \tag{4.2}$$

That is, "error-free" communication is possible asymptotically provided

$$r < 1 - P_d - 2P_{ud}. \tag{4.3}$$

This is the requirement on the *outer* code rate to have error-free communications. To get the requirement on the *overall* code rate we have to multiply by the inner code rate K/N. Thus the resulting asymptotic normalized achievable rate is given by

$$rR < \frac{K}{N}(1 - P_d - 2P_{ud}). \tag{4.4}$$

For the case of finite block length codes, we can derive an approximation to the maximum channel traffic and the maximum code rate for the packet error probability to be less than $\hat{P}_E$. It is shown in Appendix C that

$$P_c(I) \approx F\left(\frac{\sqrt{n}(1 - r - P_d - 2P_{ud})}{\sqrt{P_d - P_d^2 + 4P_{ud} - 4P_{ud}^2 - 4P_dP_{ud}}}\right). \tag{4.5}$$

By combining (4.5) with the constraint, $P_E(I) \triangleq 1 - P_c(I) \leq \hat{P}_E$, we obtain

$$r \leq 1 - P_d - 2P_{ud} - \alpha\sqrt{(P_d - P_d^2 + 4P_{ud} - 4P_{ud}^2 - 4P_dP_{ud})/n}, \qquad (4.6)$$

where α is defined in (3.12). This is the constraint on the outer code rate for the packet error probability to be less than $\hat{P}_E$ for a given inner code and the channel (number of simultaneous transmissions). Thus the normalized achievable region is given by

$$rR \leq \frac{K}{N}[1 - P_d - 2P_{ud} - \alpha\sqrt{(P_d - P_d^2 + 4P_{ud} - 4P_{ud}^2 - 4P_dP_{ud})/n}]. \qquad (4.7)$$

Throughput

The normalized throughput with the concatenated coding scheme is defined by

$$W = \frac{k}{n} \cdot \frac{K}{N} \cdot \frac{IP_c(I)}{q}. \qquad (4.8)$$

As both n and k approach infinity while $r \triangleq k/n$ is held constant, from (4.3) and (4.8) the asymptotic normalized throughput is given by

$$\lim_{n,k\to\infty} W = \frac{K}{N} \cdot \frac{I(1 - P_d - 2P_{ud})}{q}. \qquad (4.9)$$

P_d and P_{ud} are determined by the inner code and the channel. Note that the achievable regions and the throughput derived in this section are general enough to be applied to any combinations of inner block codes and RS outer codes.

4.3. Error Detecting Code / RS Code

In this section we assume that the receiver does not have side information concerning the presence of hit. However we try to get the side information by

detecting the errors in each hop caused by the multi-user interference through the use of binary error detecting code ($M_i = 2$). The idea is to encode a block of K data bits into a block of N bits and to transmit the N bits during a single hop, and on the basis of the received version of the transmitted codeword to detect the errors caused by interference. If an error is detected the entire N bits transmitted on that hop are erased. However not all error patterns are detectable so there is a nonzero probability of undetected error. We employ an RS outer code to "correct" the errors (caused by undetected errors) and the erasures (caused by detected errors).

The multi-user interference level during a hop may or may not remain constant throughout the hop depending on the availability of synchronism at the hop level. If all transmitters adjust their timings of frequency changes such that their changes occur simultaneously at each hop (*synchronous* frequency hopping), the multi-user interference level during a hop will remain the same throughout the hop. This model matches also certain real channels such as partial-band jammed channel. However, for the *asynchronous* frequency hopping multi-user systems where the timings of frequency changes do not occur simultaneously, the multi-user interference level will not remain constant throughout the hop. For both the synchronous and asynchronous frequency hopping multi-user systems, we investigate the concatenated coding scheme that employs a binary error detecting code and Reed-Solomon code.

4.3.1. Synchronous Frequency-Hopping System

We assume that the synchronization at the hop level is maintained by all users so that the multi-user interference level during a hop remains the same throughout the hop. Since the interference from the other users' packet transmissions passes through the dehopper and then is filtered, only the interference at the

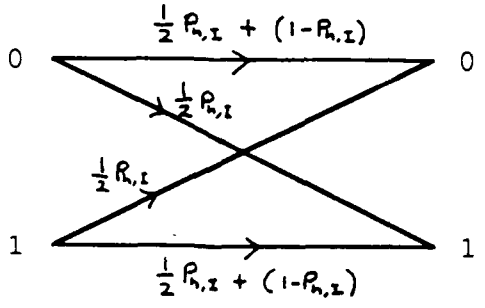

Figure 4.3: Component channel for a simple interference channel.

frequency of the signal affects the performance. We assume that the hopping pattern is essentially random, which makes the multi-user interference during a hop be independent of the interference at other hop intervals.

In each hop we have two possibilities: *hit* or *no hit*. When the signal is hit we have fixed bit error probability of 1/2 for all bits in the hop. When the signal is not hit the entire bits in the hop are error-free. In both cases the channel is modeled by a binary symmetric channel (BSC) with crossing probabilities 1/2 and 0 for the *hit* and *no hit* channel respectively. The interference channel is separated, because the j^{th} channel output does not depend on the symbols transmitted from other users. The component channel model is shown in Figure 4.3.

When error detection is being used the decoder will make a mistake and accept a codeword which is not the one transmitted if and only if the error pattern (vector) is a nonzero codeword. If $P_{N,j}$ is the probability of a particular j bit error pattern in N bits, where N is the length of the inner code, and A_j is

the number of codewords of weight j, then the probability of undetected error is given by [Mac 77]

$$P_{ud} = \sum_{j=1}^{N} A_j P_{N,j}. \tag{4.10}$$

For the above channel model, $P_{N,j}$ is given by

$$P_{N,j} = \begin{cases} p_{h,I} \cdot 2^{-N} + (1 - p_{h,I}) \cdot 1, & j = 0 \\ p_{h,I} \cdot 2^{-N} + (1 - p_{h,I}) \cdot 0, & j \geq 1. \end{cases} \tag{4.11}$$

Thus the probability of undetected error is given by

$$\begin{aligned} P_{ud} &= \textstyle\sum_{j=1}^{N} A_j P_{N,j} \\ &= p_{h,I} 2^{-N} \textstyle\sum_{j=1}^{N} A_j \\ &= (2^{-(N-K)} - 2^{-N}) p_{h,I}, \end{aligned} \tag{4.12}$$

since

$$\sum_{j=1}^{N} A_j = 2^K - 1, \tag{4.13}$$

for any linear code (A_0=1).

The probability of a detected error P_d is given by

$$\begin{aligned} P_d &= 1 - P_{N,0} - P_{ud} \\ &= (1 - 2^{-(N-K)}) p_{h,I}, \end{aligned} \tag{4.14}$$

since $1 - P_{N,0}$ is the probability of at least one bit error. Figures 4.4 and 4.5 show the variations of the reliabilty of side information, i.e., variations of P_d and P_{ud}, as a function of the inner code length N for several values of K. One observation from the figures is that the probability of undetected error approaches zero and the probability of detected error approaches the probability of a hit as N becomes large. This will be proved later.

The maximum allowable inner code rate for the reliability of side information to be above a threshold, i.e., $P_{ud} \leq \hat{P}_{ud}$ and $P_d \geq \hat{P}_d$ for some $\hat{P}_{ud}$ and $\hat{P}_d$, can

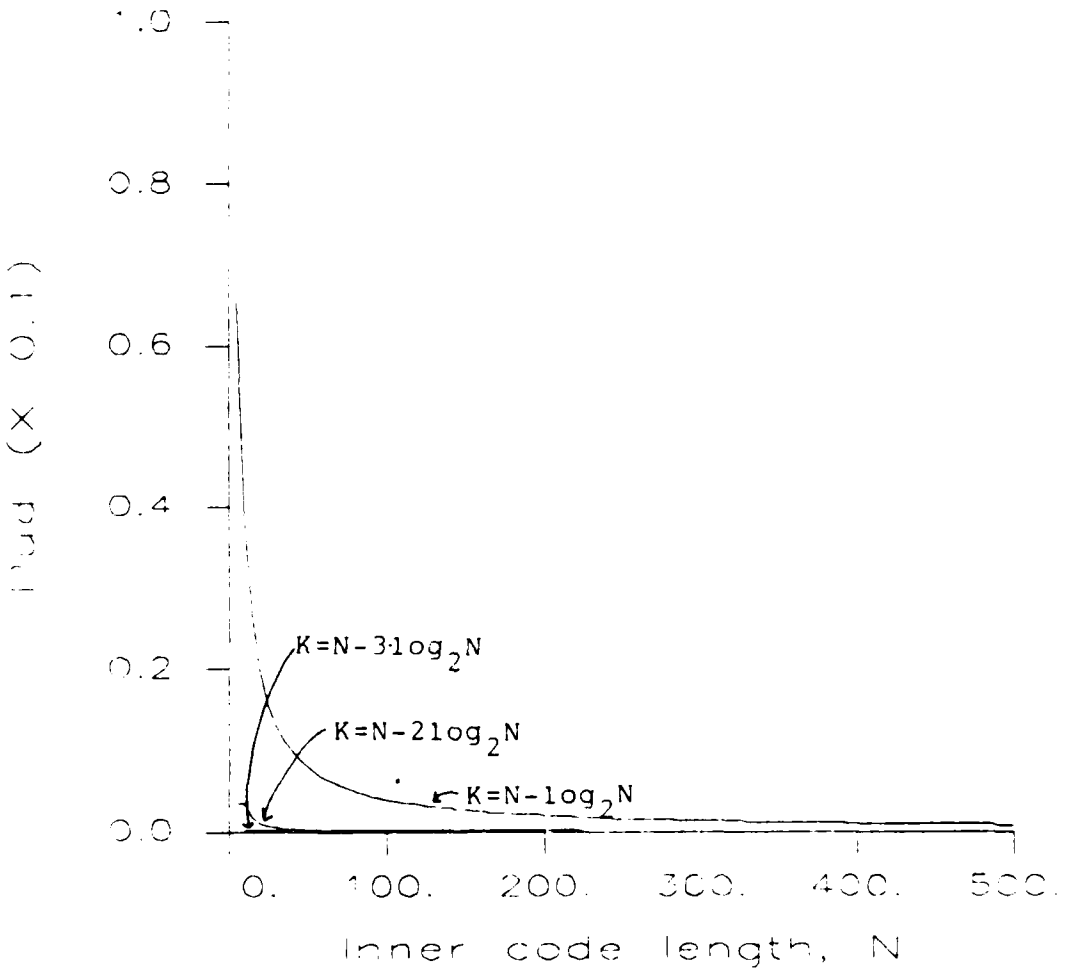

Figure 4.4: Plot of undetected error probabilty, P_{ud}, for several values of K (*synchronous* frequency-hopping, $q = 100$, $I = 50$).

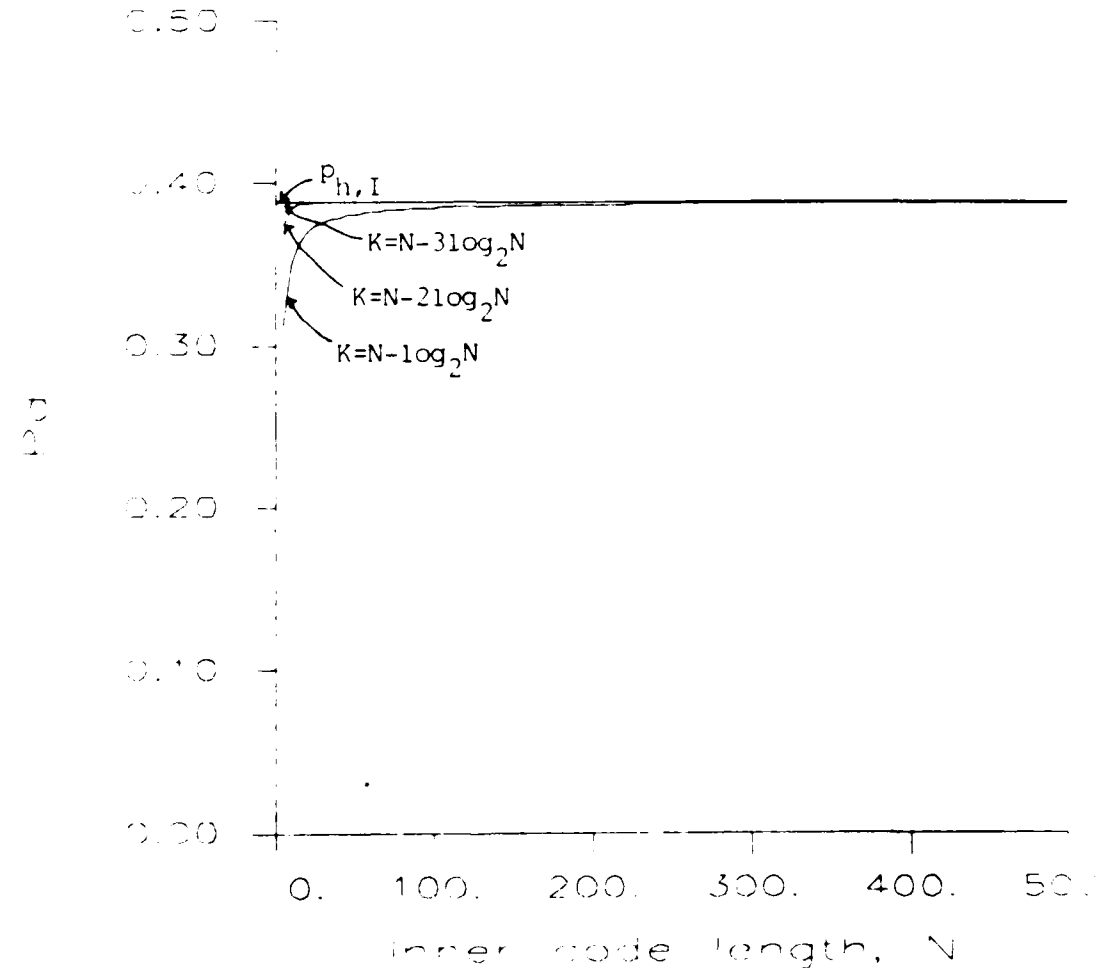

Figure 4.5: Plot of detected error probability, P_d, for several values of K (*synchronous* frequency-hopping, $q = 100$, $I = 50$).

be obtained from (4.11) and (4.13) as follows:

$$\begin{aligned} P_{ud} &= 2^{-N}(2^K - 1)p_{h,I} \\ &\leq \hat{P}_{ud} \\ \Longrightarrow K &\leq \log_2\left(\frac{\hat{P}_{ud}}{p_{h,I}} \cdot 2^N + 1\right) \\ \Longrightarrow R = \frac{K}{N} &\leq \frac{1}{N}\log_2\left(\frac{\hat{P}_{ud}}{p_{h,I}} \cdot 2^N + 1\right), \end{aligned} \tag{4.15}$$

and

$$\begin{aligned} P_d &= (1 - 2^{-(N-K)})p_{h,I} \\ &\geq \hat{P}_d \\ \Longrightarrow K &\leq N - \log_2\left(\frac{p_{h,I}}{p_{h,I} - \hat{P}_d}\right) \\ \Longrightarrow R &\leq 1 - \frac{1}{N}\log_2\left(\frac{p_{h,I}}{p_{h,I} - \hat{P}_d}\right). \end{aligned} \tag{4.16}$$

Therefore,

$$\begin{aligned} R &\leq \min\left(\frac{1}{N}\log_2\left(\frac{\hat{P}_{ud}}{p_{h,I}} \cdot 2^N + 1\right),\ 1 - \frac{1}{N}\log_2\left(\frac{p_{h,I}}{p_{h,I} - \hat{P}_d}\right)\right) \\ &= \begin{cases} \frac{1}{N}\log_2\left(\frac{\hat{P}_{ud}}{p_{h,I}} \cdot 2^N + 1\right), & \hat{P}_d + \hat{P}_{ud} \leq p_{h,I}(1 - 2^{-N}) \\ 1 - \frac{1}{N}\log_2\left(\frac{p_{h,I}}{p_{h,I} - \hat{P}_d}\right), & \hat{P}_d + \hat{P}_{ud} > p_{h,I}(1 - 2^{-N}). \end{cases} \end{aligned} \tag{4.17}$$

Figures 4.6 and 4.7 show the maximum allowable code rate to satisfy the requirement for $P_{ud} \leq \hat{P}_{ud}$ and $P_d \geq \hat{P}_d$ respectively.

From (4.11) and (4.13) we can obtain the asymptotic normalized achievable rate given by

$$\begin{aligned} rR &< \frac{K}{N}(1 - P_d - 2P_{ud}) \\ &= \frac{K}{N}[1 - (1 + 2^{-(N-K)} - 2^{-N+1})p_{h,I}], \end{aligned} \tag{4.18}$$

and the asymptotic normalized throughput given by

$$\begin{aligned} W &= \frac{k}{n}\frac{K}{N}\frac{I}{q}P_c(I) \\ &= \frac{K}{N}\frac{I}{q}[1 - (1 + 2^{-(N-K)} - 2^{-N+1})p_{h,I}]. \end{aligned} \tag{4.19}$$

If the number of redundancy bits $N - K$ is of length $\log_2 N$, then as $n \to \infty$ ($\Longrightarrow N \to \infty$, because $n = M_o = 2^{N - \log_2 N}$),

$$\begin{aligned} R &= \frac{N - \log_2 N}{N} \\ &\to 1, \end{aligned} \tag{4.20}$$

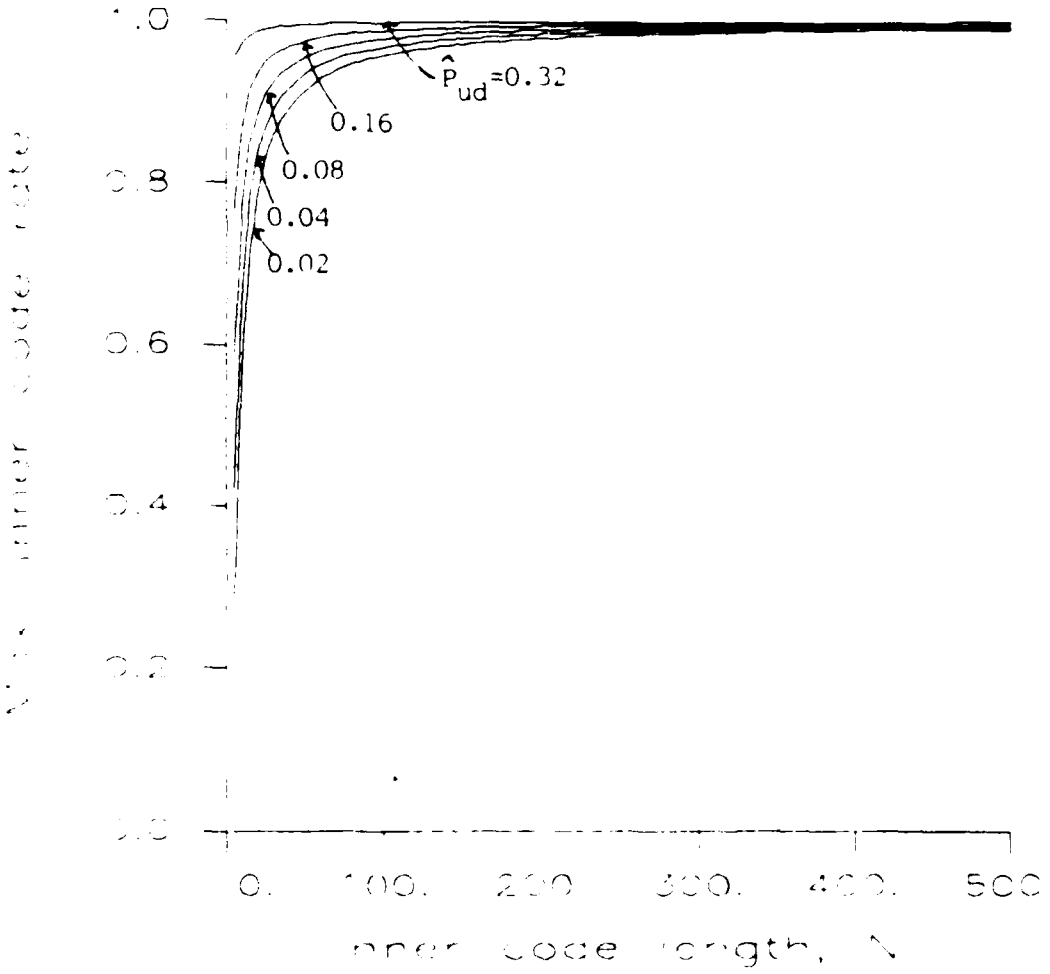

Figure 4.6: The maximum allowable code rate to satisfy $P_{ud} \leq \hat{P}_{ud}$ (*synchronous* frequency-hopping, $q = 100$, $I = 50$).

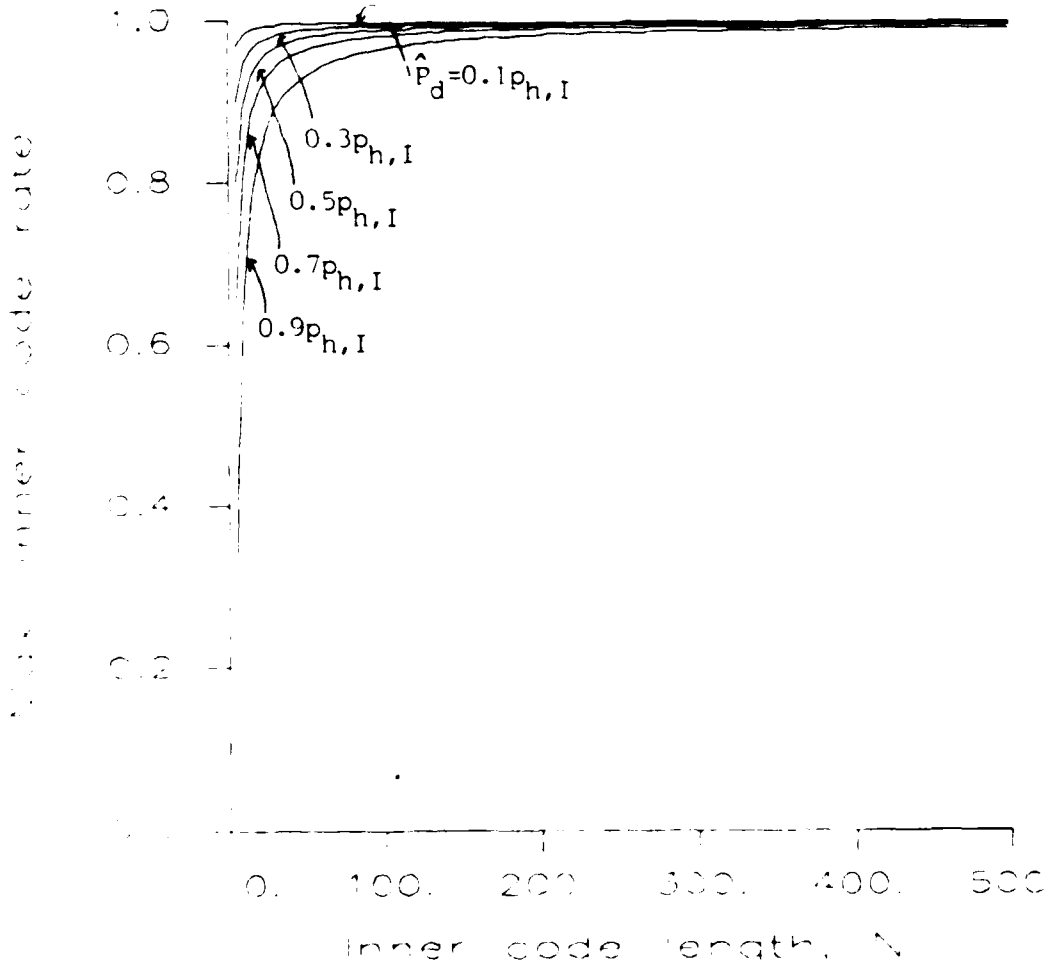

Figure 4.7: The maximum allowable code rate to satisfy $P_d \geq \hat{P}_d$ (*synchronous* frequency-hopping, $q = 100$, $I = 50$).

and

$$\begin{aligned} P_{ud} &= (2^{-(N-K)} - 2^{-N})p_{h,I} \\ &= (2^{-\log_2 N} - 2^{-N})p_{h,I} \\ &\rightarrow 0, \end{aligned} \tag{4.21}$$

and

$$\begin{aligned} P_d &= 1 - P_{N,0} - P_{ud} \\ &\rightarrow 1 - (p_{h,I}/2^N + 1 - p_{h,I}) \\ &= p_{h,I}(1 - 2^{-N}) \\ &\rightarrow p_{h,I}. \end{aligned} \tag{4.22}$$

This implies that there are no undetected errors and every hit is detected as the inner code length becomes large. Therefore, if the redundancy bits of the inner code is of length $\log_2 N$, then for large values of N one can expect the side information provided from the inner code to be increasingly reliable, and yet the fraction of the transmitted bits devoted to the redundancy is quite small. What this means is that, for large N, the super channel (combination of inner encoder, channel, and inner decoder) behaves as if perfect side information were available even though the channel provides no side information.

Therefore, the asymptotic normalized achievable region is given by

$$\begin{aligned} rR &< \tfrac{K}{N}[1 - P_d - 2P_{ud}] \\ &\rightarrow 1 - p_{h,I} \\ &= (1 - \tfrac{1}{q})^{I-1} \\ &\rightarrow e^{-\lambda}, \end{aligned} \tag{4.23}$$

as $N, I, q \rightarrow \infty$ with $\lambda \triangleq I/q$ held constant, and the asymptotic normalized throughput is given by

$$\begin{aligned} W &= \tfrac{K}{N}\tfrac{I}{q}(1 - P_d - 2P_{ud}) \\ &\rightarrow \tfrac{I}{q}(1 - \tfrac{1}{q})^{I-1} \\ &\rightarrow \lambda e^{-\lambda}, \end{aligned} \tag{4.24}$$

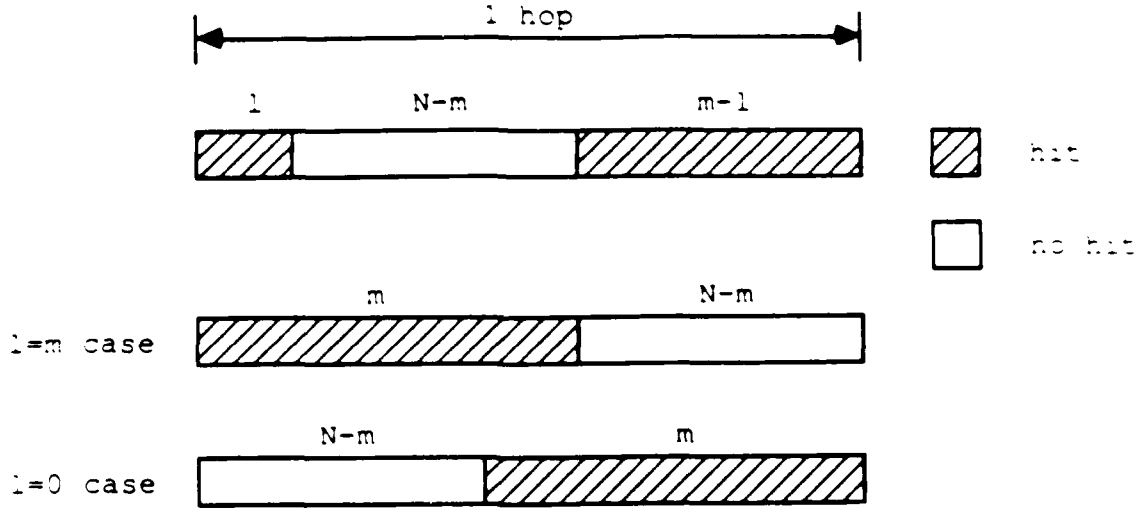

Figure 4.8: m bit hit patterns.

as $N, I, q \rightarrow \infty$ with $\lambda \triangleq I/q$ held constant. Notice that the asymptotic normalized achievable region and the normalized throughput derived are the same as those that can be obtained with perfect side information (refer to (3.7)), even though the channel provides no side information.

4.3.2. Asynchronous Frequency-Hopping System

Now we relax the assumption that the multi-user interference level remains constant throughout the hop. We consider a multi-user communication system where the signals from each user are asynchronous to other signals. Then the signal of interest will be partially overlapped by other signals as indicated in Figure 4.8.

If the signal of interest is hit by m bits, i.e., it is overlapped by other signals for the m bit intervals, $(m = 1, 2, \cdots, N)$, there will be H_m such m bit hit patterns, where

$$H_m = \begin{cases} m+1, & m = 1, 2, \cdots, N-1 \\ 1, & m = N. \end{cases} \tag{4.25}$$

The probability of undetected error in this case is given by

$$P_{ud} = \sum_{m=1}^{N} P_{ud,m} \cdot P(m \text{ bit hit}), \tag{4.26}$$

where $P_{ud,m}$ denotes the probability of undetected error given that the signal is hit by m bits, and P(m bit hit) is the probability that the signal is hit by m bits.

The total number of hit patterns can be obtained from (4.25) as

$$\begin{aligned} \textstyle\sum_{m=1}^{N} H_m &= 1 + \textstyle\sum_{m=1}^{N-1}(m+1) \\ &= \frac{N(N+1)}{2}. \end{aligned} \tag{4.27}$$

If we assume that every hit pattern is *equi-probable*, then

$$P(m \text{ bit hit}) = \begin{cases} \frac{(m+1)p_{h,I}}{\frac{N(N+1)}{2}}, & m = 1, 2, \cdots, N-1 \\ \frac{p_{h,I}}{\frac{N(N+1)}{2}}, & m = N, \end{cases} \tag{4.28}$$

where

$$p_{h,I} = 1 - \left[1 - \frac{1}{q}\left\{1 + \frac{1}{N}\left(1 - \frac{1}{q}\right)\right\}\right]^{I-1},$$

since there are N bits per hop [Ger 82].

To get $P_{ud,m}$ let us consider an m bit hit pattern as shown in Figure 4.9. Notice that only the error patterns belonging to group B can occur from the above m bit hit pattern. Thus the probability that a particular j bit error pattern in group B occurs given the above m bit hit pattern, denoted $P_{j,m,B}$, is given by

$$\begin{aligned} P_{j,m,B} &= \left(\tfrac{1}{2}\right)^{j}\left(1 - \tfrac{1}{2}\right)^{m-j} \\ &= 2^{-m}. \end{aligned} \tag{4.29}$$

To get the average number of codewords of weight j in group B, denoted $A_{j,m,B}$, let us consider the following *random coding* arguments: we choose 2^K codewords,

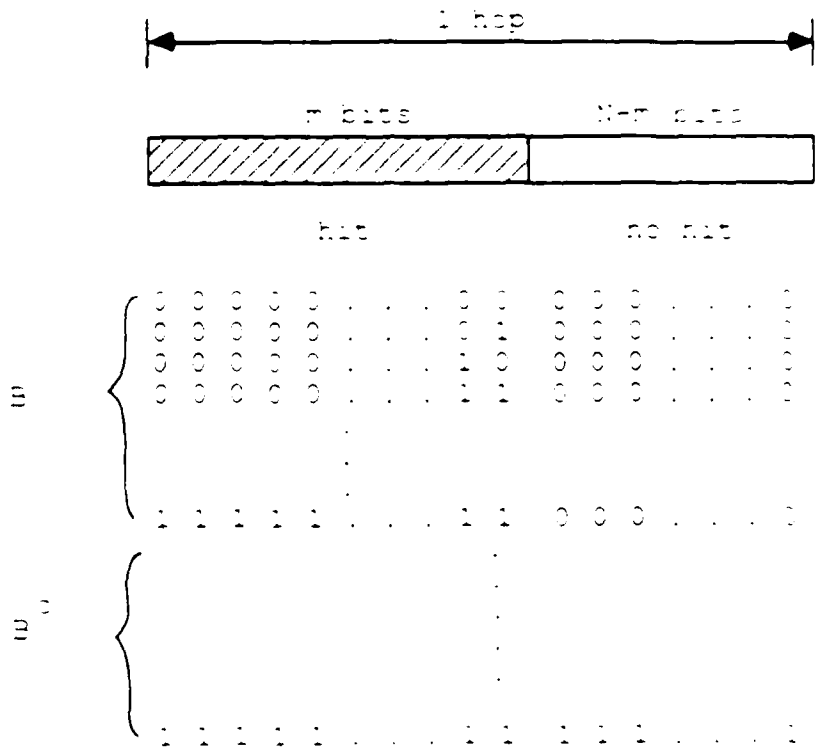

Figure 4.9: Error patterns.

each being chosen at random with equal probability among 2^N sequences and independently of the other codewords[1], and then choose one of the codewords with equal probability among 2^K codewords (call it c). Then the probability that c has weight j and is in group B is given by

$$\begin{aligned} P(\text{weight}(c) = j\ ,\ c \in B) &= P(\text{weight}(c) = j \quad c \in B) \cdot P(c \in B) \\ &= 2^{-m} \begin{pmatrix} m \\ j \end{pmatrix} \cdot \tfrac{2^m}{2^N} \\ &= 2^{-N} \begin{pmatrix} m \\ j \end{pmatrix}. \end{aligned} \tag{4.30}$$

Since there are 2^K codewords, the average number of codewords of weight j in group B, $A_{j,m,B}$, is thus given by

$$A_{j,m,B} = 2^{-(N-K)} \begin{pmatrix} m \\ j \end{pmatrix}. \tag{4.31}$$

Notice that the probability of a j bit error pattern is the same (i.e., 2^{-m}) for *all* m bit hit patterns, and the average number of codewords of weight j that can be accepted (by a mistake) as a transmitted codeword is the same for given m. Therefore, the probability of undetected error given that the signal is hit by m bits is given by

$$\begin{aligned} P_{ud,m} &= \textstyle\sum_{j=1}^{m} A_{j,m,B} P_{j,m,B} \\ &= \textstyle\sum_{j=1}^{m} 2^{-(N-K)} \begin{pmatrix} m \\ j \end{pmatrix} 2^{-m} \\ &= 2^{-(N-K)}(1 - 2^{-m}), \end{aligned} \tag{4.32}$$

for *all* m bit hit patterns. Therefore, the probability of undetected error is given

---

[1] This emsemble of codes will include some very poor codes, i.e., those for which not all codewords are distinct. Nevertheless, this technique provides some very useful insights into the fundamental behavior of coding schemes.

by

$$\begin{aligned} P_{ud} &= \sum_{m=1}^{N} P_{ud,m} \cdot P(m \text{ bit hit}) \\ &= \sum_{m=1}^{N-1} 2^{-(N-K)}(1-2^{-m})\frac{2(m+1)p_{h,I}}{N(N+1)} + 2^{-(N-K)}(1-2^{-N})\frac{2p_{h,I}}{N(N+1)} \\ &= \frac{2^{-(N-K-1)}p_{h,I}}{N(N+1)}\{(N+1)2^{-N+2} - N2^{-N+1} - 2^{-N} + 0.5(N-1)(N-2) - 2\}. \end{aligned} \tag{4.33}$$

Notice that since this is the *average* performance of all possible codes, there must exist specific codes which will do even better.

The probability of detected error P_d is given by

$$P_d = 1 - P(\text{no error}) - P_{ud}, \tag{4.34}$$

since $1 - P(\text{no error})$ is the probability of at least one error. The probability of no error is given by

$$\begin{aligned} P(\text{no error}) &= \sum_{m=0}^{N} P(\text{no error} \mid m \text{ bit hit}) \cdot P(m \text{ bit hit}) \\ &= (1-p_{h,I}) + \sum_{m=1}^{N-1} 2^{-m}\frac{2(m+1)p_{h,I}}{N(N+1)} + 2^{-N}\frac{2p_{h,I}}{N(N+1)} \\ &= 1 - p_{h,I} + \frac{2p_{h,I}}{N(N+1)}\{N2^{-N+1} - (N+1)2^{-N+2} + 2^{-N} + 3\}. \end{aligned} \tag{4.35}$$

Therefore the probability of detected error is given by

$$\begin{aligned} P_d &= p_{h,I}\{1 - \frac{2}{N(N+1)}\{N2^{-N+1} - (N+1)2^{-N+2} + 2^{-N} + 3\} \\ &\quad - \frac{2^{-(N-K-1)}}{N(N+1)}\{(N+1)2^{-N+2} - N2^{-N+1} - 2^{-N} + 0.5(N-1)(N-2) - 2\}. \end{aligned} \tag{4.36}$$

Figures 4.10 and 4.11 show the variations of the reliability of side information, i.e., variations of P_{ud} and P_d, as a function of the inner code length N for several values of K.

The requirement on the inner code rate for the reliability of side information to be above a certain threshold, i.e., $P_{ud} \leq \hat{P}_{ud}$ and $P_d \geq \hat{P}_d$ for some $\hat{P}_{ud}$ and

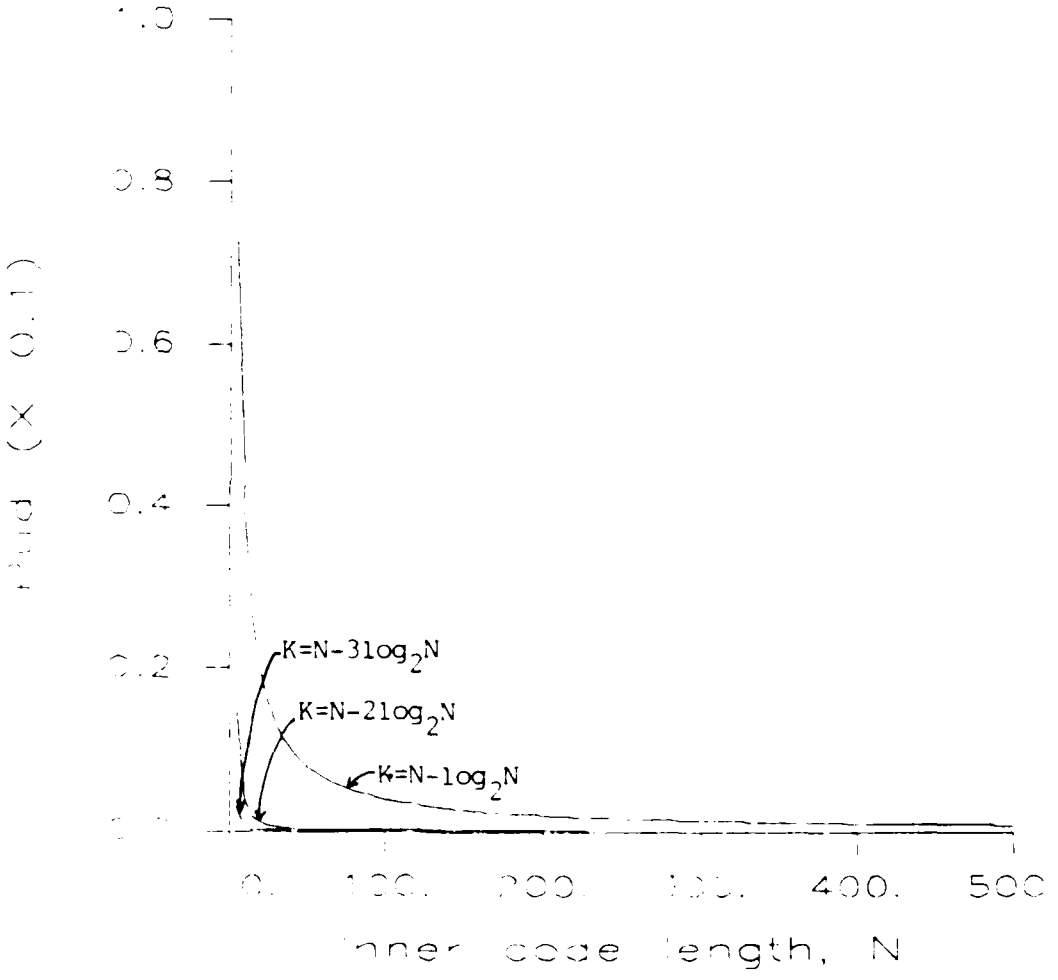

Figure 4.10: Plot of undetected error probability, P_{ud}, for several values of K (*asynchronous* frequency-hopping, q = 100, $I = 50$).

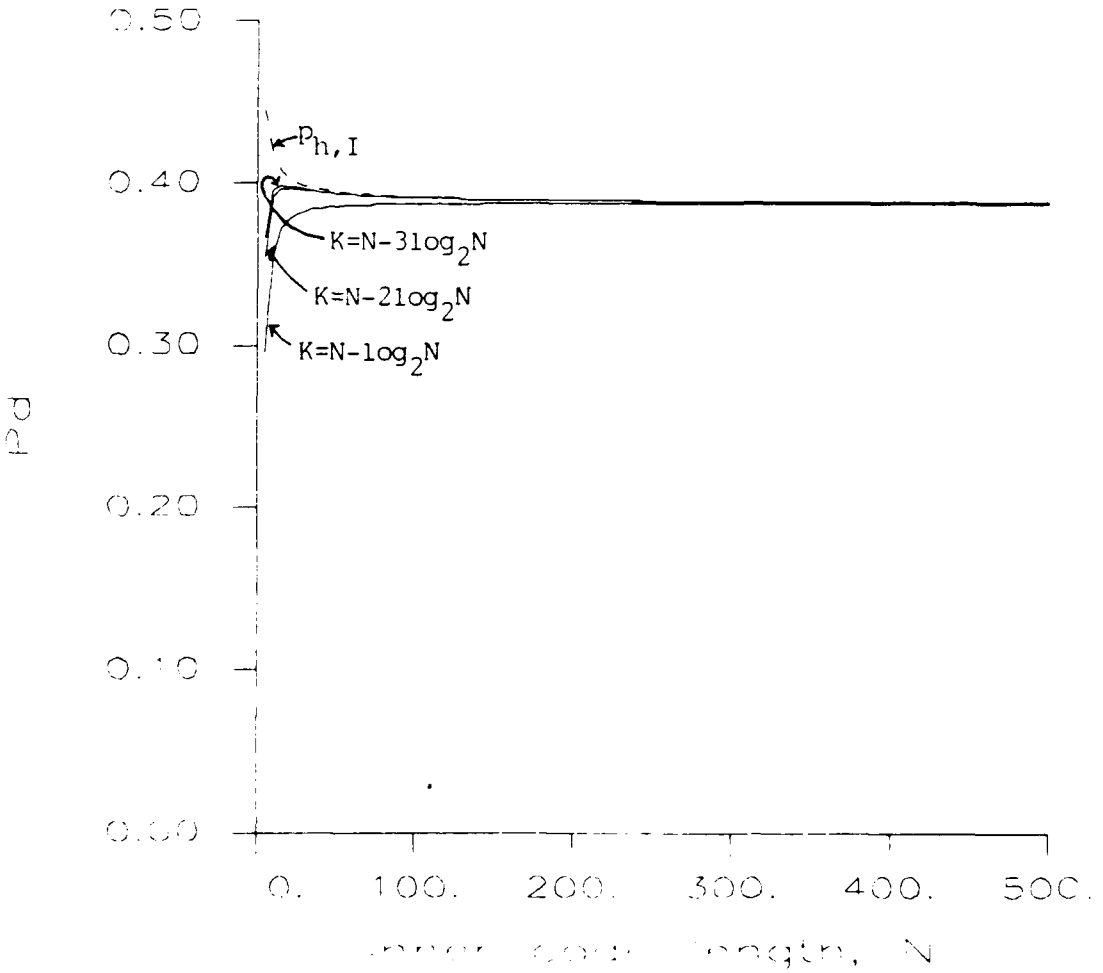

Figure 4.11: Plot of detected error probability, P_d, for several values of K (*asynchronous* frequency-hopping, $q = 100$, $I = 50$).

$\hat{P}_d$, can be obtained from (4.33) and (4.36) as follows:

$$\begin{aligned} P_{ud} &\leq \hat{P}_{ud} \\ \Longrightarrow K &\leq \log_2\left(\frac{\hat{P}_{ud}}{p_{h,I}}\frac{N(N+1)2^{N-1}}{(N+1)2^{-N+2}-N2^{-N+1}-2^{-N}+0.5(N-1)(N+2)-2}\right) \\ \Longrightarrow R &\leq \frac{1}{N}\log_2\left(\frac{\hat{P}_{ud}}{p_{h,I}}\frac{N(N+1)2^{N-1}}{(N+1)2^{-N+2}-N2^{-N+1}-2^{-N}+0.5(N-1)(N+2)-2}\right) \\ &\triangleq R_{ud}, \end{aligned} \tag{4.37}$$

and

$$\begin{aligned} P_d &\geq \hat{P}_d \\ \Longrightarrow K &\leq \log_2\left(\frac{N(N+1)2^{N-1}(1-\hat{P}_d/p_{h,I})+2N+3-3\cdot 2^N}{(N+1)2^{-N+2}-N2^{-N+1}-2^{-N}+0.5(N-1)(N+2)-2}\right) \\ \Longrightarrow R &\leq \frac{1}{N}\log_2\left(\frac{N(N+1)2^{N-1}(1-\hat{P}_d/p_{h,I})+2N+3-3\cdot 2^N}{(N+1)2^{-N+2}-N2^{-N+1}-2^{-N}+0.5(N-1)(N+2)-2}\right) \\ &\triangleq R_d. \end{aligned} \tag{4.38}$$

Therefore,

$$\begin{aligned} R &\leq \min(R_{ud}, R_d) \\ &= \begin{cases} R_{ud}, & \hat{P}_{ud}+\hat{P}_d \leq p_{h,I}(1-\frac{3\cdot 2^N-2N-3}{N(N+1)2^{N-1}}) \\ R_d, & \hat{P}_{ud}+\hat{P}_d > p_{h,I}(1-\frac{3\cdot 2^N-2N-3}{N(N+1)2^{N-1}}). \end{cases} \end{aligned} \tag{4.39}$$

Figures 4.12 and 4.13 show the maximum allowable code rate to satisfy the requirement $P_{ud} \leq \hat{P}_{ud}$ and $P_d \geq \hat{P}_d$ respectively. By comparing Figures 4.4 - 4.7 and 4.10 - 4.13 it can be observed that the reliability of the side information for the asynchronous frequency-hopping system is *slightly lower* than that for the synchronous frequency-hopping system, but as the inner block length increases the difference between them decreases and approaches to zero.

If the number of redundancy bits of the inner code, $N-K$, is of length $\log_2 N$, then the code rate R is given by

$$\begin{aligned} R &= \frac{N-\log_2 N}{N} \\ &\rightarrow 1, \end{aligned} \tag{4.40}$$

and the probability of undetected error is given by

$$\begin{aligned} P_{ud} &= \frac{2p_{h,I}}{N^2(N+1)}\left|(N+1)2^{-N+2}-N2^{-N+1}-2^{-N}+0.5(N-1)(N+2)-2\right| \\ &\rightarrow 0, \end{aligned} \tag{4.41}$$

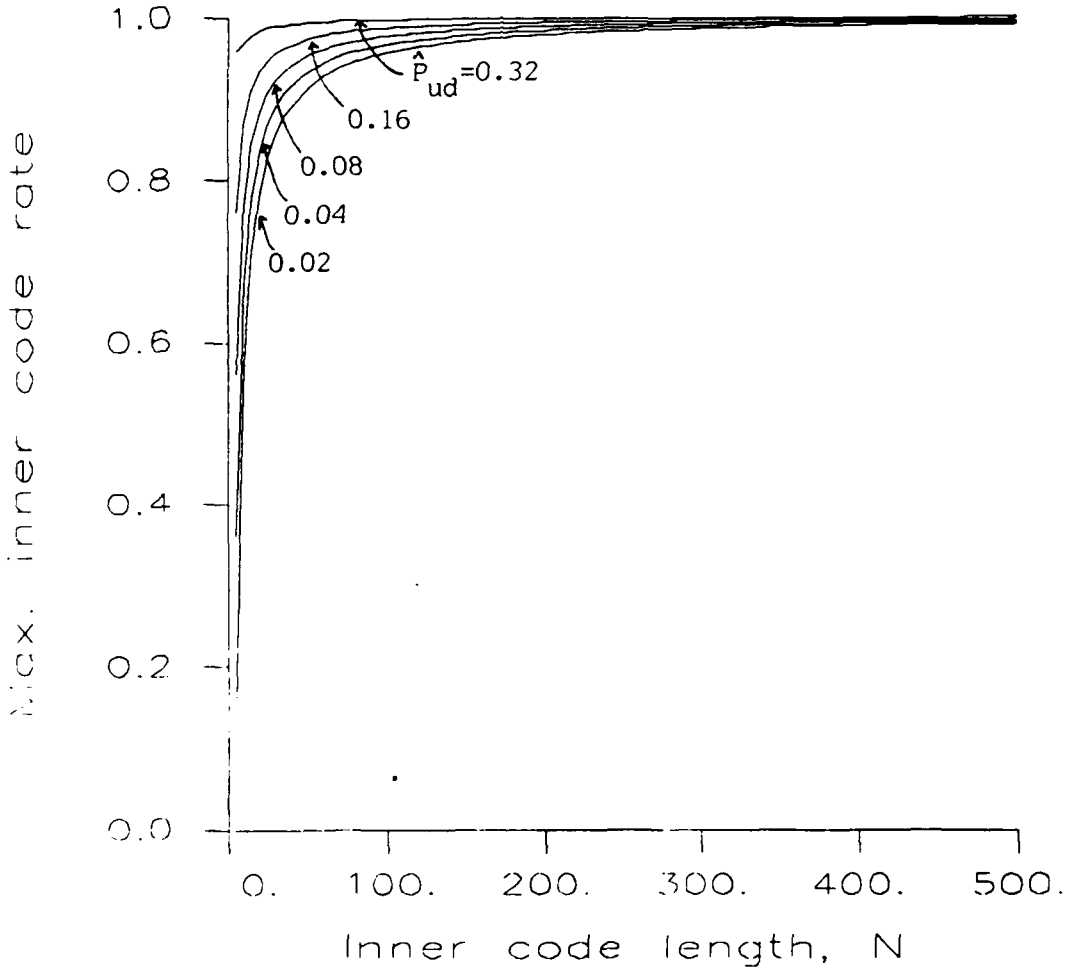

Figure 4.12: The maximum allowable code rate to satisfy $P_{ud} \leq \hat{P}_{ud}$ (*asynchronous* frequency-hopping, $q = 100$, $I = 50$).

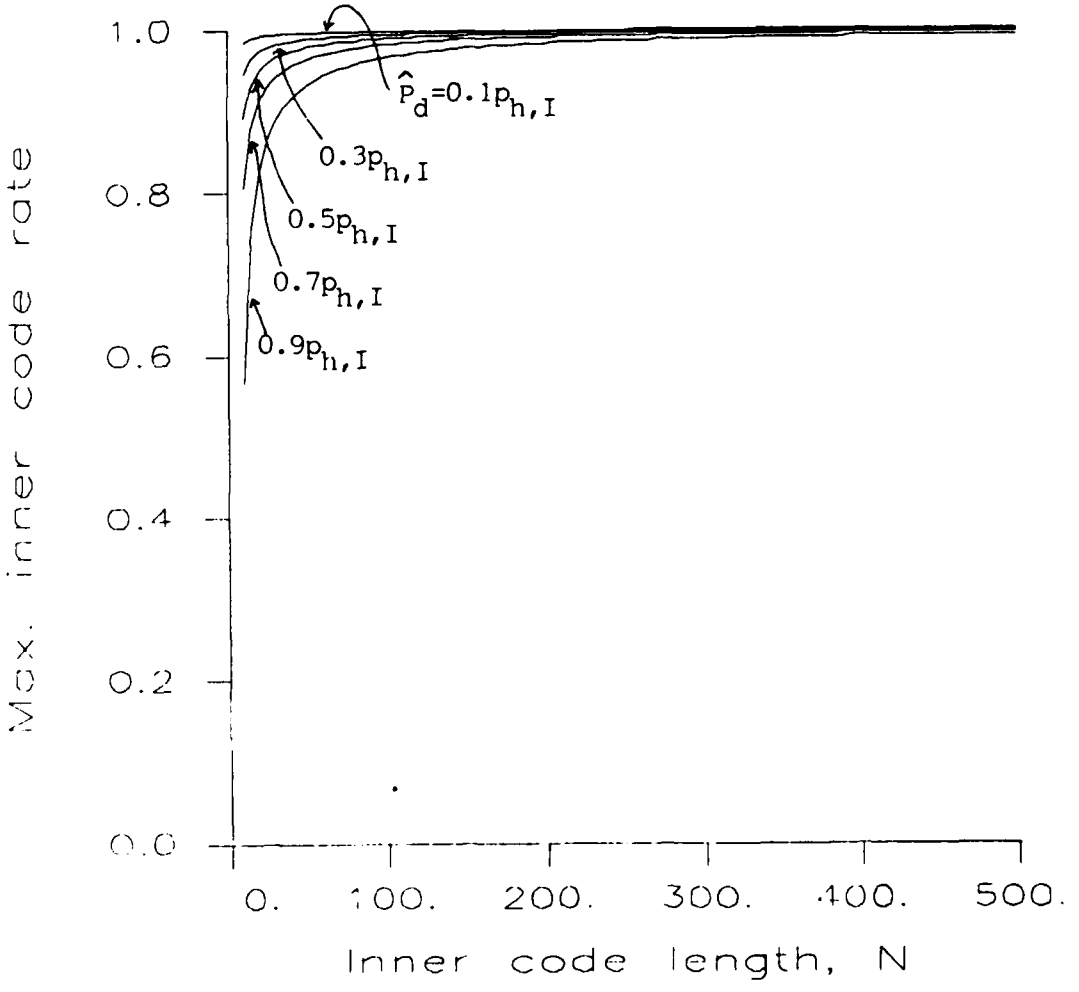

Figure 4.13: The maximum allowable code rate to satisfy $P_d \geq \hat{P}_d$ (*asynchronous* frequency-hopping, $q = 100$, $I = 50$).

and the probability of detected error is given by

$$\begin{aligned} P_d &= p_{h,I}[1 - \tfrac{2}{N(N+1)}\{N2^{-N+1} - (N+1)2^{-N+2} + 2^{-N} + 3\} \\ &\quad - \tfrac{2}{N^2(N+1)}\{(N+1)2^{-N+2} - N2^{-N+1} - 2^{-N} + 0.5(N-1)(N+2) - 2\}] \\ &\rightarrow p_{h,I}, \end{aligned} \tag{4.42}$$

as $N \rightarrow \infty$. This shows that as in synchronous frequency-hopping systems perfect side information can be obtained from the inner code *without* any loss in the inner code rate as $N \rightarrow \infty$.

Therefore, the asymptotic normalized achievable region and the normalized throughput are the same as those that can be obtained with perfect side information, That is,

$$\begin{aligned} rR &< \tfrac{K}{N}(1 - P_d - 2P_{ud}) \\ &\rightarrow (1 - p_h)^{I-1} \\ &\rightarrow e^{-\lambda}, \end{aligned} \tag{4.43}$$

and

$$\begin{aligned} W &= \tfrac{K}{N}\tfrac{I}{q}(1 - P_d - 2P_{ud}) \\ &\rightarrow \tfrac{I}{q}(1 - p_h)^{I-1} \\ &\rightarrow \lambda e^{-\lambda}, \end{aligned} \tag{4.44}$$

since

$$\begin{aligned} p_h &= \tfrac{1}{q}[1 + \tfrac{1}{N}(1 - \tfrac{1}{q})] \\ &\rightarrow \tfrac{1}{q}, \end{aligned}$$

as $N \rightarrow \infty$.

4.4. Diversity / RS code

The simplest type of block code allowing a variable amount of redundancy is the repetition code, often called *diversity*. With this code a single information symbol is encoded into a block of L identical symbols, producing an $(L, 1)$

code. Each symbol is transmitted during a single hop, so that L diversities are transmitted over the L hops. When diversity and perfect side information are employed, the inner decoder (diversity decoder) can ignore the diversity receptions that have been hit and it can extract the data from the interference-free diversity receptions. If all the diversity receptions of a symbol are hit, they are erased. The RS outer code will correct the erasures if the number of erasures produced by the inner code is within the erasure correction capability. When there is no side information, the inner decoder (a maximum likelihood decoder) counts the number of times each symbol was received and chooses the one that had the largest count, as the transmitted symbol. The RS outer code in this case will correct the errors produced by the inner decoder if the number of them is within the error correction capability.

4.4.1. Perfect Side Information

If the perfect side information is available at the receiver, a given symbol will be erased if all of its L diversity transmissions are hit: otherwise, the symbol is correctly received. In this case the probability of symbol erasure given I users, denoted $P_{I,L}$, is given by

$$P_{I,L} = [1 - (1 - p_h)^{I-1}]^L. \tag{4.45}$$

The induced super channel is an M-ary erasure channel with transition probability $P_{I,L}$ and $M = M_i = M_o$. See Figure 4.14.

Achievable Region

Since the input symbol to the (n, k) RS outer decoder is erasure with probability $P_{I,L}$ and the erasures at different hop durations are conditionally independent

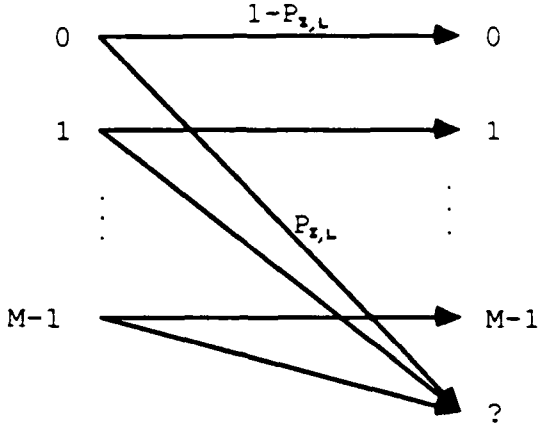

Figure 4.14: M-ary erasure channel, L diversity, perfect side information.

given I, the probability of correctly decoding a codeword (packet), $P_c(I)$, is given by

$$P_c(I) = \sum_{j=0}^{n-k} \binom{n}{j} P_{I,L}^j (1 - P_{I,L})^{n-j}. \tag{4.46}$$

As $n, k \to \infty$ while $r \triangleq k/n$ is held constant, it can be shown (see Appendix A) that $P_c(I)$ will remain 1 as long as

$$\begin{aligned} r &< 1 - P_{I,L} \\ &= 1 - [1 - (1 - p_h)^{I-1}]^L. \end{aligned} \tag{4.47}$$

Thus the asymptotic normalized achievable region of overall code rate and channel traffic is given by

$$\begin{aligned} rR &< \frac{1-[1-(1-p_h)^{I-1}]^L}{L} \\ &\to \frac{1-(1-e^{-\eta\lambda})^L}{L}, \end{aligned} \tag{4.48}$$

as $I, q \to \infty$ with $\lambda \triangleq I/q$ held constant. Figure 4.15 shows the asymptotic normalized achievable regions for various diversity levels. We can see that the optimum diversity level that maximizes the asymptotic normalized achievable

region is 1 for all channel traffic. Figure 4.16 show the variations of the normalized achievable regions as q increases. We can see that the asymptotic formula ($q = \infty$) gives a very close approximation even for small values of q.

Solving (4.47) in terms of I we can obtain the maximum number of simultaneous transmissions given by

$$I < 1 + \frac{\ln(1-(1-r)^{\frac{1}{L}})}{\ln(1-p_h)}. \tag{4.49}$$

As q approaches infinity, the asymptotic maximum number of simultaneous transmissions per frequency slot, $\lambda \triangleq I/q$, becomes

$$\lambda < \frac{1}{\eta} \ln(1-(1-r)^{\frac{1}{L}})^{-1}. \tag{4.50}$$

For the case of finite n, an approximate achievable region of channel traffic and outer code rate for $P_c(I) \geq 1 - \hat{P}_E$ is given by

$$r \leq 1 - P_{I,L} - \alpha\sqrt{P_{I,L}(1-P_{I,L})/n}, \tag{4.51}$$

which is obtained from the Gaussian approximation of $P_c(I)$ given in (4.46). The normalized achievable region can be obtained by dividing by L.

Throughput

From (4.8) and (4.49) the asymptotic normalized throughput is given by

$$\begin{aligned} W &= \frac{r\, I\, P_c(I)}{Lq} \\ &= \frac{r}{Lq}\left[1 + \frac{\ln(1-(1-r)^{\frac{1}{L}})}{\ln(1-p_h)}\right] \\ &\rightarrow \frac{r\ln(1-(1-r)^{\frac{1}{L}})^{-1}}{\eta L}, \end{aligned} \tag{4.52}$$

as $q \rightarrow \infty$. Figure 4.17 shows the asymptotic normalized throughputs in terms of the outer code rate r for various values of L. We can see that the *overall* optimum diversity level that maximizes the normalized throughput is 1, but the optimum

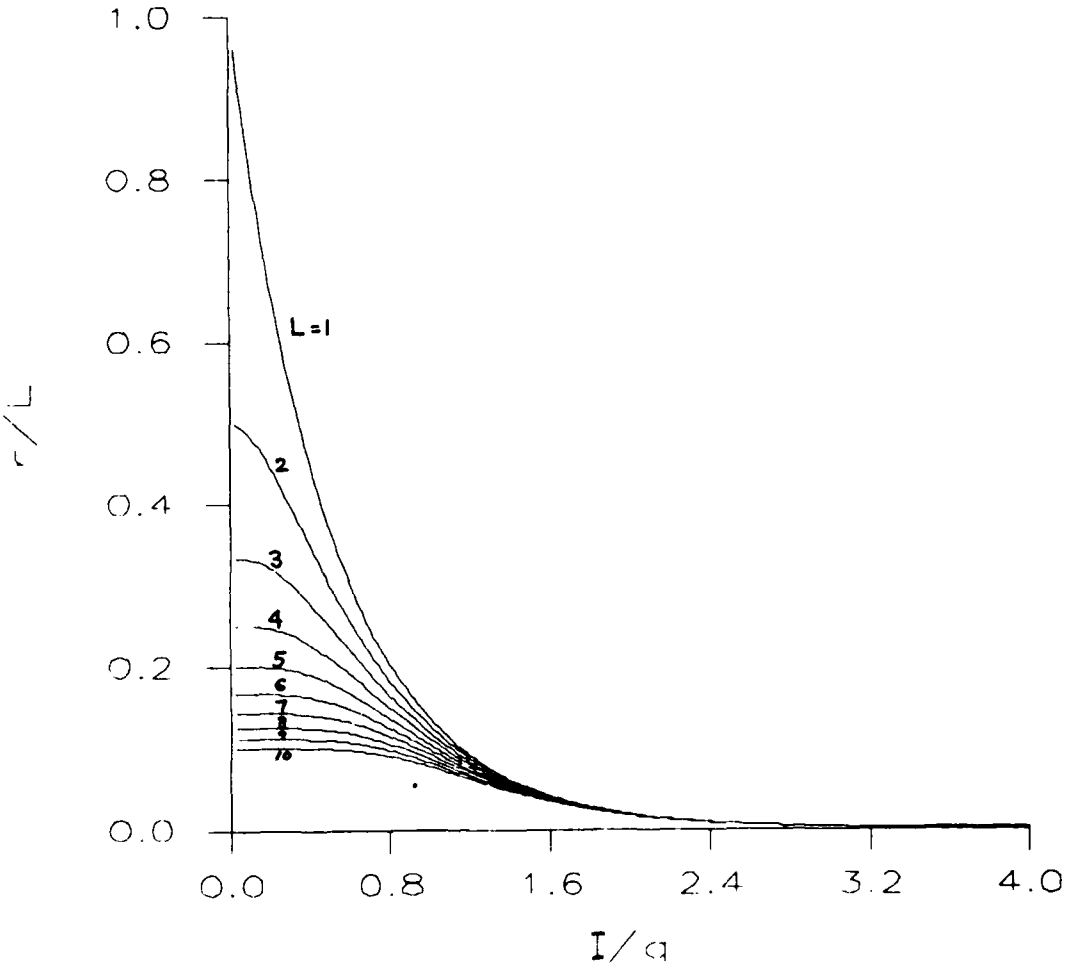

Figure 4.15: Achievable region of $(r/L, I/q)$ for various values of diversity levels L, *asynchronous* frequency-hopping, *perfect* side information.

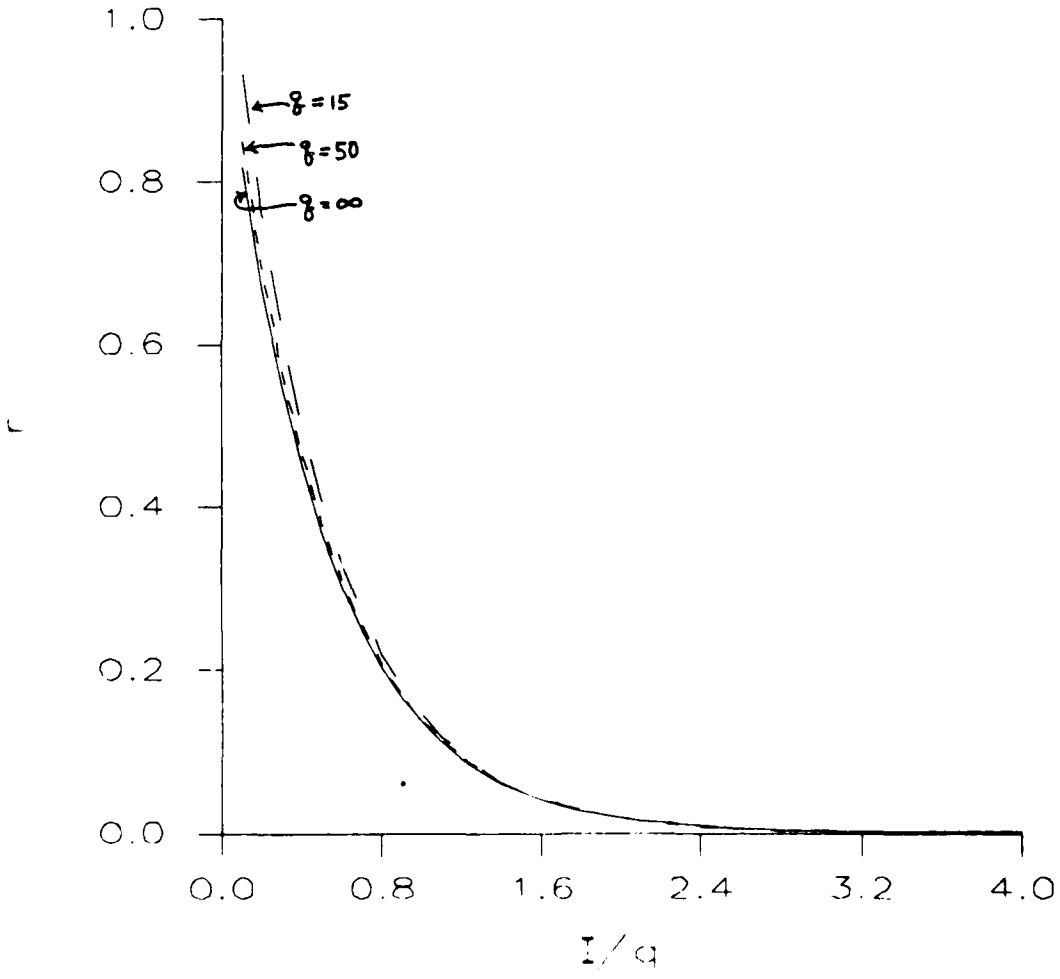

Figure 4.16: Variations of the achievable regions in terms of various values of q, *asynchronous* frequency-hopping, *perfect* side information, L=1.

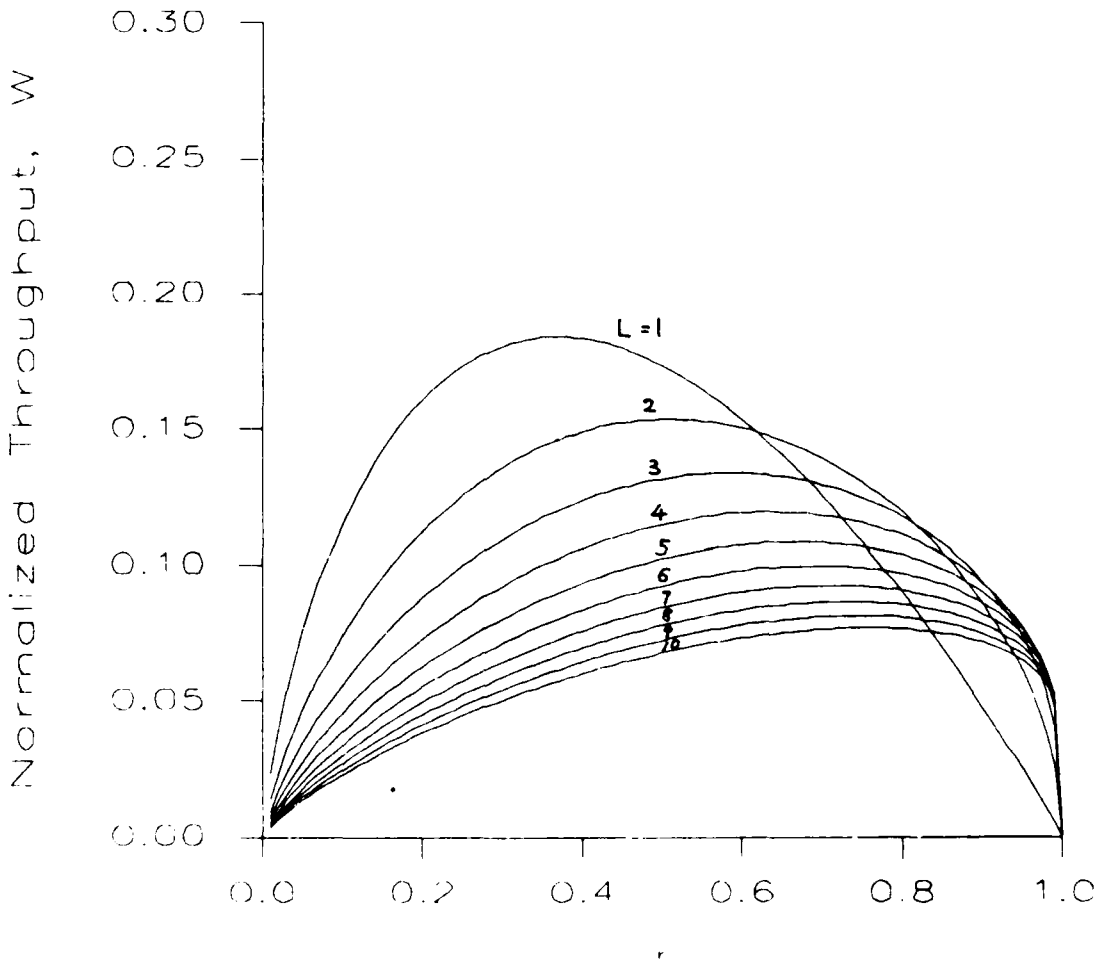

Figure 4.17: Plot of W vs. r for various values of L, *asynchronous* frequency-hopping, *perfect* side information.

deversity level is changed for different ranges of outer code rate. Figure 4.17 will be useful when decoding complexity should be considered in designing a system, because the decoding complexity of a code of rate r is proportional to $(1-r)^2$, and in some high performance applications the extreme decoding complexity may make the system impractical to build. For example, for the coding system used for deep space communication by NASA ((255,223) RS code), we can see that the optimum diversity level is 3.

4.4.2. No Side Information

When there is no side information the demodulator makes an estimate (hard decision) on the received signal, and the inner decoder (a maximum likelihood decoder) counts the number of times each symbol was received and chooses the one that had the largest count, as the transmitted symbol. In this way the inner decoder corrects some errors and passes its output to the outer decoder. However, not all errors can be corrected by the inner decoder, so there is a nonzero probability of uncorrected error. The probability of (uncorrected) error with diversity L, $P_{L,e}$, on the M-ary symmetric channel with transition probability $p_{e,I}/(M-1)$ is derived in [Sta 85] by assuming that the conditional probability of symbol error given hit is $1-1/M$. If we let $p \triangleq p_{e,I}$ and $\bar{p} \triangleq 1-p_{e,I}$, then for large enough M, $P_{L,e}$ is given by

$$\begin{aligned}
P_{1,e} &= p \\
P_{2,e} &= p \\
P_{3,e} &= 1-\bar{p}^3-3\bar{p}^2p-\bar{p}p^2 \\
P_{4,e} &= 1-\bar{p}^4-4\bar{p}^3p-6\bar{p}^2p^2-\bar{p}p^3 \\
P_{5,e} &= 1-\bar{p}^5-5\bar{p}^4p-10\bar{p}^3p^2-10\bar{p}^2p^3-\bar{p}p^4 \\
P_{6,e} &= 1-\bar{p}^6-6\bar{p}^5p-15\bar{p}^4p^2-20\bar{p}^3p^3-15\bar{p}^2p^4-\bar{p}p^5 \\
P_{7,e} &= 1-\bar{p}^7-7\bar{p}^6p-21\bar{p}^5p^2-35\bar{p}^4p^3-35\bar{p}^3p^4-21\bar{p}^2p^5-\bar{p}p^6.
\end{aligned} \tag{4.53}$$

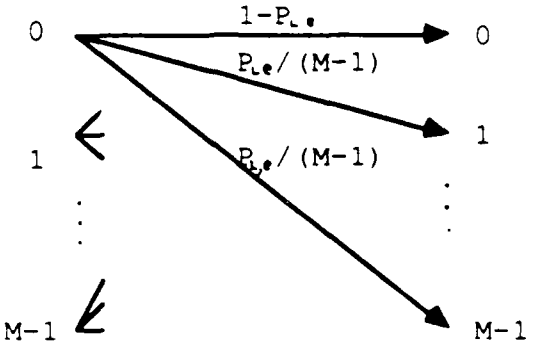

Figure 4.18: M-ary symmetric channel, L diversity, no side information.

The induced super channel is an M-ary symmetric channel with transition probability $P_{L,e}/(M-1)$ and $M = M_i = M_o$. See Figure 4.18.

Achievable Region

Since the input symbol to the RS outer decoder is in error with probability $P_{L,e}$, the probability of correctly decoding a codeword (packet) given I simultaneous transmissions $P_c(I)$ is given by

$$P_c(I) = \sum_{j=0}^{\lfloor (n-k)/2 \rfloor} \binom{n}{j} P_{L,e}^j (1 - P_{L,e})^{n-j}. \tag{4.54}$$

As $n, k \to \infty$ while $r \triangleq k/n$ is held constant, it can be shown that $P_c(I)$ will remain 1 as long as

$$r < 1 - 2P_{L,e}. \tag{4.55}$$

The asymptotic normalized achievable region is obtained by dividing the above by L, and is plotted for various values of L in Figure 4.19. We notice that the optimum diversity level depends on the channel traffic, which is not the case when perfect side information is available.

For the case of finite n, the approximate achievable region of channel traffic and outer code rate for $P_c(I) \geq 1 - \hat{P}_E$ is given by

$$r \leq 1 - \frac{2}{n}\lceil nP_{L,e} + \alpha\sqrt{nP_{L,e}(1 - P_{L,e})}\rceil, \tag{4.56}$$

which is obtained from the Gaussian approximation of $P_c(I)$ given in (4.54). The normalized achievable region can be obtained by dividing by L.

Throughput

From (4.8) and (4.55) the asymptotic normalized thrpughput is given by

$$\begin{aligned} W &= \frac{r\,I\,P_c(I)}{Lq} \\ &= \frac{I(1-2P_{L,e})}{Lq}. \end{aligned}$$

Figure 4.20 shows the asymptotic normalized throughputs in terms of code rate r for various values of L. As in perfect side information, we can see that the *overall* optimum diversity level that maximizes the throughput is 1, but the optimum diversity level is a function of outer code rate.

AD-A185 667 CODING FOR SPREAD-SPECTRUM COMMUNICATIONS NETWORKS(U) 2/2
MICHIGAN UNIV ANN ARBOR COMMUNICATIONS AND SIGNAL
PROCESSING LAB B G KIM MAR 87 022793-2-T
UNCLASSIFIED N00014-85-K-0545 F/G 25/2 NL

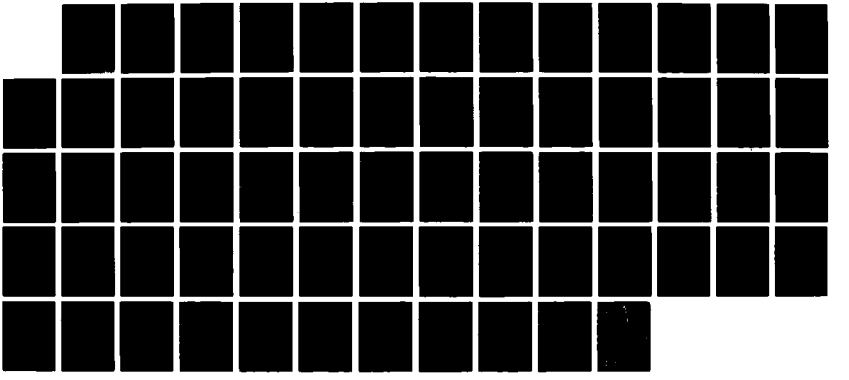

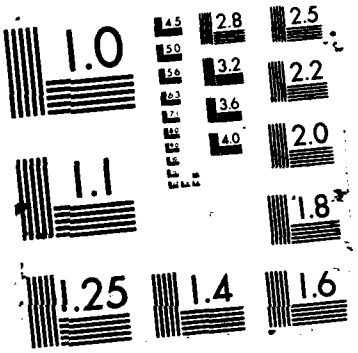
1.0
1.1
1.25
1.4
1.6
1.8
2.0
2.2
2.5
2.8
3.2
3.6
4.0
4.5
5.0
5.6
6.3
7.1
8.0

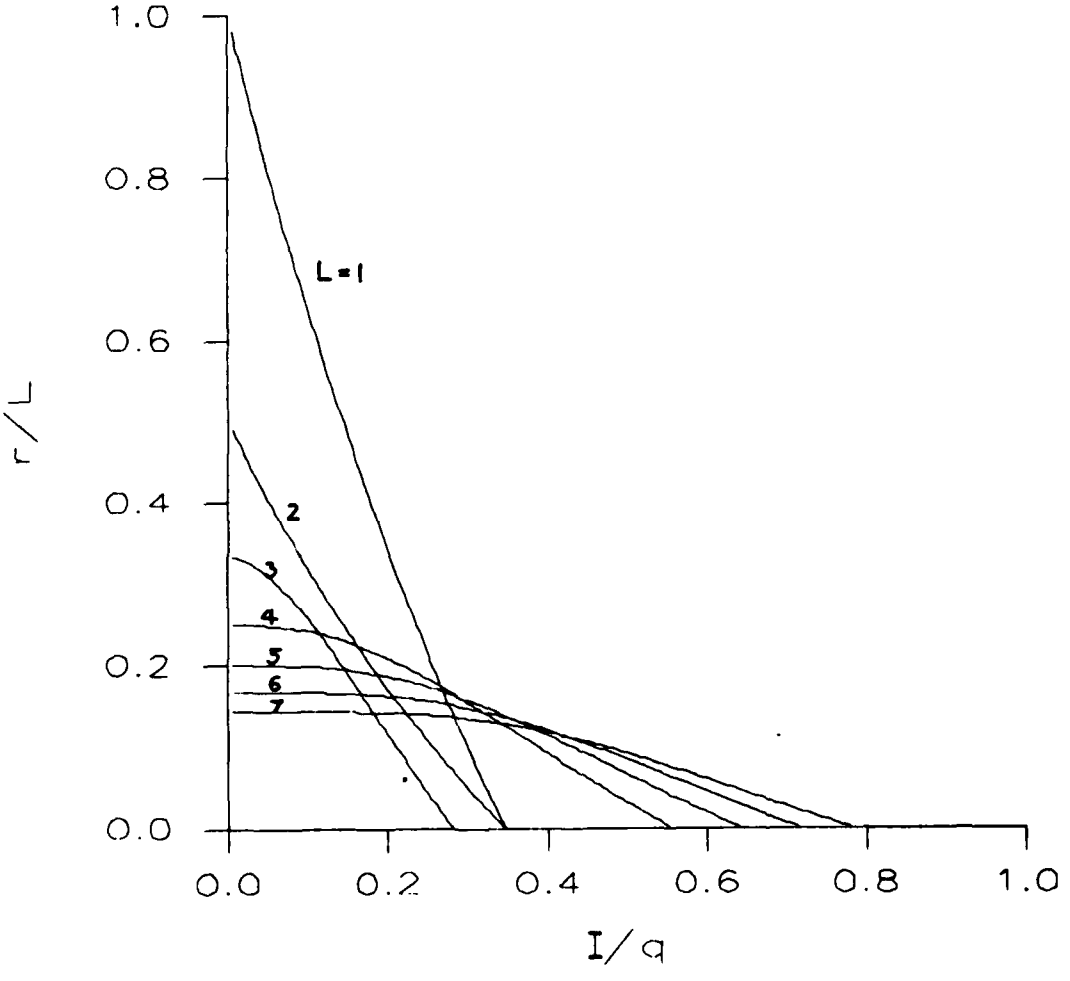

Figure 4.19: Achievable region of $(r/L, I/q)$ for various values of diversity levels L, *asynchronous* frequency-hopping, *no* side information.

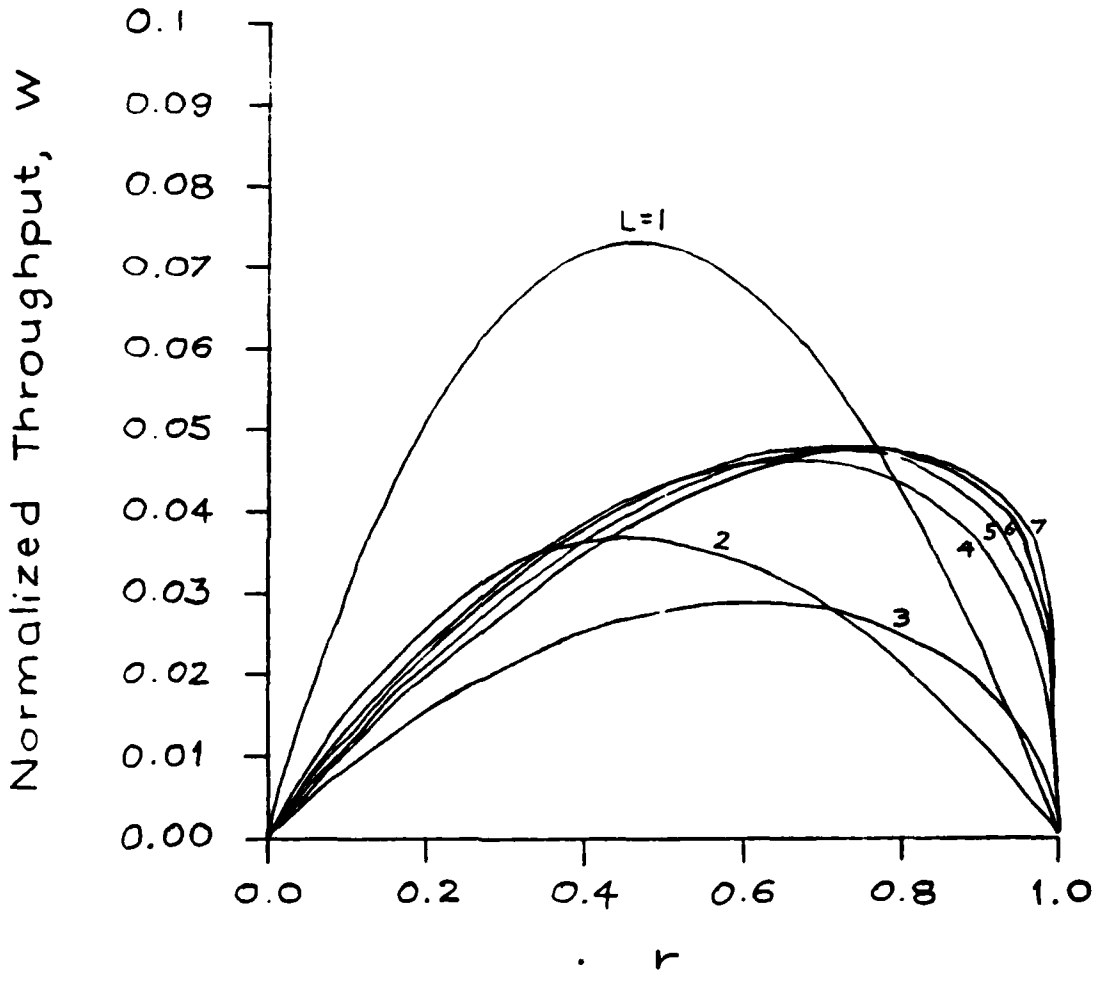

Figure 4.20: Plot of W vs. r for various values of L, *asynchronous* frequency-hopping, *no* side information.

CHAPTER V

PARALLEL DECODING FOR IMPERFECT SIDE INFORMATION

5.1. Introduction

In section 3.2 we have considered the achievable regions and throughputs of frequency-hopping (FH) multiple-access systems for which perfect side information is available at the receiver. In practice, however, the assumption regarding the perfect side information is only approximately true. In this chapter this assumption is relaxed, and we consider the performance of the FH multiple-access systems which has *imperfect* side information at the receiver.

The purpose of the side information is to determine which received symbols are to be erased. The side information regarding the presence of hit is extracted from the dehopper and demodulator. However, there is a chance that some symbols with interference will be missed (miss) and other symbols which have no interference will be erased (false alarm). We define P_F as the probability that the demodulator produces the erasure symbol given the symbol was "not hit" and P_M as the probability that the demodulator does not produce the erasure symbol given the symbol was "hit". Then P_M and P_F give us a measure of the "imperfectness" of the side information: for example, $P_M = P_F = 0$ corresponds

to the perfect side information case, and $P_M = 1, P_F = 0$ corresponds to the no side information case, because the demodulator never produces the erasure symbol when there is no side information. Thus, perfect side information and no side information are a special case of the imperfect side information.

In this chapter we assume that only imperfect side information is available at the demodulator. The demodulator decides first whether to erase the received signal or not based on the side information given to it. If the received signal is not erased, it is further processed to get the estimate of the transmitted signal. We will consider two different models for the demodulator.

The demodulator output is, in general, a sequence of errors, erasures, and correct symbols. In order to correct the errors and erasures we employ a Reed-Solomon code, and consider two different decoders for it: one is the errors-and-erasures decoder and the other is a parallel decoder.

The remainder of this chapter is organized as follows. In section 5.2 we introduce two demodulator models and derive the probabilities of error and erasure in terms of channel traffic for both demodulator models. In section 5.3 we compute the capacity of the component channel resulting from one demodulator model, and discuss an idea for improving the capacity. In section 5.4 we consider an errors-and-erasures decoder, and evaluate the performance of it over the imperfect side information channel. Based on the ideas given in section 5.3 and 5.4 we suggest a parallel decoding scheme and evaluate the performance of it over the imperfect side information channel. These are discussed in section 5.5.

5.2. Demodulator Models

In the first model (we call it "demodulator model 1: worst case"), if a received signal is hit, and not erased, it is demodulated to one of the M equally likely

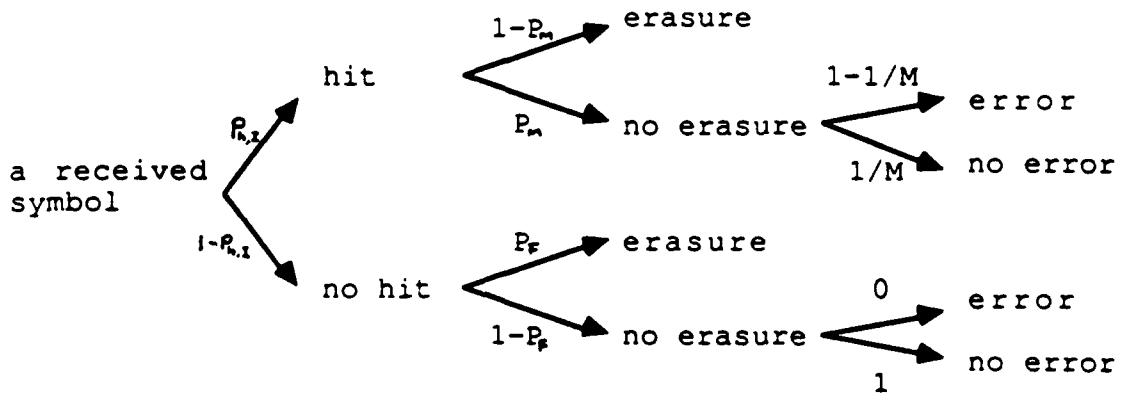

Figure 5.1: Demodulating procedures, demodulator model 1.

symbols so that the probability of symbol error is $1 - 1/M$, *independent* of the number of hits and which symbols transmitted from the interferers. If it is not hit and not erased, it is demodulated correctly. The resulting interference channel is classified as a "separated" channel by its definition given in (2.1). Demodulating procedures for demodulator model 1 are summarized in Figure 5.1, and the component channel model is shown in Figure 5.3. Thus the probability of erasure is given by

$$\begin{aligned} p_{er,I} &\triangleq \mathrm{P}(\text{erasure} \mid I \text{ users}) \\ &= \mathrm{P}(\text{erasure} \mid \text{hit}, I)\,\mathrm{P}(\text{hit} \mid I) + \mathrm{P}(\text{erasure} \mid \text{no hit}, I)\,\mathrm{P}(\text{no hit} \mid I) \\ &= (1 - P_M)p_{h,I} + P_F(1 - p_{h,I}), \end{aligned} \tag{5.1}$$

and the probability of error is given by

$$\begin{aligned} p_{e,I} &\triangleq \mathrm{P}(\text{error} \mid I \text{ users}) \\ &= \mathrm{P}(\text{error, no erasure} \mid I) + \underbrace{\mathrm{P}(\text{error, erasure} \mid I)}_{=0} \\ &= \mathrm{P}(\text{error, no erasure} \mid \text{hit}, I)\, \mathrm{P}(\text{hit} \mid I) \\ &\quad + \mathrm{P}(\text{error, no erasure} \mid \text{no hit}, I)\, \mathrm{P}(\text{no hit} \mid I) \\ &= \underbrace{\mathrm{P}(\text{error} \mid \text{no erasure, hit}, I)}_{=1-1/M}\, \mathrm{P}(\text{no erasure} \mid \text{hit}, I)\, \mathrm{P}(\text{hit} \mid I) \\ &\quad + \underbrace{\mathrm{P}(\text{error} \mid \text{no erasure, no hit}, I)}_{=0}\, \mathrm{P}(\text{no erasure} \mid \text{no hit}, I)\, \mathrm{P}(\text{no hit} \mid I) \\ &= (1 - 1/M) P_M\, p_{h,I}. \end{aligned} \tag{5.2}$$

In the second model (we call it "demodulator model 2: realistic case") both the number of hits and which symbols being transmitted from the interferers are taken into account in calculating the probability of error. If a received signal is hit by m interferers, i.e. m hits, and is not erased, the probability of symbol error, P_m, is given by (3.49). If it is not hit and not erased, it is demodulated correctly. In this case, the resulting interference channel is not separated, because the property given in (2.1) is not satisfied. Demodulating procedures for demodulator model 2 are summarized in Figure 5.2. Thus $p_{er,I}$ is the same as given in (5.1), but $p_{e,I}$ for large M is given by

$$\begin{aligned} p_{e,I} &= \mathrm{P}(\text{error} \mid I \text{ users}) \\ &= \mathrm{P}(\text{error, no erasure} \mid I) + \underbrace{\mathrm{P}(\text{error, erasure} \mid I)}_{=0} \\ &= \textstyle\sum_{m=0}^{I-1} \mathrm{P}(\text{error, no erasure} \mid m \text{ hits}, I)\, \mathrm{P}(m \text{ hits} \mid I) \\ &= \textstyle\sum_{m=0}^{I-1} \mathrm{P}(\text{error} \mid \text{no erasure}, m \text{ hits}, I) \\ &\qquad \mathrm{P}(\text{no erasure} \mid m \text{ hits}, I)\, \mathrm{P}(m \text{ hits} \mid I) \end{aligned} \tag{5.3}$$

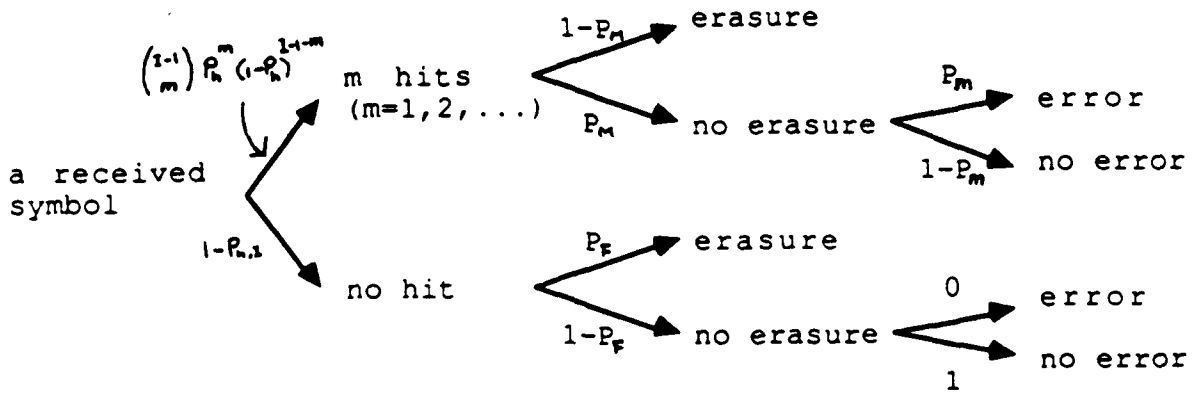

Figure 5.2: Demodulating procedures, demodulator model 2.

$$= 0 \cdot (1-P_F)(1-p_h)^{I-1} + \sum_{m=1}^{I-1} \frac{m}{m+1} P_M \begin{pmatrix} I-1 \\ m \end{pmatrix} p_h^m (1-p_h)^{I-1-m}$$

$$= P_M \left[1 - \frac{1-(1-p_h)^I}{I p_h} \right]. \tag{5.4}$$

In both models, the demodulator output is a sequence of errors, erasures, and correct symbols. Thus the component channel with imperfect side information is modeled by an M-ary errors-and-erasures channel with certain erasure probability $p_{er,I}$ and certain error probability $p_{e,I}$, which depend on P_M, P_F, and the number of simultaneous packet transmissions in a time slot. This component channel model is shown in Figure 5.3.

5.3. Component Channel Capacity

The channel capacity of an M-ary errors-and-erasures channel in information

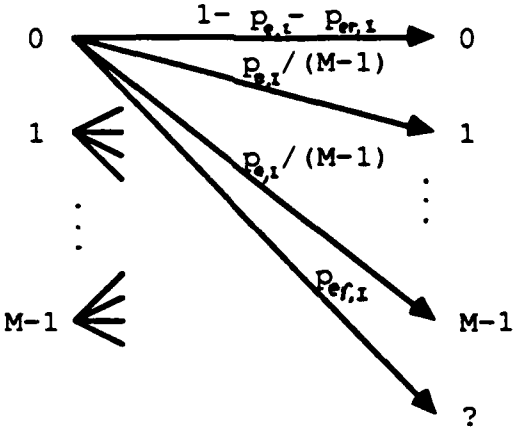

Figure 5.3: Imperfect side information channel model.

symbols per channel use is given by

$$C(I) = (1-p_{er,I}-p_{e,I}) \log_M \left(\frac{M(1-p_{er,I}-p_{e,I})}{(1-p_{er,I})} \right) + p_{e,I} \log_M \left(\frac{M p_{e,I}}{(M-1)(1-p_{er,I})} \right). \tag{5.5}$$

Notice that for $P_M = P_F = 0$ (perfect side information),

$$\begin{aligned} C(I) &= 1 - p_{er,I} \\ &= (1-p_h)^{I-1}, \end{aligned} \tag{5.6}$$

and for $P_M = 1, P_F = 0$ (no side information),

$$C(I) = (1-p_{e,I}) \log_M (M(1-p_{e,I})) + p_{e,I} \log_M (\frac{M p_{e,I}}{M-1}). \tag{5.7}$$

As mentioned in Section 5.2, since the channel resulting from demodulator model is not separated, only the channel resulting from demodulator model 1 will be considered in this section. For model 1, by applying (5.1) and (5.2) into (5.4) we

obtain

$$C(I) = (P_M p_{h,I}/M + (1-P_F)(1-p_{h,I}))\log_M\left(\frac{P_M p_{h,I}+M(1-P_F)(1-p_{h,I})}{P_M p_{h,I}+(1-P_F)(1-p_{h,I})}\right) + (P_M\frac{M-1}{M}p_{h,I})\log_M\left(\frac{P_M p_{h,I}}{P_M p_{h,I}+(1-P_F)(1-p_{h,I})}\right). \quad (5.8)$$

Figure 5.4 shows the component channel capacity in terms of the channel traffic, $\lambda = I/q$, for several values of P_M and P_F. We notice that there is a threshold in channel traffic, λ_{th}, such that for $\lambda \leq \lambda_{th}$ the channel capacity can be increased by ignoring the imperfect side information (thus do not erase) and making a hard decision demodulation of the received signals. This implies that for the lower traffic it is advantageous to make a hard decision demodulation rather than to try to make an (erroneous) erasure based on the imperfect side information. We also notice that the threshold λ_{th} increases as P_M and P_F increase, that is, as the side information becomes less reliable. On the other hand, as the alphabet set size becomes large, it can be shown from (5.4) that the component channel capacity approaches

$$\begin{aligned}\lim_{M\to\infty} C(I) &= 1 - p_{er,I} - p_{e,I} \\ &= (1-P_F)(1-p_h)^{I-1} \\ &\to (1-P_F)e^{-\eta\lambda},\end{aligned} \quad (5.9)$$

as $I, q \to \infty$ while $\lambda \triangleq I/q$ is held constant. This implies that for large enough M, the component channel capacity can be increased by ignoring the imperfect side information (thus $P_F = 0$) and making a hard decision demodulation of the received signals for all channel traffics. Notice that the resulting component channel capacity $e^{-\eta\lambda}$ is the same as that obtainable from perfect side information. It can be also noticed from (5.8) that the limiting ($M \to \infty$) value of the component channel capacity depends only on P_F (independent of P_M). This can be explained as follows. If a received signal is hit it results in either error with probability P_M (because $1 - 1/M \to 1$) or erasure with probability $1 - P_M$ (see

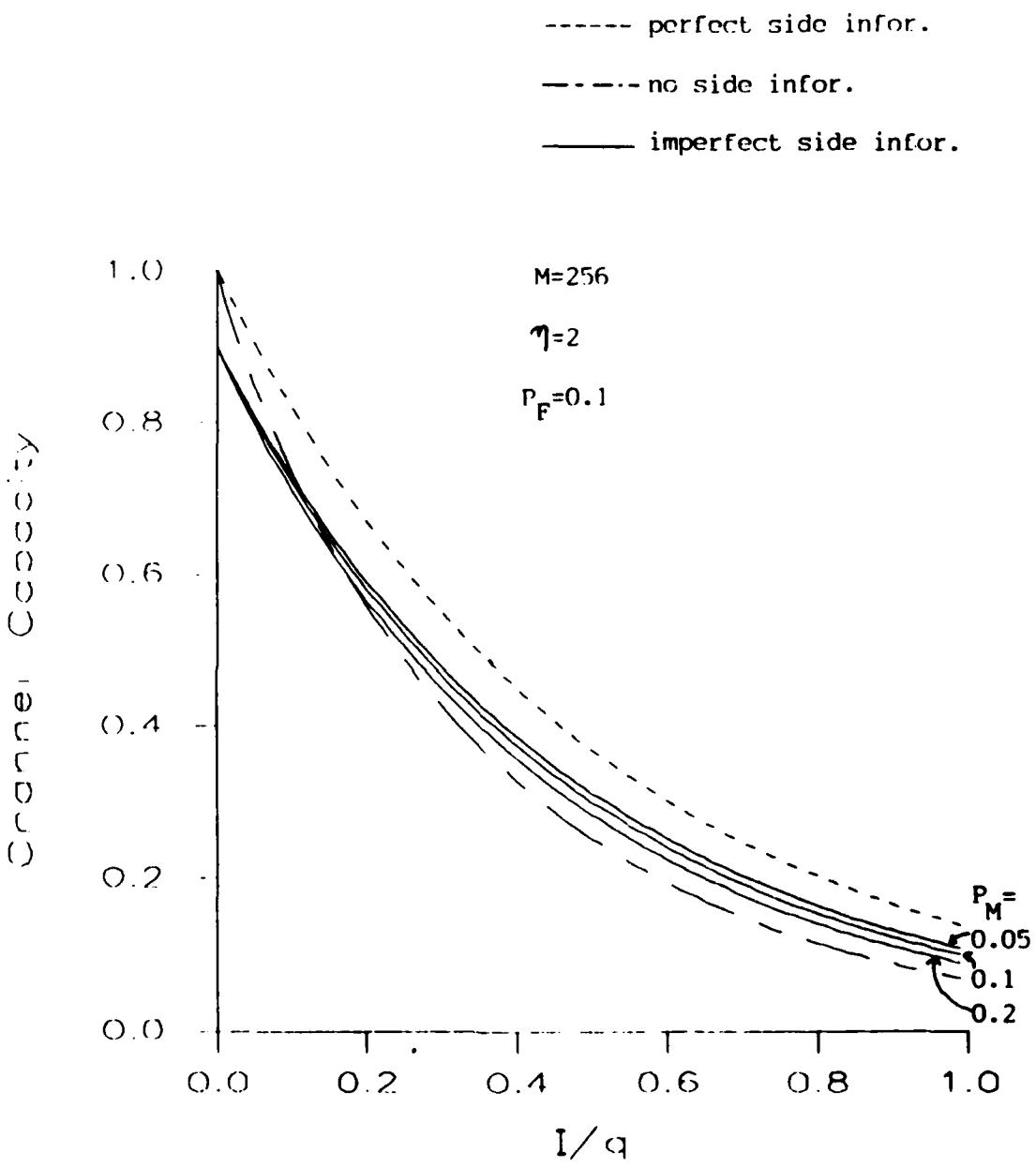

Figure 5.4: Component channel capacities vs. channel traffic.

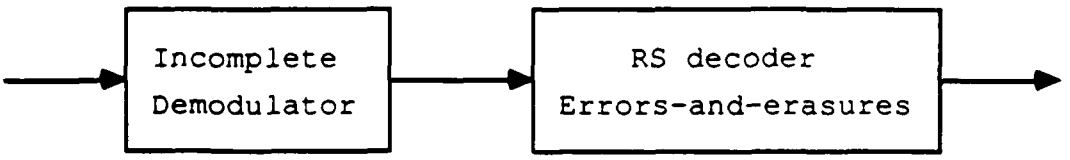

Figure 5.5: Receiver model.

Figure 5.1). However, the events of error and erasure give the *same* effect on the component channel capacity in the sense of information loss. Therefore, the component channel capacity is independent of P_M. On the other hand, when the signal is not hit, it results in erasure (i.e., information loss) with probability P_F. Therefore, the component channel capacity is a function of P_F.

5.4. Errors-and-Erasures Decoding Scheme

The block diagram of the receiver to be considered is shown in Figure 5.5. The incomplete demodulator output has an alphabet set of $\{0, 1, ..., M-1, ?\}$, and is a sequence of errors, erasures, and correct symbols. As before, let $p_{er,I}$ and $p_{e,I}$ denote the probability of symbol erasure and error given I users respectively. The RS decoder corrects the errors and erasures if the sum of the number of erasures and twice the number of errors is less than or equal to $n-k$. Therefore, the probability of correctly decoding a codeword given I simultaneous transmissions,

$P_c(I)$, is given by

$$P_c(I) = \sum_{l+2m \le n-k} \binom{n}{l,m} p_{er,I}^{l} p_{e,I}^{m} (1 - p_{er,I} - p_{e,I})^{n-l-m}. \tag{5.10}$$

Asymptotically as n and k approach infinity while the code rate $r \triangleq k/n$ is held constant, it can be shown (see Appendix C) that

$$\lim_{n,k \to \infty} P_c(I) = \begin{cases} 1, & r < 1 - p_{er,I} - 2p_{e,I} \\ 0.5, & r = 1 - p_{er,I} - 2p_{e,I} \\ 0, & r > 1 - p_{er,I} - 2p_{e,I}. \end{cases} \tag{5.11}$$

That is, "error-free" communication is possible asymptotically provided

$$r < 1 - p_{er,I} - 2p_{e,I}. \tag{5.12}$$

5.4.1. Demodulator Model 1: Worst Case

From (5.1), (5.2), and (5.11) the asymptotic achievable region of code rate and channel traffic for arbitrarily small error probability is given by

$$\begin{aligned} r &< (1 + P_M - P_F)(1 - p_h)^{I-1} - P_M \\ &\to (1 + P_M - P_F)e^{-\eta\lambda} - P_M, \end{aligned} \tag{5.13}$$

or equivalently,

$$\lambda < \frac{1}{\eta} \ln\left(\frac{1 + P_M - P_F}{r + P_M}\right), \tag{5.14}$$

as $I, q \to \infty$ while $\lambda \triangleq I/q$ is held constant.

The asymptotic normalized throughput can be obtained from (5.12) as

$$\begin{aligned} W &= \tfrac{r}{q} I\, P_c(I) \\ &\to \tfrac{I}{q}(1 - p_{er,I} - 2p_{e,I}) \\ &= \tfrac{I}{q}[(1 + P_M - P_F)(1 - p_h)^{I-1} - P_M] \\ &\to \lambda[(1 + P_M - P_F)e^{-\eta\lambda} - P_M]. \end{aligned} \tag{5.15}$$

Figures 5.6 and 5.7 show the achievable regions and the normalized throughputs for various values of P_M and P_F. We notice that as in the channel capacity case, the achievable region and the throughput can be increased by making a hard decision demodulation and error-correction decoding for the lower channel traffic.

Also, it can be shown from (5.14) that

$$\frac{\partial W}{\partial P_F} = -\lambda e^{-\eta\lambda}, \tag{5.16}$$

and

$$\frac{\partial W}{\partial P_M} = -\lambda(1 - e^{-\eta\lambda}), \tag{5.17}$$

so that

$$\frac{\partial W}{\partial P_F} \geq \frac{\partial W}{\partial P_M} \quad \text{for } \lambda \geq \frac{1}{\eta}\ln 2, \tag{5.18}$$

and

$$\frac{\partial W}{\partial P_F} < \frac{\partial W}{\partial P_M} \quad \text{for } \lambda < \frac{1}{\eta}\ln 2. \tag{5.19}$$

These imply that for $\lambda \geq \frac{1}{\eta}\ln 2$ the throughput decreases faster along the P_M axis than along the P_F axis, and for $\lambda < \frac{1}{\eta}\ln 2$ the opposite happens. The ways in which the throughput decreases as a function of P_M and P_F is shown in Figure 5.8.

Optimum code rate, optimum traffic, and maximum normalized throughput

To get the optimum channel traffic at which the normalized throughput W is maximized, we take the derivative of W w.r.t. λ, and set it to zero. This results in the following nonlinear equation:

$$e^{-\eta\lambda}(1 - \eta\lambda) = \frac{P_M}{1 + P_M - P_F}. \tag{5.20}$$

This equation will have a unique solution, because RHS is a constant between 0 and 1, and LHS is a strictly decreasing (at least from 1 to 0) function of λ as

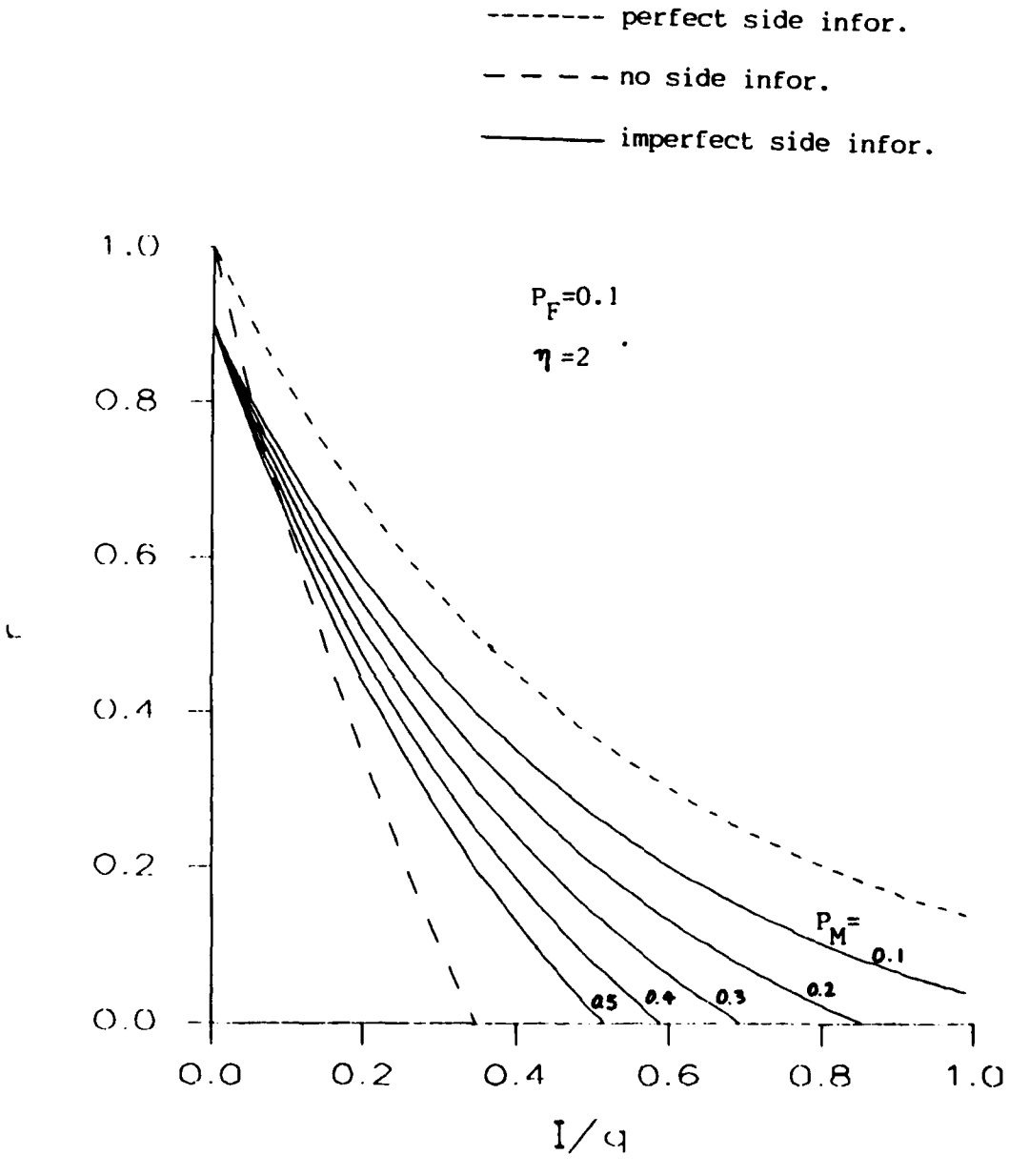

Figure 5.6: Achievable regions of code rate and channel traffic, errors-and-erasures decoding, demodulator model 1.

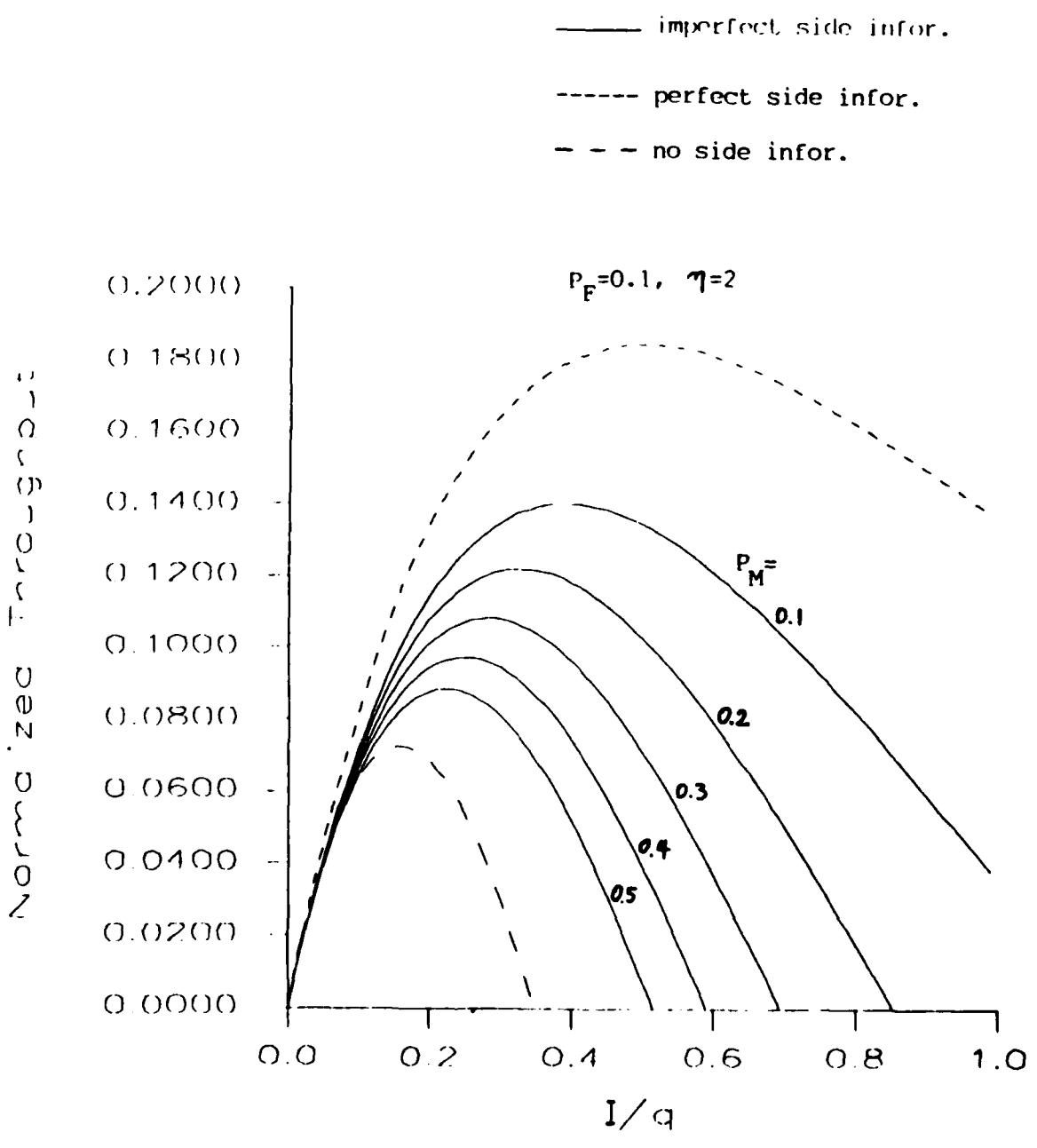

Figure 5.7: Normalized throughputs vs. channel traffic, errors-and-erasures decoding, demodulator model 1.

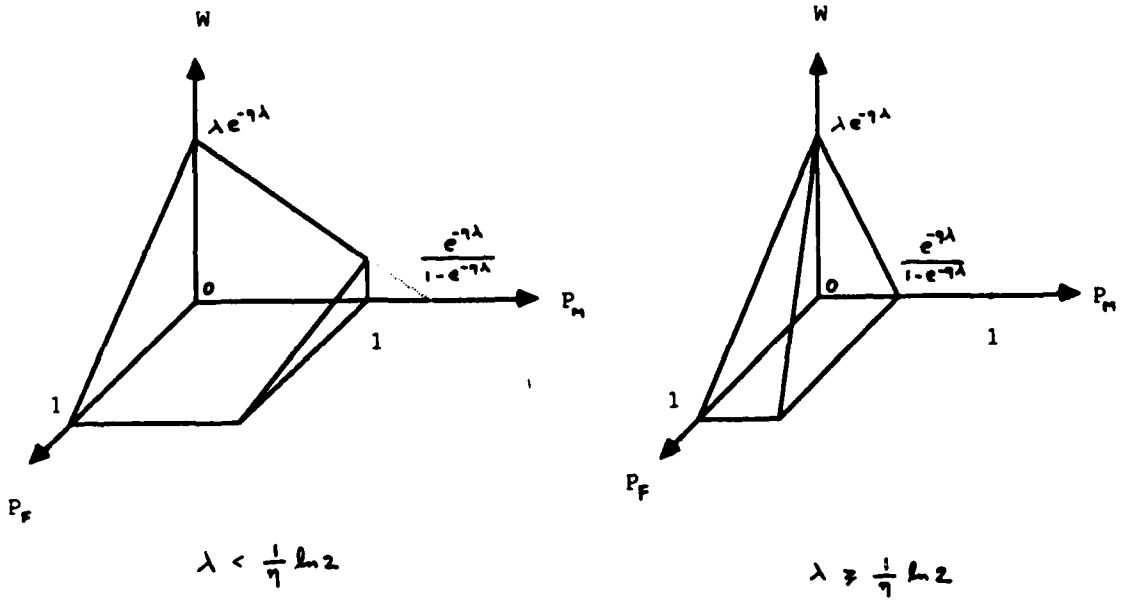

Figure 5.8: Plot of the normalized throughput vs. (P_M, P_F), errors-and-erasures decoding, demodulator model 1.

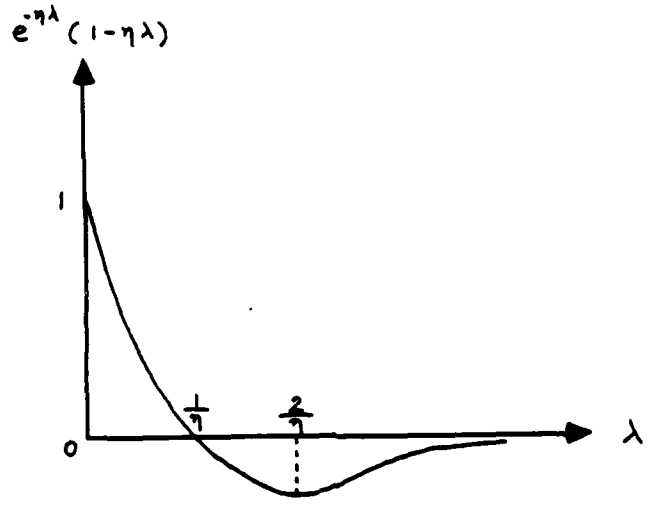

Figure 5.9: Plot of $e^{-\eta\lambda}(1-\eta\lambda)$ vs. λ.

shown in Figure 5.9. Also, by taking second derivative of W w.r.t. λ, we get

$$\frac{\partial^2 W}{\partial \lambda^2} = \eta(1 + P_M - P_F)e^{-\eta\lambda}(\eta\lambda - 2).$$

From Figure 5.9 we can see that the solution of (5.19), call it λ_{opt}, has the property $\lambda_{opt} < 1/\eta$. Thus

$$\frac{\partial^2 W}{\partial \lambda^2} \leq 0 \quad \text{at } \lambda = \lambda_{opt}.$$

Therefore there should exist a *unique* optimum channel traffic where the normalized throughput is maximized. Thus the optimum channel traffic λ_{opt} can be found from (5.19), and at λ_{opt} the optimum code rate is obtained from (5.12) and (5.19) as

$$\begin{aligned} r_{opt} &= (1 + P_M - P_F)e^{-\eta\lambda_{opt}} - P_M \\ &= \frac{\eta P_M \lambda_{opt}}{1-\eta\lambda_{opt}}, \end{aligned} \tag{5.21}$$

and at λ_{opt} and r_{opt}, the maximum normalized throughput is given by

$$W_{max} \approx \frac{\eta P_M \lambda_{opt}^2}{1 - \eta\lambda_{opt}}. \tag{5.22}$$

In Table 5.1 we list W_{max}, r_{opt}, and λ_{opt} for various values of P_M and P_F.

For the case of finite block length codes, $P_c(I)$ can be approximated as (see Appendix C)

$$P_c(I) \approx F\left(\frac{n-k-m}{\sigma}\right), \tag{5.23}$$

where

$$\begin{aligned} m &\triangleq n(p_{er,I} + 2p_{e,I}) \\ \sigma^2 &\triangleq n(p_{er,I} - p_{er,I}^2 + 4p_{e,I} - 4p_{e,I}^2 - 4p_{er,I}p_{e,I}). \end{aligned} \tag{5.24}$$

Therefore the achievable region for $P_c(I) \geq 1 - \hat{P}_E$ is approximately given by

$$r \leq (1 - p_{er,I} - 2p_{e,I}) - \alpha\sqrt{(p_{er,I} - p_{er,I}^2 + 4p_{e,I} - 4p_{e,I}^2 - 4p_{er,I}p_{e,I})/n}. \tag{5.25}$$

λ_{opt}

p_m \ p_e	0.0	0.1	0.2	0.3	0.4	0.5	0.6	0.7	0.8	0.9	1.0
0.0	0.500	0.500	0.500	0.500	0.500	0.500	0.500	0.500	0.500	0.500	0.000
0.1	0.400	0.391	0.381	0.370	0.355	0.337	0.313	0.281	0.234	0.158	0.000
0.2	0.337	0.326	0.313	0.299	0.281	0.260	0.234	0.202	0.158	0.097	0.000
0.3	0.293	0.281	0.268	0.252	0.234	0.213	0.188	0.158	0.120	0.070	0.000
0.4	0.260	0.248	0.234	0.219	0.202	0.181	0.158	0.130	0.097	0.055	0.000
0.5	0.234	0.222	0.209	0.194	0.177	0.158	0.136	0.111	0.081	0.045	0.000
0.6	0.213	0.202	0.188	0.174	0.158	0.140	0.120	0.097	0.070	0.038	0.000
0.7	0.196	0.184	0.172	0.158	0.143	0.126	0.107	0.086	0.061	0.033	0.000
0.8	0.181	0.170	0.158	0.145	0.130	0.114	0.097	0.077	0.055	0.030	0.000
0.9	0.169	0.158	0.146	0.134	0.120	0.105	0.088	0.070	0.049	0.026	0.000
1.0	0.158	0.147	0.136	0.124	0.111	0.097	0.081	0.064	0.045	0.024	0.000

r_{opt}

p_m \ p_e	0.0	0.1	0.2	0.3	0.4	0.5	0.6	0.7	0.8	0.9	1.0
0.0	0.368	0.331	0.294	0.258	0.221	0.184	0.147	0.110	0.074	0.037	0.000
0.1	0.394	0.357	0.320	0.282	0.244	0.206	0.167	0.128	0.088	0.046	0.000
0.2	0.412	0.373	0.335	0.295	0.256	0.216	0.176	0.134	0.092	0.047	0.000
0.3	0.424	0.384	0.344	0.304	0.264	0.222	0.181	0.137	0.093	0.048	0.000
0.4	0.432	0.392	0.352	0.310	0.268	0.227	0.183	0.140	0.094	0.048	0.000
0.5	0.439	0.398	0.356	0.314	0.272	0.229	0.186	0.141	0.095	0.048	0.000
0.6	0.445	0.401	0.361	0.318	0.275	0.231	0.187	0.141	0.095	0.049	0.000
0.7	0.449	0.407	0.363	0.321	0.277	0.233	0.188	0.142	0.097	0.049	0.000
0.8	0.453	0.410	0.366	0.322	0.279	0.235	0.188	0.143	0.096	0.048	0.000
0.9	0.455	0.412	0.370	0.324	0.280	0.235	0.190	0.143	0.097	0.049	0.000
1.0	0.458	0.416	0.371	0.327	0.281	0.235	0.191	0.144	0.097	0.048	0.000

W_{max}

p_m \ p_e	0.0	0.1	0.2	0.3	0.4	0.5	0.6	0.7	0.8	0.9	1.0
0.0	0.184	0.166	0.147	0.129	0.110	0.092	0.074	0.055	0.037	0.018	0.000
0.1	0.158	0.140	0.122	0.104	0.087	0.069	0.052	0.036	0.021	0.007	0.000
0.2	0.139	0.122	0.105	0.088	0.072	0.056	0.041	0.027	0.014	0.005	0.000
0.3	0.124	0.108	0.092	0.077	0.062	0.047	0.034	0.022	0.011	0.003	0.000
0.4	0.112	0.097	0.082	0.068	0.054	0.041	0.029	0.018	0.009	0.003	0.000
0.5	0.103	0.088	0.074	0.061	0.048	0.036	0.025	0.016	0.008	0.002	0.000
0.6	0.095	0.081	0.068	0.055	0.043	0.032	0.022	0.014	0.007	0.002	0.000
0.7	0.088	0.075	0.063	0.051	0.040	0.029	0.020	0.012	0.006	0.002	0.000
0.8	0.082	0.070	0.058	0.047	0.036	0.027	0.018	0.011	0.005	0.001	0.000
0.9	0.077	0.065	0.054	0.043	0.034	0.025	0.017	0.010	0.005	0.001	0.000
1.0	0.072	0.061	0.051	0.040	0.031	0.023	0.015	0.009	0.004	0.001	0.000

Table 5.1: λ_{opt}, r_{opt}, and W_{max}, errors-and-erasures decoding, demodulator model 1, η=2.

5.4.2. Demodulator Model 2: Realistic Case

By applying (5.1) and (5.3) into (5.11), the asymptotic achievable region of code rate and channel traffic can be obtained as

$$\begin{aligned} r &< 1 - p_{er,I} - 2p_{e,I} \\ &= (1 - P_M - P_F)(1 - p_h)^{I-1} + P_M\left(\tfrac{2-2(1-p_h)^I}{Ip_h} - 1\right) \\ &\to (1 - P_M - P_F)e^{-\eta\lambda} + P_M\left(\tfrac{2}{\eta}\left(\tfrac{1-e^{-\eta\lambda}}{\lambda}\right) - 1\right), \end{aligned} \tag{5.26}$$

as $I, q \to \infty$ while $\lambda \triangleq I/q$ is held constant. Thus the asymptotic normalized throughput is obtained from (5.25) as

$$\begin{aligned} W &= \tfrac{r}{q} I P_c(I) \\ &\to \tfrac{I}{q}(1 - p_{er,I} - 2p_{e,I}) \\ &= \tfrac{I}{q}\left[(1 - P_M - P_F)(1 - p_h)^{I-1} + P_M\left(\tfrac{2-2(1-p_h)^I}{Ip_h} - 1\right)\right] \\ &\to \lambda\left[(1 - P_M - P_F)e^{-\eta\lambda} + P_M\left(\tfrac{2}{\eta}\left(\tfrac{1-e^{-\eta\lambda}}{\lambda}\right) - 1\right)\right]. \end{aligned} \tag{5.27}$$

Figures 5.10 and 5.11 show the achievable regions and the normalized throughputs for various values of P_M and P_F. We can see again that the performance can be improved by making a hard decision demodulation and error-correction decoding for the lower traffic. In Figures 5.12 and 5.13 we compare the performances obtained from the two demodulator models.

From (5.26) it can be shown that

$$\frac{\partial W}{\partial P_F} = -\lambda e^{-\eta\lambda}, \tag{5.28}$$

and

$$\frac{\partial W}{\partial P_M} = -\lambda e^{-\eta\lambda} + \frac{2}{\eta}(1 - e^{-\eta\lambda}) - \lambda, \tag{5.29}$$

so that

$$\frac{\partial W}{\partial P_F} \geq \frac{\partial W}{\partial P_M} \quad \text{for } \lambda \geq 1.594/\eta, \tag{5.30}$$

and

$$\frac{\partial W}{\partial P_F} < \frac{\partial W}{\partial P_M} \quad \text{for } \lambda < 1.594/\eta. \tag{5.31}$$

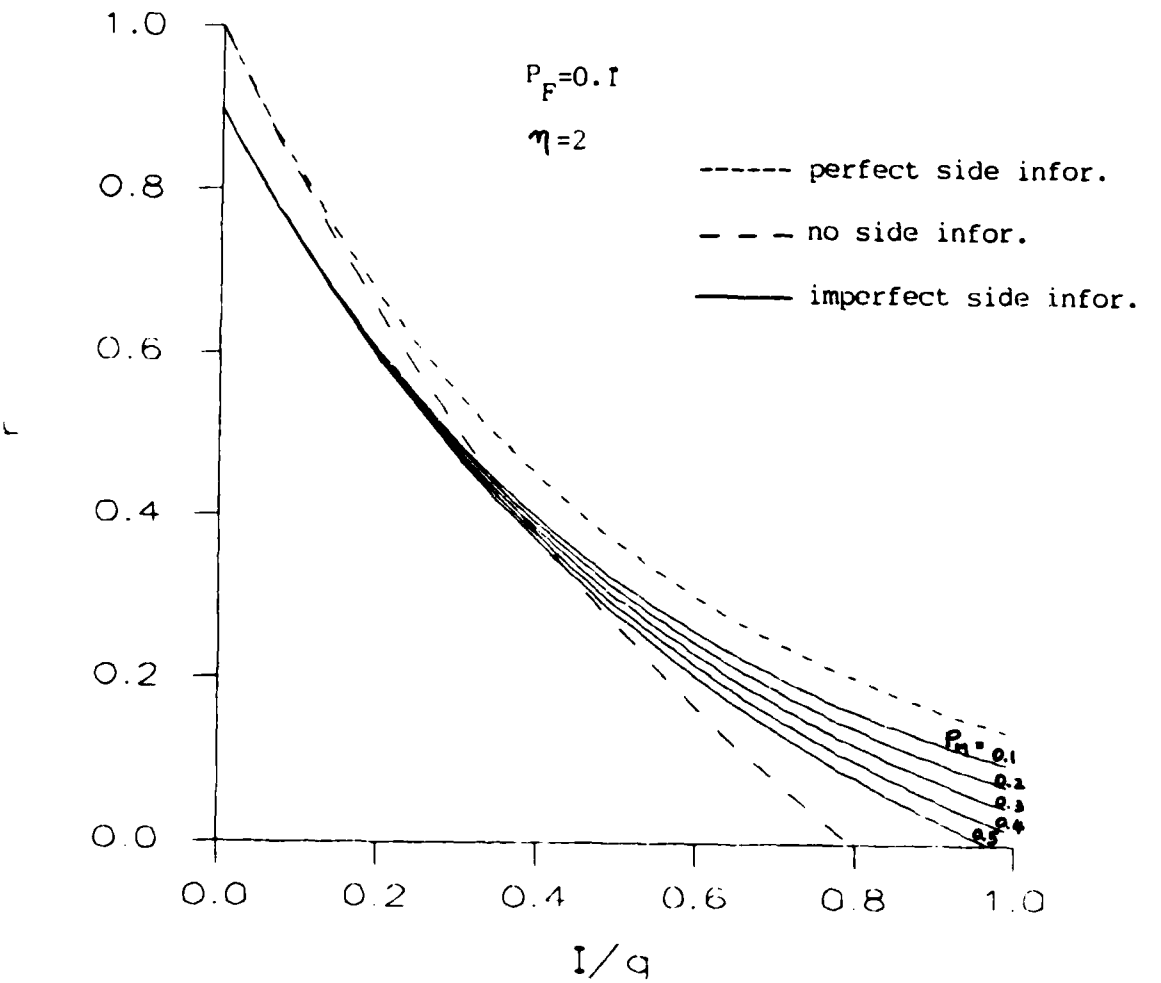

Figure 5.10: Achievable regions of code rate and channel traffic, errors-and-erasures decoding, demodulator model 2.

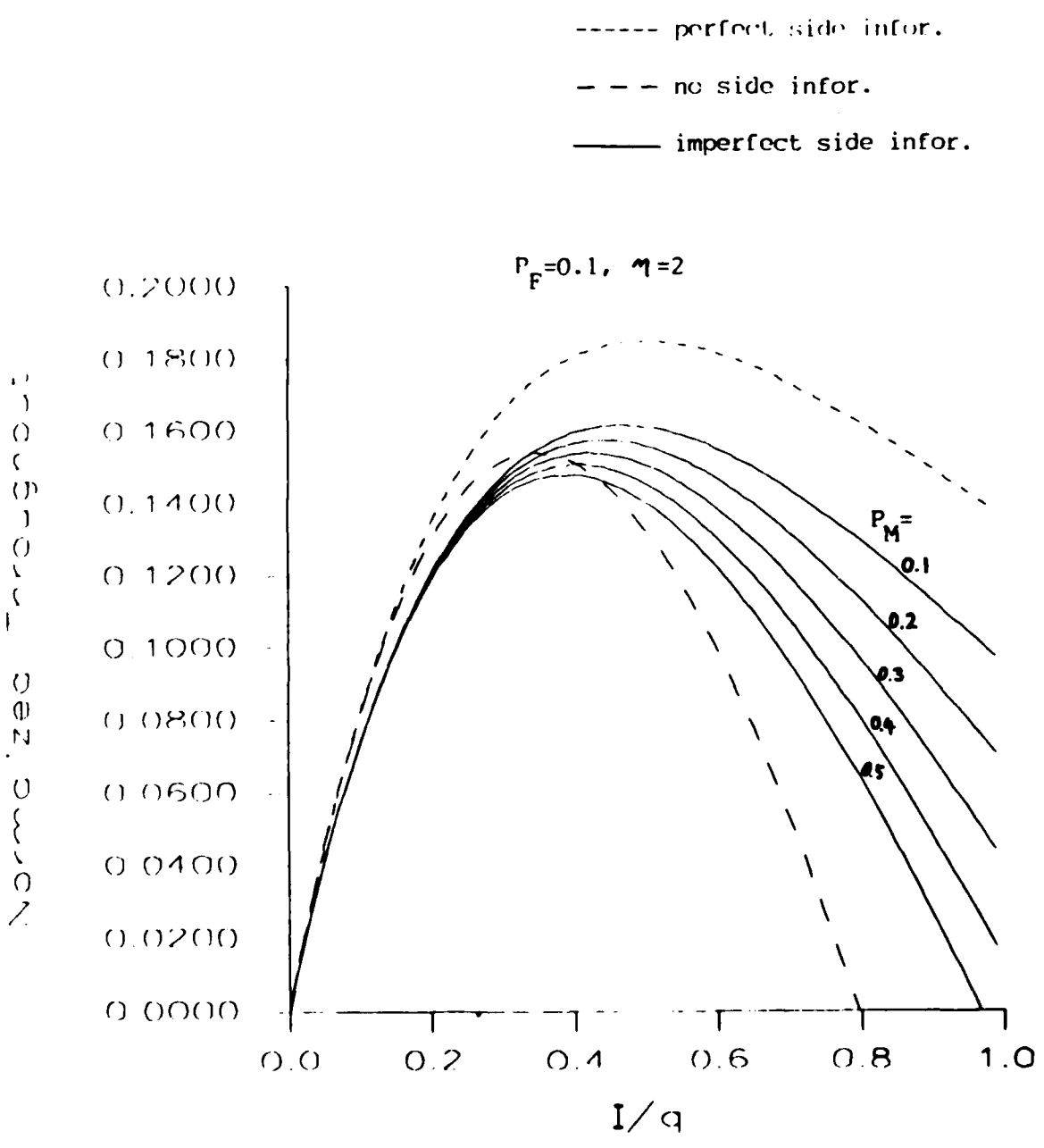

Figure 5.11: Normalized throughputs vs. channel traffic, errors-and-erasures decoding, demodulator model 2.

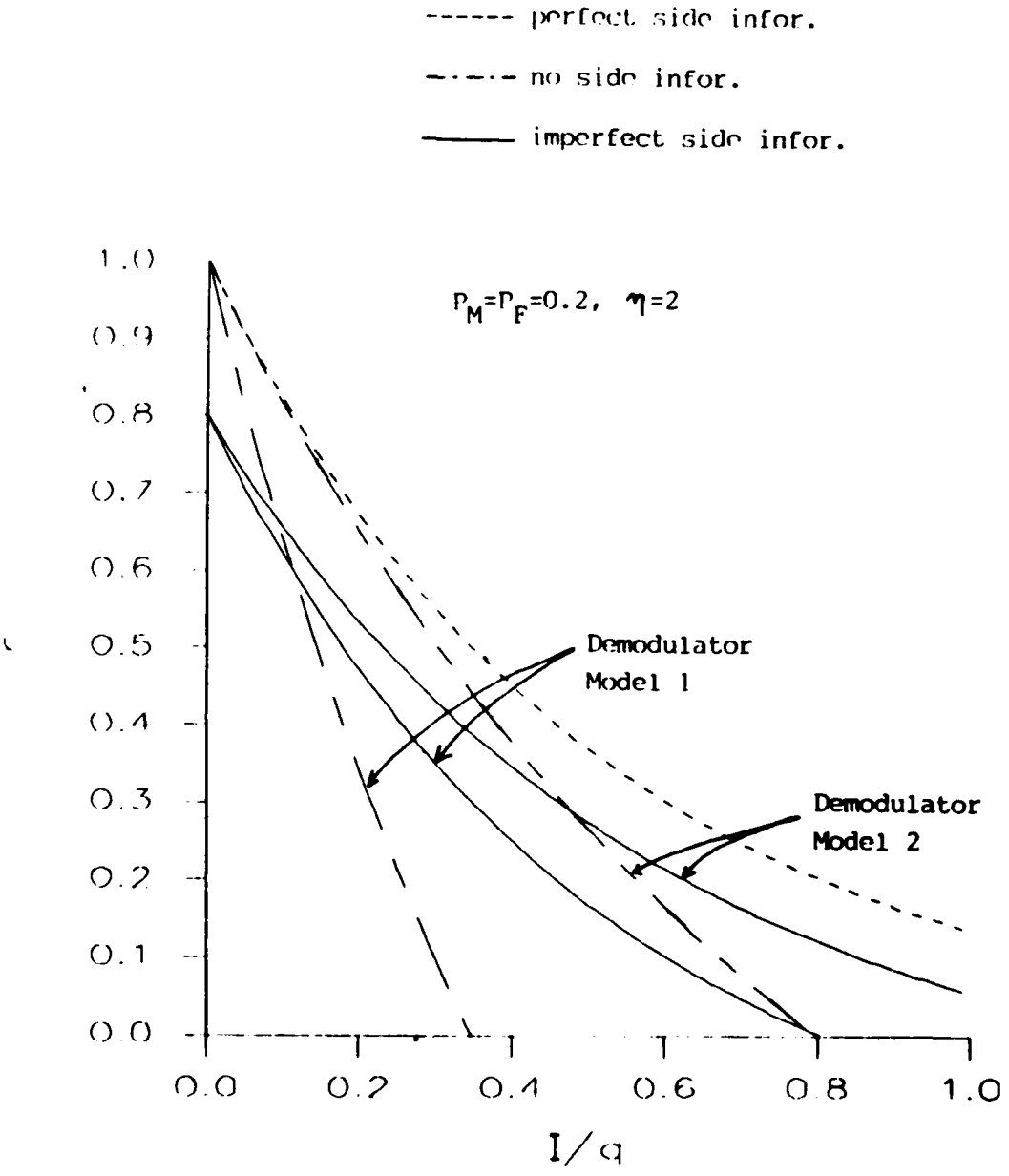

Figure 5.12: Comparison of the achievable regions obtained from the two demodulator models, errors-and-erasures decoding.

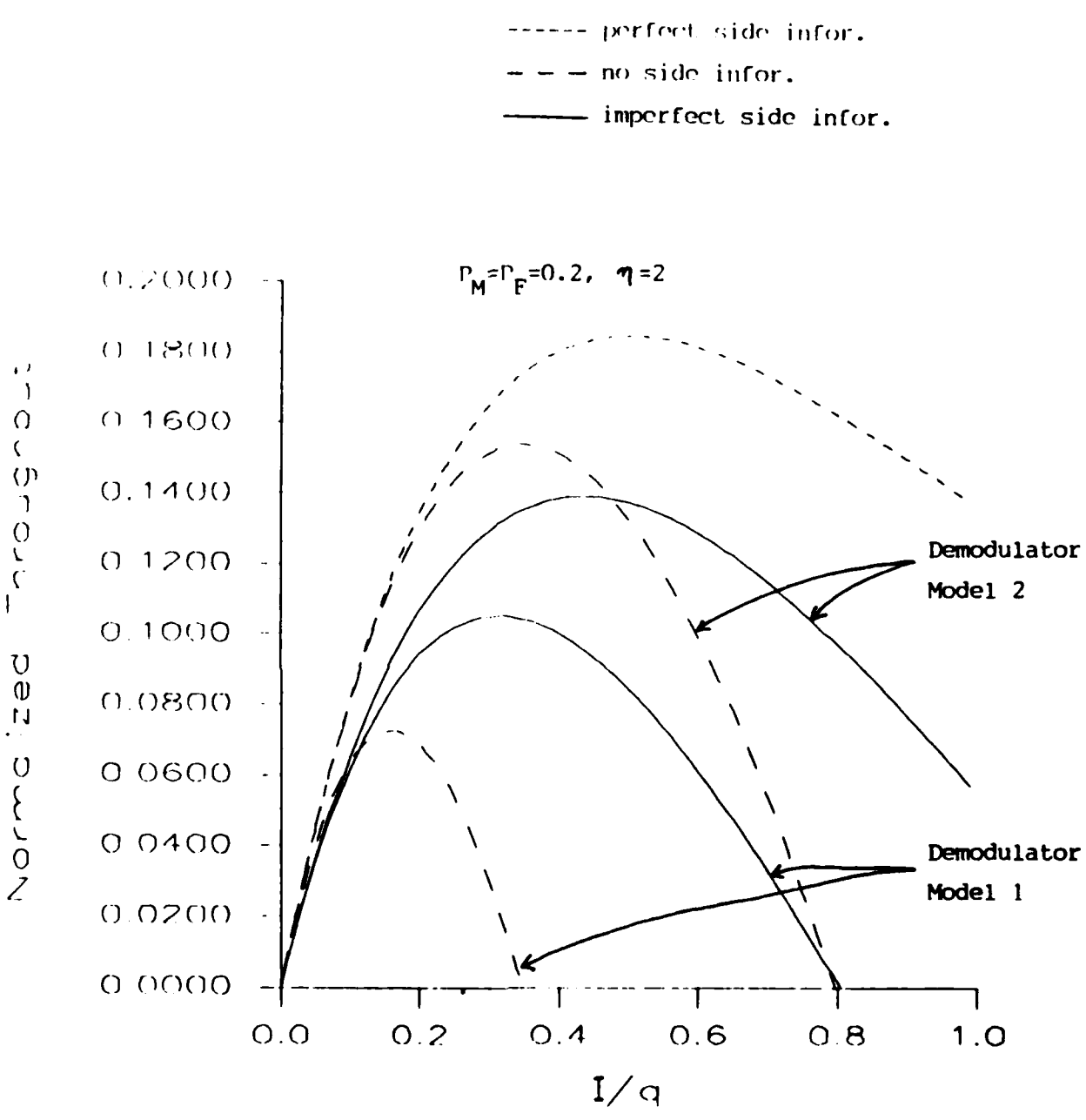

Figure 5.13: Comparison of the normalized throughputs obtained from the two demodulator models, errors-and-erasures decoding.

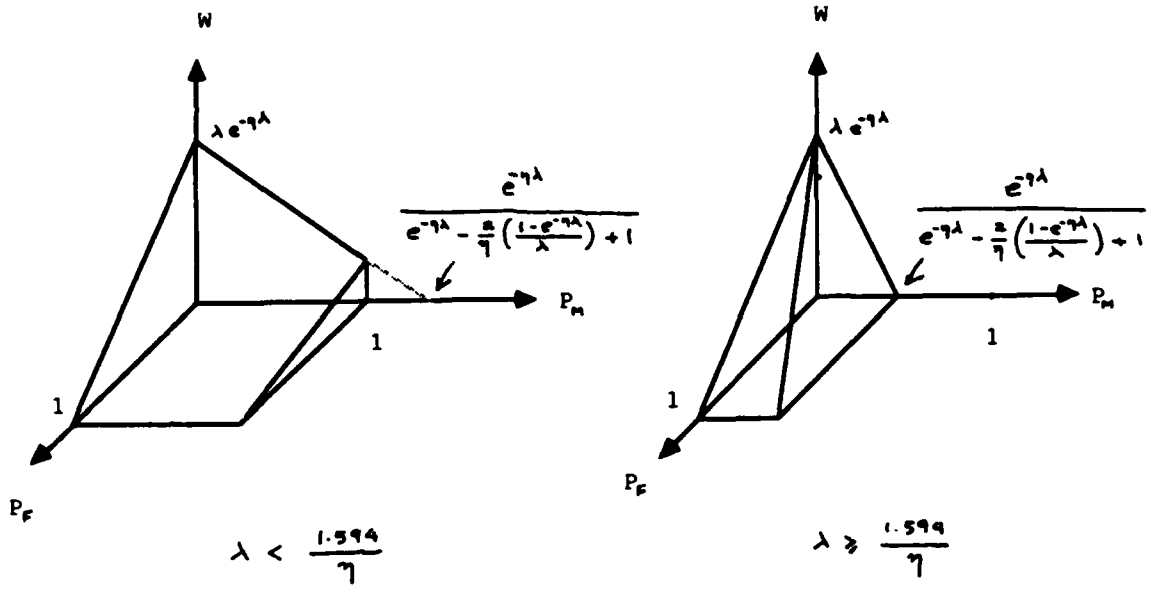

Figure 5.14: Plot of the normalized throughput vs. (P_M, P_F), errors-and-erasures decoding, demodulator model 2.

These imply that for $\lambda \geq 1.594/\eta$ the throughput decreases faster along the P_M axis than along the P_F axis, and for $\lambda < 1.594/\eta$ the opposite happens. The ways in which the throughput decreases as a function of P_M and P_F is shown in Figure 5.14.

Optimum code rate, optimum traffic, and maximum normalized throughput

To get the optimum channel traffic at which the normalized throughput W is maximized, we take the derivative of W w.r.t. λ, and set it to zero. This results in the following nonlinear equation:

$$(1 + P_M - P_F) - \eta(1 - P_M - P_F)\lambda = P_M e^{\eta\lambda}. \tag{5.32}$$

From Figure 5.15 we can see that there exist a unique solution because LHS and RHS meet at exactly one point. Also, by taking second derivative of W w.r.t. λ,

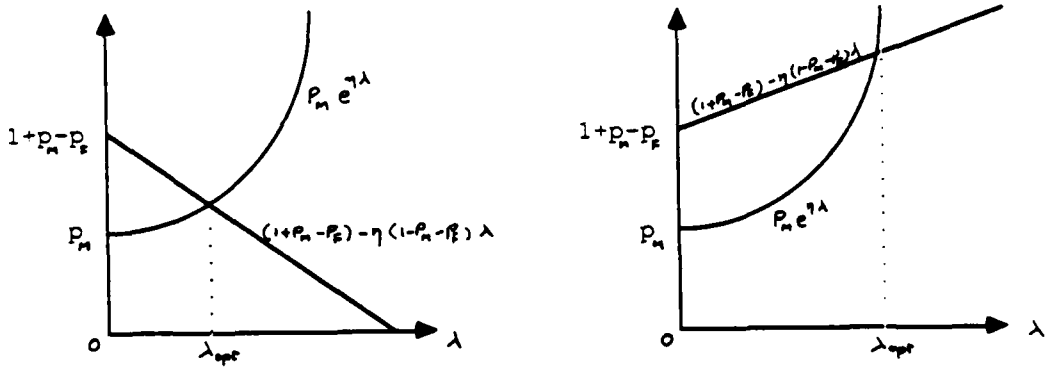

Figure 5.15: Plot of $P_M e^{\eta\lambda}$ and $(1+P_M-P_F)-\eta(1-P_M-P_F)\lambda$ vs. λ.

we get

$$\frac{\partial^2 W}{\partial \lambda^2} = -\eta e^{-\eta\lambda}[2(1-P_F)-\eta(1-P_M-P_F)\lambda].$$

For $1-P_M-P_F \leq 0$ case, it is obvious $\frac{\partial^2 W}{\partial \lambda^2} \leq 0$. For $1-P_M-P_F > 0$ case, the solution of (5.31), call it λ_{opt}, has the property $\lambda_{opt} < (1+P_M-P_F)/[\eta(1-P_M-P_F)]$. Thus

$$\frac{\partial^2 W}{\partial \lambda^2} \leq 0 \quad \text{at } \lambda = \lambda_{opt}.$$

Therefore the unique optimum channel traffic λ_{opt} can be found from (5.31), and at λ_{opt} the optimum code rate is obtained from (5.25) as

$$r_{opt} = (1-P_M-P_F)e^{-\eta\lambda_{opt}} + P_M\left(\frac{2}{\eta}\left(\frac{1-e^{-\eta\lambda_{opt}}}{\lambda_{opt}}\right)-1\right), \tag{5.33}$$

and at λ_{opt} and r_{opt}, the maximum normalized throughput is obtained from (5.26) and (5.31) as

$$W_{max} = \frac{1}{\eta}[(1-P_M-P_F)e^{-\eta\lambda_{opt}} + P_M(1-2\lambda_{opt})]. \tag{5.34}$$

λ_{opt}

P_M \ P_E	0.0	0.1	0.2	0.3	0.4	0.5	0.6	0.7	0.8	0.9	1.0
0.0	0.500	0.500	0.500	0.500	0.500	0.500	0.500	0.500	0.500	0.500	0.000
0.1	0.470	0.467	0.463	0.459	0.453	0.446	0.436	0.421	0.397	0.347	0.000
0.2	0.446	0.441	0.436	0.429	0.421	0.410	0.397	0.377	0.347	0.292	0.000
0.3	0.427	0.421	0.414	0.406	0.397	0.384	0.369	0.347	0.315	0.259	0.000
0.4	0.410	0.404	0.397	0.388	0.377	0.364	0.347	0.325	0.292	0.237	0.000
0.5	0.397	0.390	0.382	0.372	0.361	0.347	0.330	0.307	0.274	0.220	0.000
0.6	0.384	0.377	0.369	0.359	0.347	0.333	0.315	0.292	0.259	0.207	0.000
0.7	0.374	0.366	0.357	0.347	0.335	0.321	0.303	0.280	0.247	0.196	0.000
0.8	0.364	0.356	0.347	0.337	0.325	0.310	0.292	0.269	0.237	0.186	0.000
0.9	0.355	0.347	0.338	0.327	0.315	0.301	0.283	0.259	0.228	0.178	0.000
1.0	0.347	0.339	0.330	0.319	0.307	0.292	0.274	0.251	0.220	0.172	0.000

r_{opt}

P_M \ P_E	0.0	0.1	0.2	0.3	0.4	0.5	0.6	0.7	0.8	0.9	1.0
0.0	0.368	0.331	0.294	0.258	0.221	0.184	0.147	0.110	0.074	0.037	0.000
0.1	0.381	0.344	0.308	0.270	0.234	0.196	0.159	0.121	0.083	0.044	0.000
0.2	0.393	0.356	0.318	0.281	0.243	0.205	0.166	0.128	0.088	0.047	0.000
0.3	0.401	0.364	0.326	0.288	0.250	0.212	0.172	0.133	0.092	0.049	0.000
0.4	0.410	0.372	0.333	0.295	0.256	0.217	0.177	0.136	0.094	0.050	0.000
0.5	0.416	0.378	0.339	0.300	0.261	0.221	0.180	0.139	0.096	0.051	0.000
0.6	0.423	0.384	0.344	0.305	0.265	0.225	0.184	0.142	0.098	0.052	0.000
0.7	0.428	0.389	0.350	0.310	0.269	0.228	0.186	0.143	0.100	0.053	0.000
0.8	0.433	0.394	0.354	0.313	0.272	0.231	0.189	0.145	0.101	0.054	0.000
0.9	0.438	0.398	0.357	0.317	0.276	0.233	0.191	0.147	0.102	0.054	0.000
1.0	0.442	0.402	0.361	0.320	0.278	0.236	0.193	0.149	0.103	0.054	0.000

W_{max}

P_M \ P_E	0.0	0.1	0.2	0.3	0.4	0.5	0.6	0.7	0.8	0.9	1.0
0.0	0.184	0.166	0.147	0.129	0.110	0.092	0.074	0.055	0.037	0.018	0.000
0.1	0.179	0.160	0.142	0.124	0.106	0.087	0.069	0.051	0.033	0.015	0.000
0.2	0.175	0.157	0.138	0.120	0.102	0.084	0.066	0.048	0.031	0.014	0.000
0.3	0.171	0.153	0.135	0.117	0.099	0.081	0.063	0.046	0.029	0.013	0.000
0.4	0.168	0.150	0.132	0.114	0.096	0.079	0.061	0.044	0.027	0.012	0.000
0.5	0.165	0.147	0.129	0.112	0.094	0.076	0.059	0.042	0.026	0.011	0.000
0.6	0.162	0.144	0.126	0.109	0.092	0.075	0.058	0.041	0.025	0.011	0.000
0.7	0.159	0.142	0.125	0.107	0.090	0.073	0.056	0.040	0.025	0.010	0.000
0.8	0.157	0.140	0.122	0.105	0.088	0.071	0.055	0.039	0.024	0.010	0.000
0.9	0.155	0.138	0.120	0.104	0.087	0.070	0.053	0.038	0.023	0.010	0.000
1.0	0.153	0.136	0.118	0.102	0.085	0.069	0.053	0.037	0.022	0.009	0.000

Table 5.2: λ_{opt}, r_{opt}, and W_{max}, errors-and-erasures decoding, demodulator model 2, η=2.

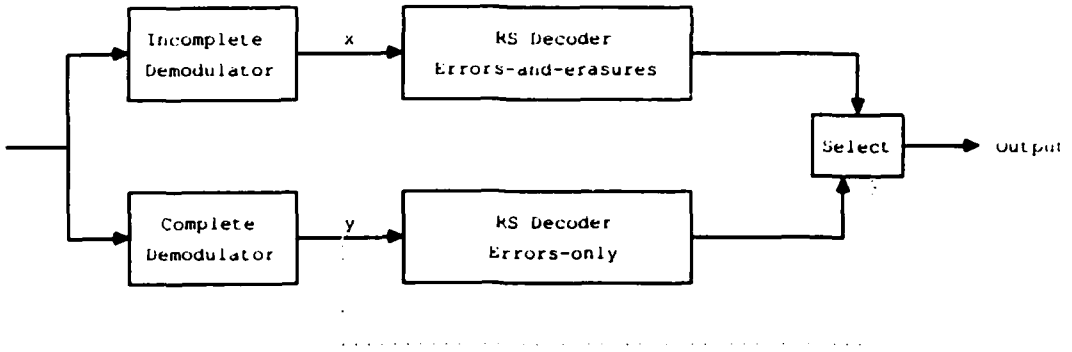

Figure 5.16: Parallel decoding system.

In Table 5.2 we list W_{max}, r_{opt}, and λ_{opt} for various values of P_M and P_F.

For finite block length codes, the achievable regions for $P_c(I) \geq 1 - \hat{P}_E$ is approximately given by (5.24) with $p_{e,I}$ and $p_{er,I}$ given in (5.3) and (5.1) respectively.

5.5. Parallel Decoding Scheme

We have observed in sections 5.3 and 5.4 that there is a threshold in channel traffic such that for the lower traffic it is advantageous to ignore the imperfect (unreliable) side information and make a hard decision demodulation of the received signals, and for the higher traffic to try to erase the unreliable symbols. This suggests the following parallel decoding scheme whose block diagram is shown in Figure 5.16. The output of the demodulator is a pair (x, y): the first component is the input to the errors-and-erasures decoder and the second component is the input to the errors-only decoder. The output of the incomplete

demodulator, x, is either a symbol estimate or an erasure, and it is in the alphabet set of $\{0, 1, ..., M-1, ?\}$. On the other hand, the complete demodulator makes a hard decision demodulation of the symbol transmitted, and its output, y, is in the alphabet set of $\{0, 1, ..., M-1\}$. If x is not an erasure, then x and y are identical. We will assume throughout that RS decoder never errors (produces the wrong codeword) but always fails (gives up) when the number of errors and erasures exceeds the capability of the code. In fact, if a Reed-Solomon code is being used and the decoder is attempting to correct t errors, the probability of a decoding failure is approximately $t!$ times the probability of a decoding error [Ber 80]: as $n \rightarrow \infty$, $t = n(\frac{1-r}{2}) \rightarrow \infty \Rightarrow t! \rightarrow \infty \Rightarrow$ P(decoding error) $\rightarrow 0$. Therefore a codeword (packet) error occurs if both decoders fail and at least one symbol out of the complete demodulator is in error.

Previous studies on parallel decoder begin with [Pur 82], in which the use of a parallel combination of erasures-decoding and errors-decoding for Reed-Solomon codes was introduced. Soon after, it is applied in [Pur 83] and [McC 83] to increase the jamming margin against a *partial-band jammer*. In all of those works, the *perfect side information* was assumed to be available at the receiver. For the *partial-band jamming, no side information* environment, Castor [Cas 86] analyzed a parallel combination of diversity decoder/errors-and-erasures decoder and diversity decoder/errors-only decoder. In this section we will evaluate the performance of the suggested parallel decoding scheme under the *multiple-access, imperfect side information* environment.

5.5.1. Achievable Region and Throughput

Let us first define the following random variables:

$Z_1 \triangleq$ the number of symbols in the received packet for which

x is erasure and y is in error,

$Z_2 \triangleq$ the number of symbols in the received packet for which x is not erasure and y is in error,

$Z_3 \triangleq$ the number of symbols in the received packet for which x is erasure and y is not in error.

Then there are $Z_1 + Z_3$ erasures and Z_2 errors at the input of the errors-and-erasures decoder, and $Z_1 + Z_2$ errors at the input of the errors-only decoder. Therefore the packet (codeword) error probability given I simultaneous transmissions, $P_E(I)$, is given by

$$\begin{aligned} P_E(I) &= P(Z_1 + Z_3 + 2Z_2 > n-k \cap Z_1 + Z_2 > \lfloor \tfrac{n-k}{2} \rfloor \cap Z_1 + Z_2 > 0) \\ &= P(Z_1 + Z_3 + 2Z_2 > n-k \cap Z_1 + Z_2 > \lfloor \tfrac{n-k}{2} \rfloor). \end{aligned} \tag{5.35}$$

This implies that the performance (in terms of packet error probability) is the same whether the complete demodulator output is selected or not. Therefore we will consider the modified parallel decoding scheme which has no path from the complete demodulator to the selector, i.e., without the dotted line in Figure 5.16.

Since the events of Z_1, Z_2, and Z_3 are mutually exclusive and they are independent from symbol to symbol within a codeword, the joint distribution of Z_1, Z_2, and Z_3 may be calculated as [Kal 85]

$$P(Z_1 = j,\ Z_2 = l,\ Z_3 = m) = \binom{n}{j,l,m} p_1^j\, p_2^l\, p_3^m (1 - p_1 - p_2 - p_3)^{n-j-l-m}, \tag{5.36}$$

where

$$\begin{aligned} p_1 &\triangleq P(\text{ a received symbol is erased and in error } |\ I \text{ users }) \\ p_2 &\triangleq P(\text{ a received symbol is not erased and in error } |\ I \text{ users }) \\ p_3 &\triangleq P(\text{ a received symbol is erased and not in error } |\ I \text{ users }). \end{aligned} \tag{5.37}$$

Thus the codeword error probability given I users, $P_E(I)$, is given by

$$P_E(I) = \sum_{j=0}^{n} \sum_{l=h(j)}^{n-j} \sum_{m=g(j,l)}^{n-j-l} P(Z_1 = j,\ Z_2 = l,\ Z_3 = m), \tag{5.38}$$

where

$$\begin{aligned} h(j) &\triangleq \max\{0, \lfloor \tfrac{n-k}{2} \rfloor - j + 1\}, \\ g(j,l) &\triangleq \max\{0, n-k-j-2l+1\}. \end{aligned}$$

To get the limiting value of $P_E(I)$ as $n, k \to \infty$, let us define the following random variables:

$$\begin{aligned} X_n &\triangleq Z_1 + 2Z_2 + Z_3 \\ Y_n &\triangleq Z_1 + Z_2 \\ U_n &\triangleq \tfrac{X_n - E(X_n)}{\sqrt{Var(X_n)}} \\ V_n &\triangleq \tfrac{Y_n - E(Y_n)}{\sqrt{Var(Y_n)}}. \end{aligned} \tag{5.39}$$

Then, X_n is the sum of the number of erasures and twice the number of errors at the input of the errors-and-erasures decoder, and Y_n is the sum of the number of errors at the input of the errors-only decoder. Therefore,

$$\begin{aligned} P_E(I) &= P(X_n > n-k,\ Y_n > \lfloor \tfrac{n-k}{2} \rfloor) \\ &= P(U_n > \tfrac{n-k-E(X_n)}{\sqrt{Var(X_n)}},\ V_n > \tfrac{\lfloor \frac{n-k}{2} \rfloor - E(Y_n)}{\sqrt{Var(Y_n)}}) \\ &= P(U_n > a\sqrt{n},\ V_n > b\sqrt{n}), \end{aligned} \tag{5.40}$$

where

$$\begin{aligned} E(X_n) &= n(p_1 + 2p_2 + p_3) \\ E(Y_n) &= n(p_1 + p_2) \\ Var(X_n) &= n(p_1 - p_1^2 + 4p_2 - 4p_2^2 + p_3 - p_3^2 - 4p_1p_2 - 2p_1p_3 - 4p_2p_3) \\ Var(Y_n) &= n(p_1 + p_2)(1 - p_1 - p_2) \\ a &\triangleq \tfrac{1 - r - p_1 - 2p_2 - p_3}{\sqrt{(p_1 - p_1^2 + 4p_2 - 4p_2^2 + p_3 - p_3^2 - 4p_1p_2 - 2p_1p_3 - 4p_2p_3)}} \\ b &\triangleq \tfrac{1 - r - 2p_1 - 2p_2}{\sqrt{(p_1 + p_2)(1 - p_1 - p_2)}}. \end{aligned} \tag{5.41}$$

By the central limit theorem, as the code length n becomes large, it is well known that the distributions of U_n and V_n approach the standard normal distribution

with mean zero and variance one. That is, as $n \to \infty$,

$$F_G(u) - \epsilon_1 \leq F_{U_n}(u) \leq F_G(u) + \epsilon_1, \tag{5.42}$$

and

$$F_G(v) - \epsilon_2 \leq F_{V_n}(v) \leq F_G(v) + \epsilon_2, \tag{5.43}$$

for arbitrarily small positive ϵ_1 and ϵ_2, where

$$\begin{aligned} F_{U_n}(u) &\triangleq P(U_n \leq u) \\ F_{V_n}(v) &\triangleq P(V_n \leq v) \\ F_G(u) &\triangleq \textstyle\int_{-\infty}^{u} \frac{1}{\sqrt{2\pi}} e^{-x^2/2} dx. \end{aligned} \tag{5.44}$$

Thus, as $n, k \to \infty$ while $r \triangleq k/n$ is held constant

$$\begin{aligned} P_E(I) &= P(U_n > a\sqrt{n},\ V_n > b\sqrt{n}) \\ &\leq P(U_n > a\sqrt{n}) \\ &= 1 - F_{U_n}(a\sqrt{n}) \\ &\leq 1 - F_G(a\sqrt{n}) + \epsilon_1 \\ &\to 0, \end{aligned} \tag{5.45}$$

if $a > 0$. Similarly,

$$\begin{aligned} P_E(I) &\leq P(V_n > b\sqrt{n}) \\ &= 1 - F_{V_n}(b\sqrt{n}) \\ &\leq 1 - F_G(b\sqrt{n}) + \epsilon_2 \\ &\to 0, \end{aligned} \tag{5.46}$$

if $b > 0$. Therefore, the codeword (packet) error probability $P_E(I)$ approaches zero asymptotically if

$$a > 0 \text{ or } b > 0, \tag{5.47}$$

$$\iff r < 1 - p_1 - 2p_2 - p_3 \text{ or } r < 1 - 2p_1 - 2p_2 \tag{5.48}$$

$$\iff r < \max\{1 - p_1 - 2p_2 - p_3,\ 1 - 2p_1 - 2p_2\}. \tag{5.49}$$

Also, it can be shown that as $n \to \infty$,

$$P_E(I) \to 1,$$

if $a < 0$ and $b < 0$, i.e., $r > \max\{1 - p_1 - 2p_2 - p_3,\ 1 - 2p_1 - 2p_2\}$:

$$\begin{aligned} P_E(I) &= P(U_n > a\sqrt{n} \cap V_n > b\sqrt{n}) \\ &= 1 - P(U_n \le a\sqrt{n} \cup V_n \le b\sqrt{n}) \\ &\ge 1 - \underbrace{P(U_n \le a\sqrt{n})}_{\to 0,\ \text{if } a<0} - \underbrace{P(V_n \le b\sqrt{n})}_{\to 0,\ \text{if } b<0} \\ &\to 1, \end{aligned}$$

as $n \to \infty$. Therefore, (5.48) represents the asymptotic achievable regions of code rate and channel traffic for arbitrarily small error probability. The asymptotic normalized throughput is thus given by

$$\begin{aligned} W &= \frac{r\,I\,(1-P_E(I))}{q} \\ &= \frac{I}{q} \max\{1 - p_1 - 2p_2 - p_3,\ 1 - 2p_1 - 2p_2\}. \end{aligned} \tag{5.50}$$

The remaining problem is to find the probabilities p_1, p_2, and p_3 in terms of the number of packet transmissions.

5.5.2. Demodulator Model 1: Worst Case

In computing (5.48) and (5.49) we need only the probabilities $p_1 + p_2$, $p_1 + p_3$ and p_2, which can be derived as follows:

$$\begin{aligned} p_1 + p_2 &= \mathrm{P}(\text{erasure, error} \mid I \text{ users}) \\ &\quad + \mathrm{P}(\text{no erasure, error} \mid I \text{ users}) \\ &= \mathrm{P}(\text{error} \mid I \text{ transmissions}) \\ &= \underbrace{\mathrm{P}(\text{error} \mid \text{hit},\ I)}_{=1-1/M}\,\mathrm{P}(\text{hit} \mid I) \\ &\quad + \underbrace{\mathrm{P}(\text{error} \mid \text{no hit},\ I)}_{=0}\,\mathrm{P}(\text{no hit} \mid I) \\ &= (1 - 1/M)p_{h,I}, \end{aligned} \tag{5.51}$$

$$\begin{aligned} p_1 + p_3 &= \mathrm{P}(\text{erasure, error} \mid I) \\ &\quad + \mathrm{P}(\text{erasure, no error} \mid I) \\ &= \mathrm{P}(\text{erasure} \mid I) \\ &= \mathrm{P}(\text{erasure} \mid \text{hit, } I)\mathrm{P}(\text{hit} \mid I) \\ &\quad + \mathrm{P}(\text{erasure} \mid \text{no hit, } I)\mathrm{P}(\text{no hit} \mid I) \\ &= (1 - P_M)p_{h,I} + P_F(1 - p_{h,I}), \end{aligned} \tag{5.52}$$

$$\begin{aligned} p_2 &= \mathrm{P}(\text{no erasure, error} \mid I) \\ &= \mathrm{P}(\text{error} \mid \text{no erasure, } I)\mathrm{P}(\text{no erasure} \mid I) \\ &= \mathrm{P}(\text{error} \mid \text{no erasure, hit, } I)\mathrm{P}(\text{no erasure} \mid \text{hit, } I)\mathrm{P}(\text{hit} \mid I) \\ &\quad + \underbrace{\mathrm{P}(\text{error} \mid \text{no erasure, no hit, } I)}_{=0}\mathrm{P}(\text{no erasure} \mid \text{no hit, } I)\mathrm{P}(\text{no hit} \mid I) \\ &= \mathrm{P}(\text{error} \mid \text{no erasure, hit, } I)P_M\, p_{h,I}. \end{aligned} \tag{5.53}$$

Since both the complete demodulator and the incomplete demodulator produce *identical* symbols if the symbol produced by the latter is not an erasure, the probability of symbol error at the complete demodulator output given no erasure at the incomplete demodulator output is the same as that at the incomplete demodulator output given no erasure. That is,

$$\begin{aligned} P(\text{error}_{[\text{comp}]} \mid \text{no erasure}_{[\text{incomp}]}, \text{ hit, } I) &= P(\text{error}_{[\text{incomp}]} \mid \text{no erasure}_{[\text{incomp}]}, \text{ hit, } I) \\ &= 1 - 1/M. \end{aligned}$$

Thus p_2 is given by

$$p_2 = (1 - 1/M)P_M p_{h,I}. \tag{5.54}$$

Therefore,

$$1 - 2p_1 - 2p_2 = 1 - 2p_{h,I}, \tag{5.55}$$

and

$$1 - p_1 - 2p_2 - p_3 = 1 - P_F - (1 + P_M - P_F)p_{h,I}. \tag{5.56}$$

The resulting asymptotic achievable regions for arbitrarily small error probability is given by

$$r < \max\{1 - 2p_{h,I},\ 1 - P_F - (1 + P_M - P_F)p_{h,I}\}, \tag{5.57}$$

and the asymptotic normalized throughput is given by

$$\begin{aligned} W &= \tfrac{rIP_c(I)}{q} \\ &= \tfrac{I}{q}\max\{1 - 2p_{h,I},\ 1 - P_F - (1 + P_M - P_F)p_{h,I}\} \\ &= \tfrac{I}{q}\max\{2(1-p_h)^{I-1} - 1,\ (1 + P_M - P_F)(1-p_h)^{I-1} - P_M\}. \end{aligned} \tag{5.58}$$

Since

$$1 - 2p_{h,I} \geq 1 - P_F - (1 + P_M - P_F)p_{h,I}, \tag{5.59}$$

for

$$\begin{aligned} I &\leq 1 + \tfrac{\ln(\frac{1-P_M}{1-P_M+P_F})}{\ln(1-p_h)} \\ &\triangleq I_{th}, \end{aligned} \tag{5.60}$$

the achievable regions are

$$r < \begin{cases} 2(1-p_h)^{I-1} - 1, & I \leq I_{th} \\ (1 + P_M - P_F)(1-p_h)^{I-1} - P_M, & I > I_{th}, \end{cases} \tag{5.61}$$

$$\to \begin{cases} 2e^{-\eta\lambda} - 1, & \lambda \leq \lambda_{th} \\ (1 + P_M - P_F)e^{-\eta\lambda} - P_M, & \lambda > \lambda_{th}, \end{cases}$$

where

$$\lambda_{th} \triangleq \frac{1}{\eta}\ln\left(\frac{1 - P_M + P_F}{1 - P_M}\right), \tag{5.62}$$

as $I, q \to \infty$ while $\lambda \triangleq I/q$ is held constant. Similarly the asymptotic normalized throughput is given by

$$\begin{aligned} W &= \tfrac{I}{q}\, r\, P_c(I) \\ &= \begin{cases} \frac{I}{q}[2(1-p_h)^{I-1} - 1], & I \leq I_{th} \\ \frac{I}{q}[(1 + P_M - P_F)(1-p_h)^{I-1} - P_M], & I > I_{th}, \end{cases} \\ &\to \begin{cases} \lambda(2e^{-\eta\lambda} - 1), & \lambda \leq \lambda_{th} \\ \lambda[(1 + P_M - P_F)e^{-\eta\lambda} - P_M], & \lambda > \lambda_{th}. \end{cases} \end{aligned} \tag{5.63}$$

We can see that for lower traffic ($\lambda \leq \lambda_{th}$) it is advantageous to select the "errors-only" decoder, and for higher traffic ($\lambda > \lambda_{th}$) it is advantageous to select the "errors-and-erasures" decoder. This implies that the parallel decoder *adapts* to the level of channel traffic by switching between two decoding modes. Figures 5.17 and 5.18 show the achievable regions and the normalized throughputs for various values of P_M and P_F respectively. The shaded area in the lower traffic region indicates the performance improvement over the errors-and-erasures decoding scheme. Notice that the performance improvement becomes more significant as the side information is less reliable, i.e., higher P_M and P_F.

On the other hand, the requirement on (P_M, P_F) pair for the errors-only decoder to perform better than the errors-and-erasures decoder can be obtained from (5.58) as

$$P_M + \left(\frac{1 - p_{h,I}}{p_{h,I}}\right) P_F \geq 1, \tag{5.64}$$

and as $I, q \to \infty$ while $\lambda \triangleq I/q$ is held constant it becomes

$$P_M + \left(\frac{e^{-\eta\lambda}}{1 - e^{-\eta\lambda}}\right) P_F \geq 1. \tag{5.65}$$

Figure 5.19 indicates regions of (P_M, P_F) pair where one decoding scheme performs better than the other for given λ. Notice that as the channel traffic increases, the errors-and-erasures decoder performs better even for less reliable side information, and as the channel traffic decreases, the errors-only decoder performs better even for more reliable side information.

Optimum code rate, optimum traffic, and maximum normalized throughput

In Figure 5.20 we show the typical form of the normalized throughput, where λ_{o1} and λ_{o2} denote the optimum channel traffic at which $\lambda(2e^{-\eta\lambda} - 1)$ and $\lambda[(1 + P_M - P_F)e^{-\eta\lambda} - P_M]$ are maximized respectively, and W_{o1} and W_{o2} are the maximum values at λ_{o1} and λ_{o2} respectively. It has been shown in (3.47) and

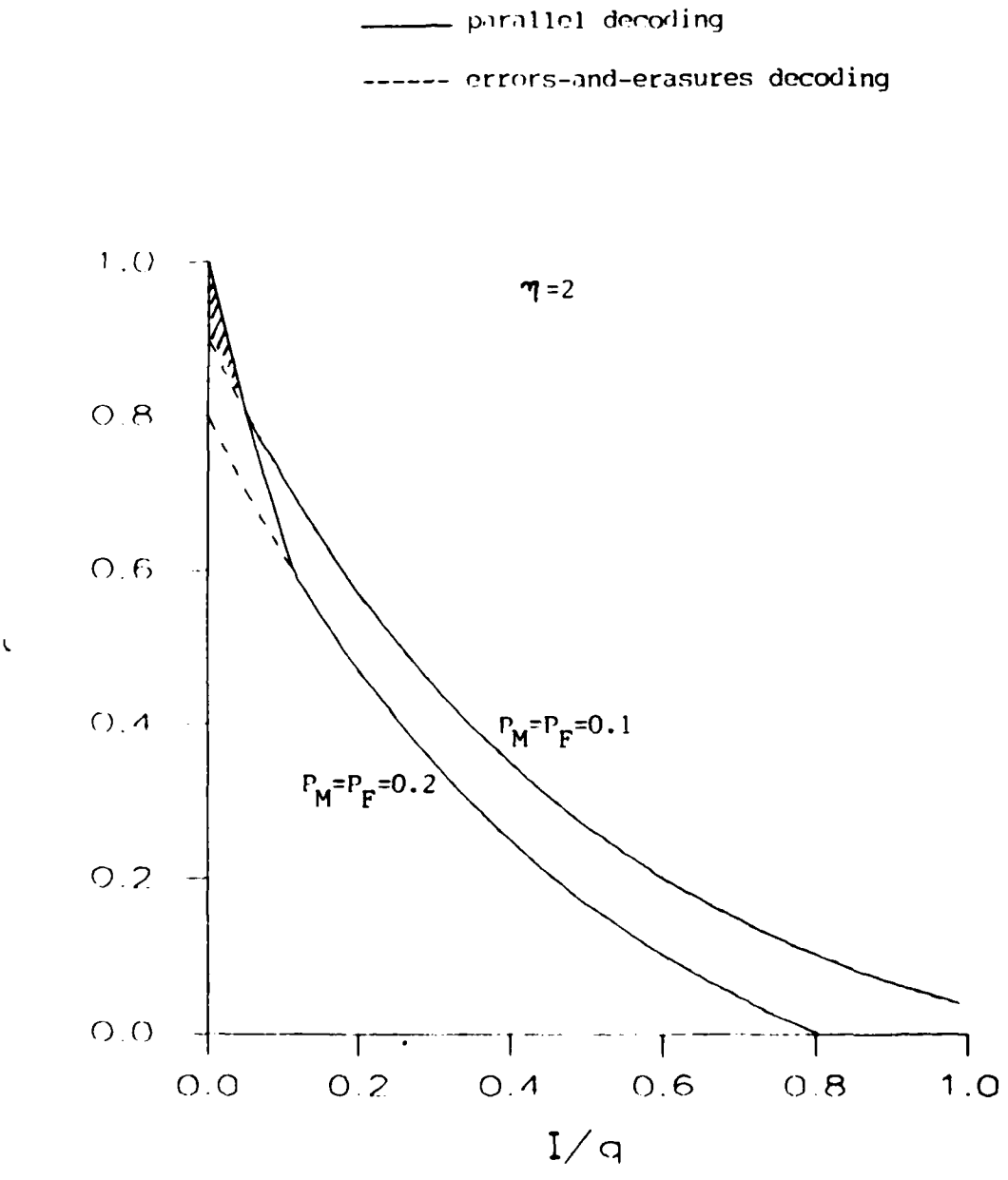

Figure 5.17: Achievable regions of code rate and channel traffic, parallel decoding, demodulator model 1.

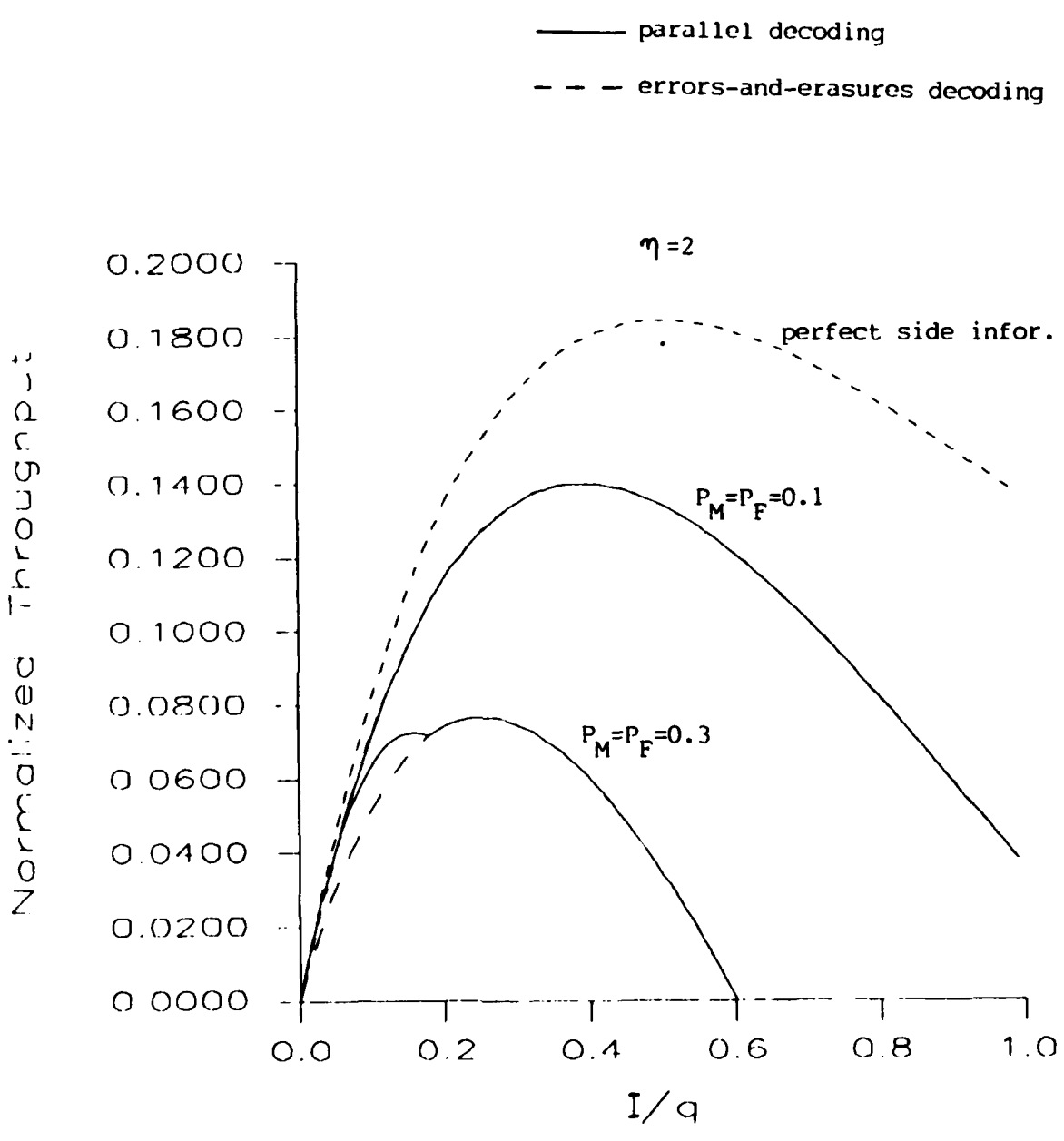

Figure 5.18: Normalized throughputs vs. channel traffic, parallel decoding, demodulator model 1.

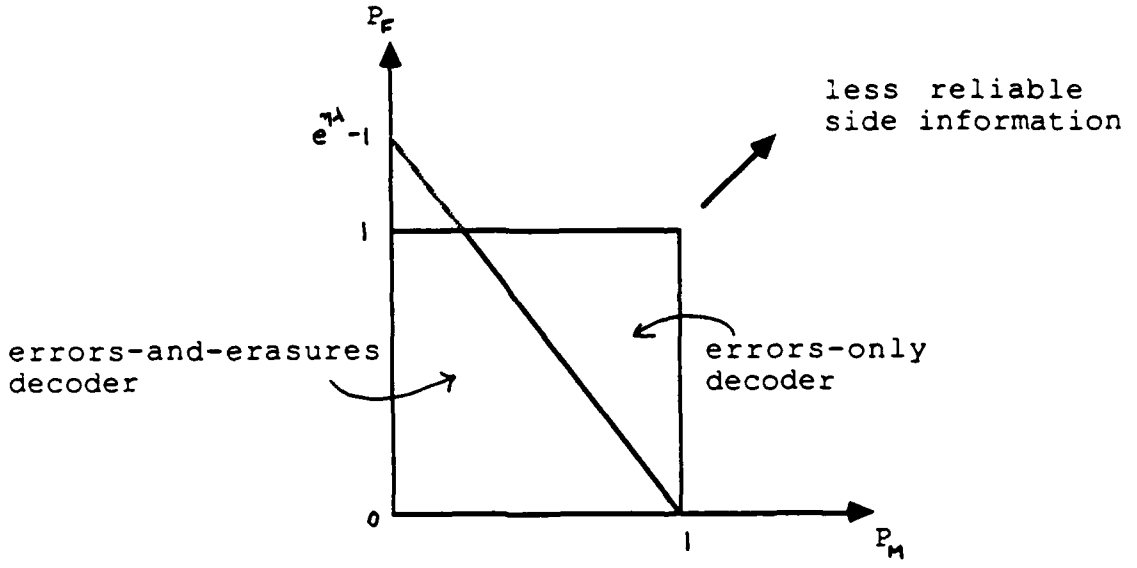

Figure 5.19: Regions of preferences, demodulator model 1.

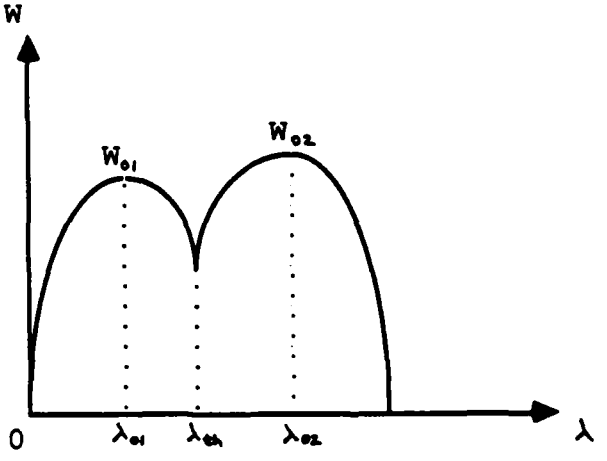

Figure 5.20: Typical form of the normalized throughput of parallel decoding system.

(3.48) that

$$\lambda_{o1} = 0.3148/\eta, \text{ and } W_{o1} = 0.1448/\eta. \tag{5.66}$$

To get W_{o2}, we take the derivative of $\lambda[(1 + P_M - P_F)e^{-\eta\lambda} - P_M]$ and set it to zero:

$$\begin{aligned} \frac{\partial}{\partial\lambda}\{\lambda[(1 + P_M - P_F)e^{-\eta\lambda} - P_M]\} &= (1 + P_M - P_F)e^{-\eta\lambda}(1 - \eta\lambda) - P_M \\ &= 0 \end{aligned}$$

$$\Longrightarrow e^{-\eta\lambda}(1 - \eta\lambda) = \frac{P_M}{1 + P_M - P_F}. \tag{5.67}$$

The above nonlinear equation will have a unique solution, which is λ_{o2}, by the arguments given in subsection 5.4.1. Therefore W_{o2} is obtained from (5.62) and (5.66) as

$$\begin{aligned} W_{o2} &= \lambda_{o2}[(1 + P_M - P_F)e^{-\eta\lambda_{o2}} - P_M] \\ &= \frac{\eta P_M \lambda_{o2}^2}{1 - \eta\lambda_{o2}}. \end{aligned} \tag{5.68}$$

From (5.65) and (5.67) it can be shown that $W_{o2} \geq W_{o1}$ if

$$\begin{aligned} \lambda_{o2} &\geq \frac{-0.1448 + \sqrt{(0.1448)^2 + 0.5792 P_M}}{2\eta P_M} \\ &\triangleq \lambda_T. \end{aligned} \tag{5.69}$$

Therefore we get the following results:

$$\begin{cases} \text{if } \lambda_{o2} < \lambda_T, & \begin{cases} W_{max} = 0.1448/\eta \\ r_{opt} = 0.4611 \\ \lambda_{opt} = 0.314/\eta, \end{cases} \\ \text{if } \lambda_{o2} \geq \lambda_T, & \begin{cases} W_{max} = \frac{\eta P_M \lambda_{o2}^2}{1 - \eta\lambda_{o2}} \\ r_{opt} = \frac{\eta P_M \lambda_{o2}}{1 - \eta\lambda_{o2}} \\ \lambda_{opt} = \lambda_{o2}. \end{cases} \end{cases} \tag{5.70}$$

5.5.3. Demodulator Model 2: Realistic Case

The probabilities $p_1 + p_2$, $p_1 + p_3$, and p_2 can be derived as follows:

$$\begin{aligned} p_1 + p_2 &= \mathrm{P}(\text{error} \mid I \text{ users}) \\ &= 1 - \tfrac{1-(1-p_h)^I}{Ip_h}, \end{aligned} \tag{5.71}$$

$$\begin{aligned} p_1 + p_3 &= \mathrm{P}(\text{erasure} \mid I \text{ users}) \\ &= \textstyle\sum_{m=0}^{I-1} \mathrm{P}(\text{erasure} \mid m \text{ hits}, I)\mathrm{P}(m \text{ hits} \mid I) \\ &= P_F(1-p_{h,I}) + (1-P_M)\textstyle\sum_{m=1}^{I-1} \binom{I-1}{m} p_h^m (1-p_h)^{I-1-m} \\ &= P_F(1-p_{h,I}) + (1-P_M)p_{h,I}, \end{aligned} \tag{5.72}$$

$$\begin{aligned} p_2 &= \mathrm{P}(\text{error, no erasure} \mid I \text{ users}) \\ &= \textstyle\sum_{m=0}^{I-1} \mathrm{P}(\text{error, no erasure} \mid m \text{ hits}, I)\mathrm{P}(m \text{ hits} \mid I) \\ &= \textstyle\sum_{m=0}^{I-1} \mathrm{P}(\text{error} \mid \text{no erasure}, m \text{ hits}, I) \\ &\qquad \mathrm{P}(\text{no erasure} \mid m \text{ hits}, I)\mathrm{P}(m \text{ hits} \mid I) \\ &= 0 \cdot (1-P_F)(1-p_h)^{I-1} + \textstyle\sum_{m=1}^{I-1} \frac{m}{m+1} P_M \binom{I-1}{m} p_h^m (1-p_h)^{I-1-m} \\ &= P_M\left[1 - \tfrac{1-(1-p_h)^I}{Ip_h}\right]. \end{aligned} \tag{5.73}$$

Thus,

$$1 - 2p_1 - 2p_2 = \frac{2-2(1-p_h)^I}{Ip_h} - 1, \tag{5.74}$$

and

$$1 - p_1 - 2p_2 - p_3 = (1-P_M-P_F)(1-p_h)^{I-1} + P_M\left(\frac{2-2(1-p_h)^I}{Ip_h} - 1\right). \tag{5.75}$$

Therefore, the resulting asymptotic achievable regions for arbitrarily small error probability is given by

$$\begin{aligned} r &< \max\left\{\tfrac{2-2(1-p_h)^I}{Ip_h} - 1,\ (1-P_M-P_F)(1-p_h)^{I-1} + P_M\left(\tfrac{2-2(1-p_h)^I}{Ip_h} - 1\right)\right\} \\ &\to \max\left\{\tfrac{2}{\eta}\tfrac{1-e^{-\eta\lambda}}{\lambda} - 1,\ (1-P_M-P_F)e^{-\eta\lambda} + P_M\left(\tfrac{2}{\eta}\tfrac{1-e^{-\eta\lambda}}{\lambda} - 1\right)\right\}, \end{aligned} \tag{5.76}$$

and the asymptotic normalized throughput is given by

$$\begin{aligned} W &= \max\left\{\tfrac{2-2(1-p_h)^I}{qp_h} - \tfrac{I}{q},\ (1-P_M-P_F)\tfrac{I}{q}(1-p_h)^{I-1} + P_M\left(\tfrac{2-2(1-p_h)^I}{qp_h} - \tfrac{I}{q}\right)\right\} \\ &\to \max\left\{\tfrac{2-2e^{-\eta\lambda}}{\eta} - \lambda,\ (1-P_M-P_F)\lambda e^{-\eta\lambda} + P_M\left(\tfrac{2-2e^{-\eta\lambda}}{\eta} - \lambda\right)\right\}, \end{aligned} \tag{5.77}$$

as $I, q \to \infty$ while $\lambda \triangleq I/q$ is held constant. It can be easily shown that

$$\frac{2-2e^{-\eta\lambda}}{\eta} - \lambda \geq (1-P_M-P_F)\lambda e^{-\eta\lambda} + P_M\left(\frac{2-2e^{-\eta\lambda}}{\eta} - \lambda\right), \tag{5.78}$$

if

$$\frac{2e^{\eta\lambda}-2}{\eta\lambda} - e^{\eta\lambda} \geq \frac{1-P_M-P_F}{1-P_M}. \tag{5.79}$$

Let

$$f(\lambda) \triangleq \frac{2e^{\eta\lambda}-2}{\eta\lambda} - e^{\eta\lambda}. \tag{5.80}$$

Then it can be shown for both η=1 and 2 that

$$\begin{aligned} f'(\lambda) &= \tfrac{2e^{\eta\lambda}}{\eta\lambda^2}[e^{-\eta\lambda} - (\eta^2\lambda^2/2 + \eta\lambda - 1)] \\ &< 0, \end{aligned} \tag{5.81}$$

for all $\lambda > 0$. This implies that $f(\lambda)$ is a decreasing function of λ, whose maximum is 1. But, since the RHS of (5.78) is a constant between $(-\infty, 1]$, there exists a *unique* threshold in channel traffic, denoted λ'_{th}, such that the achievable region and the asymptotic normalized throughput are given by

$$r < \begin{cases} \frac{2-2e^{-\eta\lambda}}{\eta\lambda} - 1, & \lambda \leq \lambda'_{th} \\ (1-P_M-P_F)e^{-\eta\lambda} + P_M\left(\frac{2-2e^{-\eta\lambda}}{\eta\lambda} - 1\right), & \lambda > \lambda'_{th}, \end{cases} \tag{5.82}$$

and

$$W = \begin{cases} \frac{2-2e^{-\eta\lambda}}{\eta} - \lambda, & \lambda \leq \lambda'_{th} \\ (1-P_M-P_F)\lambda e^{-\eta\lambda} + P_M\left(\frac{2-2e^{-\eta\lambda}}{\eta} - \lambda\right), & \lambda > \lambda'_{th}. \end{cases} \tag{5.83}$$

The achievable regions and the asymptotic normalized throughputs are plotted in Figures 5.21 and 5.22 for various values of P_M and P_F respectively. The shaded area in the lower traffic region indicates the performance improvement over the errors-and-erasures decoding scheme. As in subsection 5.5.2, the performance improvement becomes more significant as the side information becomes less reliable, i.e., higher P_M and P_F. By comparing Figures 5.17, 5.18, 5.21, and 5.22, one can also observe that the performance improvement in the lower traffic region is even higher with the demodulator model 2 (realistic model) than with the demodulator model 1 (worst case).

The requirement on (P_M, P_F) pair for the errors-only decoder to perform better than the errors-and-erasures decoder can be obtained from (5.77) as

$$[1 + e^{\eta\lambda} - \frac{2}{\eta}(\frac{e^{\eta\lambda} - 1}{\lambda})]P_M + P_F \geq 1 + e^{\eta\lambda} - \frac{2}{\eta}(\frac{e^{\eta\lambda} - 1}{\lambda}). \tag{5.84}$$

Figure 5.23 indicates regions of (P_M, P_F) pair where one decoding scheme performs better than the other for given λ. We can see similar phenomenon as in demodulator model 1.

Optimum code rate, optimum traffic, and maximum normalized throughput

Let W_{o1} and W_{o2} be the maximum values of $(2 - 2e^{-\eta\lambda})/\eta - \lambda$ and $(1 - P_M - P_F)\lambda e^{-\eta\lambda} + P_M[(2 - 2e^{-\eta\lambda})/\eta - \lambda]$ respectively, and λ_{o1} and λ_{o2} be the channel traffics at which W_{o1} and W_{o2} are achieved respectively. It has been shown in (3.53) and (3.55) that

$$\lambda_{o1} = 0.6931/\eta \text{ and } W_{o1} = 0.3069/\eta. \tag{5.85}$$

In section 5.4.2 it has been shown that λ_{o2} is the (unique) solution of (5.31). Thus,

$$W_{o2} = \frac{1}{\eta}[(1 - P_M - P_F)e^{-\eta\lambda_{o2}} + P_M(1 - 2\lambda_{o2})]. \tag{5.86}$$

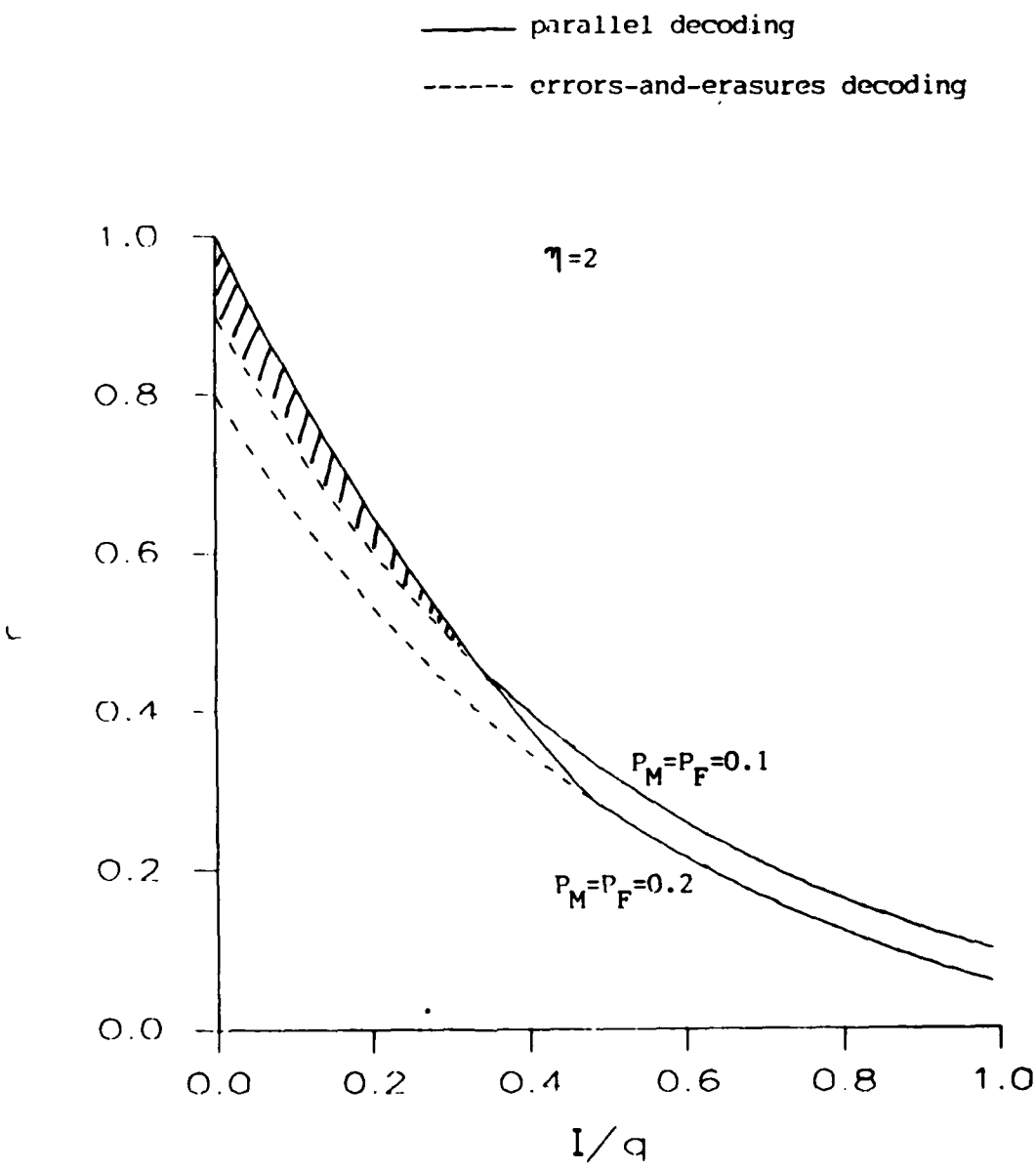

Figure 5.21: Achievable regions of code rate and channel traffic, parallel decoding, demodulator model 2.

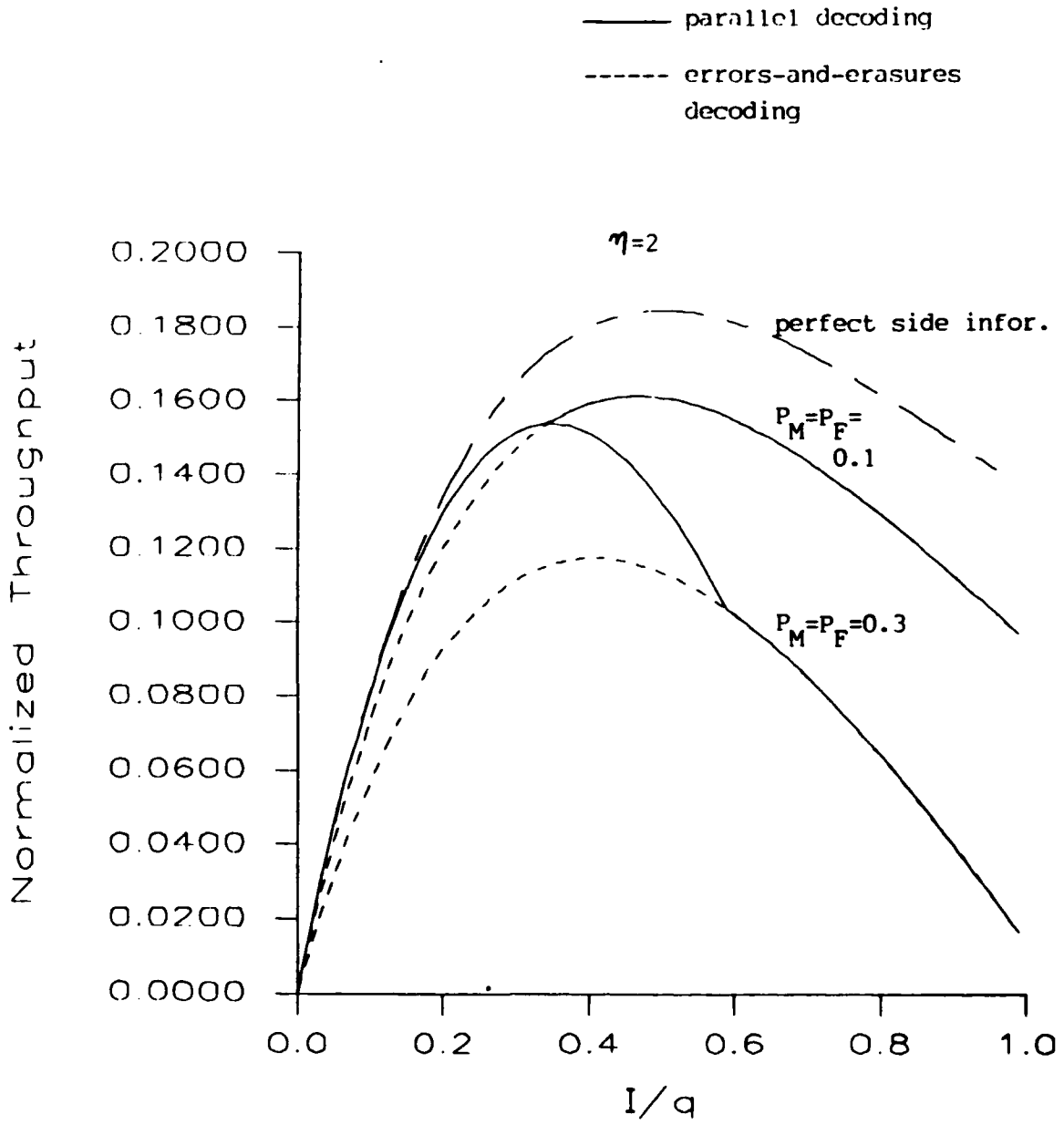

Figure 5.22: Normalized throughputs vs. channel traffic, parallel decoding, demodulator model 2.

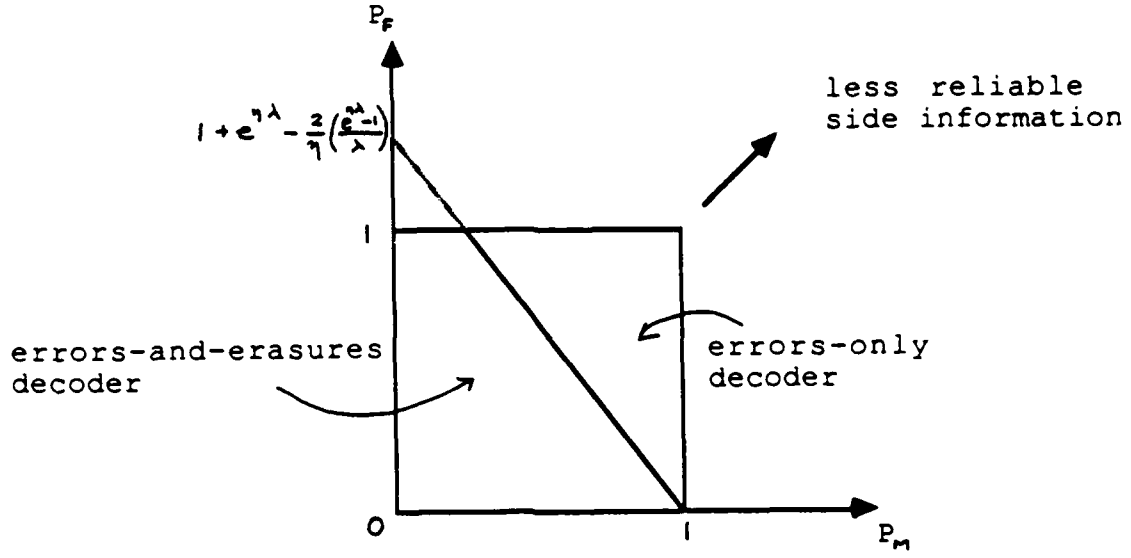

Figure 5.23: Region of preferences, demodulator model 2.

Therefore,

$$
\begin{aligned}
W_{max} &= \max\{W_{o1}, W_{o2}\}, \\
\lambda_{opt} &= \begin{cases} 0.6932/\eta, & W_{o1} \geq W_{o2} \\ \lambda_{o2}, & W_{o1} < W_{o2}, \end{cases} \\
r_{opt} &= \begin{cases} 0.4427, & W_{o1} \geq W_{o2} \\ (1-P_M-P_F)e^{-\eta\lambda_{o2}} + P_M\left(\frac{2-2e^{-\eta\lambda_{o2}}}{\eta\lambda_{o2}} - 1\right), & W_{o1} < W_{o2}. \end{cases}
\end{aligned}
\tag{5.87}
$$

CHAPTER VI

CONCLUSIONS

In this thesis we have examined the multiple-access capability of frequency-hop packet radio networks from a coding point of view. The achievable region of code rate and channel traffic and the normalized throughput were considered as performance measures. We modeled the communication system from the modulator input to the demodulator output as an I-user interference channel, and evaluated the performance of several codes for the interference channels with perfect side information, no side information, and imperfect side information.

For channels with perfect side information, we have considered the performance of Reed-Solomon codes with erasures-correction. The achievable region of code rate and channel traffic, and the optimal code rate, optimal channel traffic at which the normalized throughput is maximized have been derived. It is found that the maximum sum capacity is achieved by the optimal rate Reed-Solomon code with bounded distance decoding. Also, it is shown that the maximum normalized throughput obtained with frequency-hopped spread-spectrum modulation and Reed-Solomon coding is the same as that with narrowband ALOHA system without frequency-hopping. This implies that frequency-hopped spread-spectrum modulation can be just as bandwidth-efficient as narrowband modulation in the sense that for a given bandwidth it can achieve the same throughput. However, for the narrowband ALOHA system without frequency-hopping the

throughput of e^{-1} is achieved when the packet error probability is 0.632 (which is too large in practical sense) and with binary feedback, while for the frequency-hopped spread-spectrum modulation it is achieved with arbitrarily small packet error probability and without feedback.

Next we considered the performance of Reed-Solomon codes for channels with no side information. It is found that the maximum normalized throughput achievable without side information is only 39.3 % (worst case) of that achievable with perfect side information. This gives us a quantitative measure of the importance of side information in improving the multiple-access capability of frequency-hop packet radio networks.

We investigated a technique for obtaining the side information. This is done by partitioning the data stream into blocks and encoding each block by an *error-detecting code*, and transmitting the encoded block (codeword) during a single hop. On the basis of the received version of the codeword the decoder makes a statistical decision about which of the channel states (*hit* or *no hit*) each codeword was transmitted over. Clearly, as the code rate decreases, the error detection capability increases, therefore the reliability of the side information obtained will increase. However, decreasing the code rate implies a decrease in the efficient use of the channel. With this notion in mind, the relationship between the reliability of side information and code rate has been investigated, and the maximum allowable code rate to obtain a certain reliability of side information has been derived for both synchronous and asynchronous frequency-hopping systems.

The above combination of (inner) encoder, channel, and (inner) decoder generates in general an errors-and-erasures channel. To correct the errors (caused by undetected errors) and the erasures (caused by detected errors) we employed an outer code (Reed-Solomon code). In this way the inner decoder informs the outer decoder which symbols (inner codewords) in the received packet have been

hit by symbols from other packets. It is shown that asymptotically perfect side information can be generated from the inner code *without* any loss in code rate for both synchronous and asynchronous frequency-hopping systems, so that the normalized throughput achievable with perfect side information can be achieved through the use of this *concatenated coding scheme*, even though the channel provides *no* side information.

Finally, we considered a *parallel decoding scheme* for channels with *imperfect side information.* In fact, perfect side information and no side information are special cases of imperfect side information. When imperfect side information is available at the demodulator its output is, in general, a sequence of errors, erasures, and correct symbols. In order to correct the errors and erasures we employed a Reed-Solomon code, and considered two different decoding schemes for it: one is the errors-and-erasures decoding and the other is a parallel decoding.

We first evaluated the performance of errors-and-erasures decoder, and found that there is a threshold in channel traffic such that for the lower traffic region the performance can be increased by making a hard decision demodulation and employing errors-only decoding, rather than trying to make an (erroneous) erasure based on the imperfect (unreliable) side information and employing errors-and-erasures decoding.

Based on this observation we suggested a parallel decoding scheme, and analyzed the performance of it for channels with imperfect side information. We found that the parallel decoder gives better performances than errors-and-erasures decoder, and the performance improvement becomes more significant as the side information becomes less reliable.

APPENDICES

APPENDIX A

Proof of (3.4)

Proof of

$$\lim_{n,k\to\infty} \sum_{j=0}^{n-k} \binom{n}{j} p_{h,I}^{j}(1-p_{h,I})^{n-j} = \begin{cases} 1, & 1-r > p_{h,I} \\ 0.5, & 1-r = p_{h,I} \\ 0, & 1-r < p_{h,I}, \end{cases} \tag{A.1}$$

where $r \triangleq k/n$.

Let

$$\begin{aligned} p_{h,I} &\triangleq P(\text{erasure}) \\ X_n &\triangleq \text{number of erasures in a codeword} \\ Y_n &\triangleq X_n/n. \end{aligned} \tag{A.2}$$

Then

$$\begin{aligned} \textstyle\sum_{j=0}^{n-k} \binom{n}{j} p_{h,I}^{j}(1-p_{h,I})^{n-j} &= P(0 \le X_n \le n-k) \\ &= P(0 \le Y_n \le 1-r). \end{aligned} \tag{A.3}$$

From the weak law of large numbers [Dav 70],

$$\lim_{n\to\infty} P(|Y_n - p_{h,I}| > \epsilon) = 0, \tag{A.4}$$

for any $\epsilon > 0$. This implies

$$\lim_{n,k\to\infty} P(0 \le Y_n \le 1-r) = \begin{cases} 1, & 1-r \ge p_{h,I}+\epsilon \Leftrightarrow 1-r > p_{h,I} \\ 0, & 1-r \le p_{h,I}-\epsilon \Leftrightarrow 1-r < p_{h,I}. \end{cases} \tag{A.5}$$

Also, DeMoivre-Laplace limit theorem [Fel 70] implies that as $n \rightarrow \infty$,

$$P(0 \leq X_n \leq n-k) \longrightarrow F\left(\frac{n-k-np_{h,I}}{\sqrt{np_{h,I}(1-p_{h,I})}}\right), \tag{A.6}$$

where

$$F(x) \triangleq \int_{-\infty}^{x} (2\pi)^{-\frac{1}{2}} e^{-u^2/2} du.$$

Therefore,

$$\lim_{n,k\rightarrow\infty} P(0 \leq X_n \leq n-k) = 0.5, \text{ if } 1-r = p_{h,I}. \quad \text{Q.E.D.} \tag{A.7}$$

APPENDIX B

Derivation of P_m.

Let $N_{m,j}$ denote the number of distinct tone positions in the frequency slot, each containing exactly j signals given m hits (i.e., $m+1$ signals in the same frequency slot). Then the tone position occupancy distribution within a frequency slot can be represented by $[N_{m,1}, N_{m,2}, \cdots, N_{m,m+1}]$. For example, consider the case of m=3: [2,1,0,0] corresponds to a situation in which one tone position is occupied by two users and two tone positions are singly occupied. Consider another example, m=5 case: [3,0,1,0,0,0] corresponds to a situation in which one tone position is occupied by three users and three tone positions are singly occupied. Using this notation we can derive P_m as follows.

$$
\begin{aligned}
P_1 &= 0\,P(\text{two users transmit the same symbol}) \\
&\quad + \tfrac{1}{2}P(\text{two users transmit different symbols}) \\
&= 0\,P([0,1]) + \tfrac{1}{2}P([2,0]) \\
&= 0\tfrac{1}{M} + \tfrac{1}{2}(1 - \tfrac{1}{M}) \\
&= \tfrac{1}{2}(\tfrac{M-1}{M}).
\end{aligned}
$$

$$
\begin{aligned}
P_2 &= 0\,P(\text{three users transmit the same symbol}) \\
&\quad +\tfrac{1}{2}P(\text{two users transmit same symbol, the third user} \\
&\qquad \text{transmit a different symbol}) \\
&\quad +\tfrac{2}{3}P(\text{all three users transmit different symbols}) \\
&= 0\,P([0,0,1]) + \tfrac{1}{2}P([1,1,0]) + \tfrac{2}{3}P([3,0,0]) \\
&= 0\tfrac{1}{M^2} + \tfrac{1}{2}\tfrac{3(M-1)}{M^2} + \tfrac{2}{3}\tfrac{(M-1)(M-2)}{M^2} \\
&= \tfrac{4M^2-3M-1}{6M^2}.
\end{aligned}
$$

$$
\begin{aligned}
P_3 &= 0P([0,0,0,1]) + \tfrac{1}{2}P([1,0,1,0]) + \tfrac{1}{2}P([0,2,0,0]) + \tfrac{2}{3}P([2,1,0,0]) \\
&\quad +\tfrac{3}{4}P([4,0,0,0]) \\
&= 0\tfrac{1}{M^3} + \tfrac{1}{2}\tfrac{4(M-1)}{M^3} + \tfrac{1}{2}\tfrac{3(M-1)}{M^3} + \tfrac{2}{3}\tfrac{6(M-1)(M-2)}{M^3} + \tfrac{3}{4}\tfrac{(M-1)(M-2)(M-3)}{M^3} \\
&= \tfrac{3M^3-2M^2-M}{4M^3}.
\end{aligned}
$$

$$
\begin{aligned}
P_4 &= 0P([0,0,0,0,1]) + \tfrac{1}{2}P([1,0,0,1,0]) + \tfrac{1}{2}P([0,1,1,0,0]) + \tfrac{2}{3}P([2,0,1,0,0]) \\
&\quad +\tfrac{2}{3}P([1,2,0,0,0]) + \tfrac{3}{4}P([3,1,0,0,0]) + \tfrac{4}{5}P([5,0,0,0,0]) \\
&= 0\tfrac{1}{M^4} + \tfrac{1}{2}\tfrac{5(M-1)}{M^4} + \tfrac{1}{2}\tfrac{10(M-1)}{M^4} + \tfrac{2}{3}\tfrac{10(M-1)(M-2)}{M^4} \\
&\quad +\tfrac{2}{3}\tfrac{15(M-1)(M-2)}{M^4} + \tfrac{3}{4}\tfrac{10(M-1)(M-2)(M-3)}{M^4} + \tfrac{4}{5}\tfrac{(M-1)(M-2)(M-3)(M-4)}{M^4} \\
&= \tfrac{24M^4-15M^3-10M^2+1}{30M^4}.
\end{aligned}
$$

$$
\begin{aligned}
P_5 &= 0P([0,0,0,0,0,1]) + \tfrac{1}{2}P([1,0,0,0,1,0]) + \tfrac{1}{2}P([0,1,0,1,0,0]) \\
&\quad +\tfrac{2}{3}P([2,0,0,1,0,0]) + \tfrac{1}{2}P([0,0,2,0,0,0]) + \tfrac{2}{3}P([1,1,1,0,0,0]) \\
&\quad +\tfrac{3}{4}P([3,0,1,0,0,0]) + \tfrac{2}{3}P([0,3,0,0,0,0]) + \tfrac{3}{4}P([2,2,0,0,0,0]) \\
&\quad +\tfrac{4}{5}P([4,1,0,0,0,0]) + \tfrac{5}{6}P([6,0,0,0,0,0]) \\
&= 0\tfrac{1}{M^5} + \tfrac{1}{2}\tfrac{6(M-1)}{M^5} + \tfrac{1}{2}\tfrac{15(M-1)}{M^5} + \tfrac{2}{3}\tfrac{15(M-1)(M-2)}{M^5} \\
&\quad +\tfrac{1}{2}\tfrac{10(M-1)}{M^5} + \tfrac{2}{3}\tfrac{60(M-1)(M-2)}{M^5} + \tfrac{3}{4}\tfrac{20(M-1)(M-2)(M-3)}{M^5} + \tfrac{2}{3}\tfrac{15(M-1)(M-2)}{M^5} \\
&\quad +\tfrac{3}{4}\tfrac{45(M-1)(M-2)(M-3)}{M^5} + \tfrac{4}{5}\tfrac{15(M-1)(M-2)(M-3)(M-4)}{M^5} + \tfrac{5}{6}\tfrac{(M-1)(M-2)(M-3)(M-4)(M-5)}{M^5} \\
&= \tfrac{10M^5-6M^4-5M^3+M}{12M^5}.
\end{aligned}
$$

.

.

.

Notice that in general as M becomes large, P_m is dominated by the last term, i.e., $\frac{m}{m+1}P(\,[m+1,0,\cdots,0]\,)$, because

$$\begin{aligned} P(\,[m+1,0,\cdots,0]\,) &= \frac{(M-1)(M-2)\cdots(M-m)}{M^m} \\ &\rightarrow 1, \end{aligned} \tag{B.1}$$

for large enough M. Therefore, $P_m = \frac{m}{m+1}$ for large enough M.

APPENDIX C

Proof of (4.2)

Proof of

$$\lim_{n,k\to\infty} P_c(I) = \begin{cases} 1, & 1-r > 2P_{ud} + P_d \\ 0.5, & 1-r = 2P_{ud} + P_d \\ 0, & 1-r < 2P_{ud} + P_d, \end{cases}$$

where $r \triangleq k/n$.

Let random variables X_i, Y_n, and Z_n be defined as

$$X_i = \begin{cases} 0, & \text{if the received symbol is } \textit{correct} \\ 1, & \text{if the received symbol is } \textit{erased} \\ 2, & \text{if the received symbol is } \textit{in error}, \end{cases} \qquad i = 1, 2, \cdots, n, \tag{C.1}$$

and

$$Y_n \triangleq \sum_{i=1}^{n} X_i, \tag{C.2}$$

and

$$Z_n \triangleq \frac{Y_n - \mathrm{E}(Y_n)}{\sqrt{\mathrm{Var}(Y_n)}}, \tag{C.3}$$

where $\mathrm{E}(Y_n)$ and $\mathrm{Var}(Y_n)$ are the mean and the variance of Y_n respectively.

Then Y_n is the total number of erasures and twice the number of errors in the received packet (codeword). Therefore the probability of correctly decoding a packet $P_c(I)$ is given by

$$P_c(I) = P(Y_n \leq n-k). \tag{C.4}$$

Since the X_i, $i = 1, 2, \cdots, n$, are mutually independent (due to the random frequency-hopping), by the central limit theorem [Dav 70]

$$\lim_{n\to\infty} P(Z_n \le z) = \int_{-\infty}^{z} \frac{1}{\sqrt{2\pi}} e^{-u^2/2}\, du. \tag{C.5}$$

It can be shown that

$$\begin{aligned} \mathrm{E}(Y_n) &= n(P_d + 2P_{ud}) \\ \mathrm{Var}(Y_n) &= n(P_d - P_d^2 + 4P_{ud} - 4P_{ud}^2 - 4P_dP_{ud}), \end{aligned} \tag{C.6}$$

since

$$\begin{aligned} P(X_i = 1) &= P_d, \\ P(X_i = 2) &= P_{ud}, \end{aligned}$$

for $i = 1, 2, \cdots, n$. Therefore,

$$\begin{aligned} P_c(I) &= P(Y_n \le n - k) \\ &= P\left(Z_n \le \frac{n-k-\mathrm{E}(Y_n)}{\sqrt{\mathrm{Var}(Y_n)}}\right) \\ &= P\left(Z_n \le \underbrace{\frac{\sqrt{n}(1-r-P_d-2P_{ud})}{\sqrt{P_d - P_d^2 + 4P_{ud} - 4P_{ud}^2 - 4P_dP_{ud}}}}_{\triangleq s}\right) \\ &\to \int_{-\infty}^{s} \frac{1}{\sqrt{2\pi}} e^{-u^2/2}\, du \\ &= \begin{cases} 1, & 1 - r - P_d - 2P_{ud} > 0 \\ 0.5, & 1 - r - P_d - 2P_{ud} = 0 \\ 0, & 1 - r - P_d - 2P_{ud} < 0. \end{cases} \quad Q.E.D. \end{aligned} \tag{C.7}$$

BIBLIOGRAPHY

BIBLIOGRAPHY

[Abr 70] N.Abramson, "The ALOHA System - Another alternative for computer communications," *Proc. Fall Joint Computer Conf.*, pp.281-285, 1970.

[Ahl 71] R. Ahlswede, "Multi-user communication channels," *Proc. 2nd Int. Symp. Infor. Theory*, Tsahkadsor, Armenian S.S.R. 1971, Hungarian Acad. Sc., pp.23-52.

[Ber 68] E.R.Berlekamp, *Algebraic Coding Theory*, McGraw-Hill, New York, 1968.

[Ber 80] E.R.Berlekamp, "The technology of error-correcting codes," (Appendix B), *Proceedings of the IEEE*, pp.564-592, May 1980.

[Ber 84] E.R.Berlekamp, *Algebraic Coding Theory*, Aegean Park Press, 1984.

[Bla 83] R.E.Blahut, *Theory and Practice of Error Control Codes*, Addison-Wesley Pub. Co., 1983.

[Cas 86] K.G.Castor and W.E.Stark, "Parallel decoding of diversity / Reed-Solomon coded SSFH communications with repetition thresholding," *Proc. of the 1986 Conf. on Information Sciences and Systems*, March 1986.

[Cla 82] G.C.Clark and J.B.Cain, *Error Control Coding for Digital Communications*, Plenum Press, New York, 1982.

[Coo 78] G.R.Cooper and R.W.Nettleton, "A spread spectrum technique for high capacity mobile communications," *IEEE Tr. on Vehicular Technology*, vol. VT-27, no.4, pp.264-275, Nov. 1978.

[Dav 70] W.B.Davenport, Jr., *Probability and Random Processes*, McGraw-Hill, Kogakusha Ltd., 1970.

[Fel 70] W.Feller, *An Introduction to Probability Theory and Its Applications*, Vol.I, 3rd Ed., p.186, John Wiley and Sons, New York, 1970.

[For 66] G.D.Forney, *Concatenated Codes*, MIT Press, Cambridge, MA, 1966.

[Gam 80] A.E.Gamal and T.M.Cover, "Multiple user information theory," *Proc. of IEEE*, vol.68, no.12, pp.1466-1483, Dec. 1980.

[Ger 82] E.A.Geraniotis and M.B.Pursley, "Error probabilities for slow frequency-hopped spread-spectrum multiple-access communications over fading channels," *IEEE Tr.Comm.*, pp.996-1009, May 1982.

[Goo 80] D.J.Goodman, P.S.Henry, and V.K.Prabhu, "Frequency-hopped multilevel FSK for mobile radio," *Bell System Technical Journal*, vol.59, no.7, pp.1257-1275, Sep. 1980.

[Haj 82] B.E.Hajek, "Recursive retransmission control - Application to a frequency-hopped spread-spectrum system," Proc. *1982 Conf. on Information Sciences and Systems*, Princeton University, pp.116-120., March 1982.

[Haj 83] B.E.Hajek, "Adaptive packet radio networks," unpublished report, Oct. 1983.

[Heg 85] M.Hegde and W.E.Stark, "Multiple-access capability of frequency hop spread-spectrum communication," *Proc. of Milcom*, pp.575-579, Oct. 1985.

[Kal 85] J.G.Kalbfleisch, *Probability and Statistical Inference, Vol 1.: Probability*, 2nd ed., Springer-Verlag, New York, 1985.

[Kle 76] L. Kleinrock, *Queueing Systems*, vol.2: *Computer Applications*, Wiley, New York, 1976.

[Leb 71] I.L.Lebow, K.L.Jordan, and P.R.Drouilhet Jr., "Satellite communications to mobile platforms," *Proceedings of IEEE*, vol.59, pp.139-159, Feb. 1971.

[Leh 84] J.S.Lehnert, "Direct-sequence spread-spectrum signaling with applications to packet radio systems," *Tech. Report T-153*, Coordinated Science Laboratory, University of Illinois, Nov. 1984.

[Mac 77] F.J.MacWilliams and N.J.A.Sloane, *The Theory of Error-Correcting Codes*, Amsterdam, The Netherlands, North-Holland, 1977.

[McC 83] J.R.McChesney, J.Carmody, and M.B.Pursley, "A jam resistant digital voice modem for Air Force tactical voice communicattions," *Proceedings of the 1983 IEEE Military Communication Conference*, Oct. 1983.

[McE 82] R.J.McEliece and M.B.Pursley, "Error-control coding for slow-frequency-hopped spread-spectrum communications," *Abst. of Papers, 1982 IEEE Int. Symp. Information Theory*, Les Arcs, France, p.42, June 1982.

[McE 84] R.J.McEliece and W.E.Stark, "Channels with block interference," *IEEE Tr. on Information Theory*, pp.44-53, Jan. 1984.

[Mus 82] J.M.Musser and J.N.Daigle, "Throughput analysis of an asynchronous code division multiple access system," *Proc. of ICC*, 2F.2.1-2F.2.7, 1982.

[Pap 65] A.Papoulis, *Probability, Random Variables, and Stochastic Processes*, McGraw-Hill Inc., Kogakusha, Ltd., 1965.

[Pet 72] W.W.Peterson and E.J.Weldon.Jr., *Error-Correcting Codes*, 2nd Ed.,MIT Press, Cambridge, MA, 1972.

[Pur 81a] M.B.Pursley and B.E.Hajek, "Spread-spectrum random access communications for HF channels," *Coordinated Science Laboratory Tech. Report R-919*, Univ. of Illinois, Sep. 1981.

[Pur 81b] M.B.Pursley, "Spread-spectrum multiple-access communications," in *Multi-User Communication Systems*, G.Longo (ed.), Springer-Verlag, Vienna and New York, pp.139-199, 1981.

[Pur 82] M.B.Pursley, "Coding and diversity for channels with fading and pulsed interference," *Proceedings of the 1982 Conference on Information Sciences and Systems*, Princeton Univ., pp.413-418, Mar. 1982.

[Pur 83] M.B.Pursley and W.E.Stark, "Anti-jam capability of frequency-hop spread-spectrum with Reed-Solomon coding," *Proceedings of the 1983 IEEE Military Communication Conference*, Oct. 1983.

[Pur 83a] M.B.Pursley, "Throughput of frequency-hopped spread-spectrum communications for packet radio networks," *Proc. of the 1983 Conf. on Information Sciences and Systems*, Johns Hopkins Univ., pp.550-556, March 1983.

[Pur 83b] M.B.Pursley, "Adaptive spread-spectrum radio networks," *Coordinated Science Laboratory Rep-131*, University of Illinois, Dec. 1983.

[Pur 84] M.B.Pursley, "Frequency-hop transmission for satellite packet switching and terrestrial packet radio networks," *Coordinated Science Labo-*

ratory Tech. Rep., June 1984. Also published in *IEEE Tr. on Information Theory*, Sep. 1986.

[Pur 86] M.B.Pursley, "Frequency-hop transmission for satellite packet switching and terrestrial packet radio networks," *IEEE Tr. on Information Theory*, Sep. 1986.

[Pur 87] M.B.Pursley, "The role of spread spectrum in packet radio networks," *Proc. of IEEE*, Jan. 1987, To be published.

[Ray 81] D. Raychaudhuri, "Performance analysis of random access packet switched code division multiple access systems," *IEEE Tr. on Comm.*, Vol. Com.-29, No. 6, pp.895-901, June 1981.

[San 81] D. Sant, "Spread spectrum and satellite systems," *IEEE Milcom Conf. Proc.*, Oct. 1981.

[Sat 77] H. Sato, "Two-user communication channels," *IEEE Tr. on Information Theory*, vol. IT-23, pp.295-304, May 1977.

[Sil 84] J.A.Silvester, "Performance of spread spectrum," *Allerton Conf. on Compter, Communication, and Control*, pp.30-39, Oct. 1984.

[Sou 84] E.S.Sousa and J.A.Silvester, "A spreading code protocol for a distributed spread spectrum packet radio network," *Proc. IEEE Global Communications Conf.*, pp. 481-486, Nov. 1984.

[Sta 85] W.E.Stark, "Coding for frequency-hopped spread-spectrum communication with partial-band interference - Part II: coded performance," *IEEE Tr. Communication*, pp.1045-1057, Oct. 1985.

[Sti 73] I.G.Stiglitz, "Multiple-access considerations - a satellite example," *IEEE Tr. on Communication*, vol. COM-21, pp.577-582, May 1973.

[Tan 81] A.S.Tanenbaum, *Computer Networks*, Prentice-Hall Inc., New Jersey, 1981.

[Wie 82] J.E.Wieselthier, "Spread spectrum multiple access issues in the HF intra task force communication network," *5th MIT/ONR Workshop on C^3 systems*, Naval Postgraduate School, Monterey, Aug. 1982.

[Wie 83] J.E.Wieselthier and A.Ephremides, "A distributed reservation scheme for spread spectrum multiple access channels," *Proc. GLOBECOM* , pp.659-665, 1983.

[Wie 86] J.E.Wieselthier and A.Ephremides, "A distributed reservation-based CDMA protocol that does not require feedback information," *1986 IEEE Int. Symp. Information Theory*, Ann Arbor, Oct. 1986.

END

12-87

DTIC